DETERMINATION OF FUNCTIONAL IMPACTS OF DIFFERENTIALLY EXPRESSED PHOP GENE ON MYCOBACTERIAL VIRULENCE IN CAUSING TUBERCULOUS MENINGITIS

CHALA CHABURTE GALATA

PhD

The Hong Kong Polytechnic University

2022

The Hong Kong Polytechnic University

Department of Health Technology and Informatics

Determination of functional impacts of differentially expressed PhoP gene on mycobacterial virulence in causing tuberculous meningitis

Chala Chaburte Galata

A thesis submitted in partial fulfillment of the requirements

for the degree of Doctor of Philosophy

May 2022

CERTIFICATION OF ORIGINALITY

I hereby declare that this thesis is my own work and that, to the best of my knowledge and belief, it reproduces no material previously published or written, nor material that has been accepted for the award of any other degree or diploma, except where due acknowledgment has been made in the text.

Signed:

_____

Chala Chaburte Galata

ABSTRACT

Tuberculous meningitis is a life-threatening extrapulmonary tuberculosis caused by *Mycobacterium tuberculosis* (*M. tuberculosis)* in the central nervous system. Such a serious clinical manifestation of tuberculosis is associated with an increased level of virulence in some strains of the causative agent. The situation is further aggravated by the lack of effective vaccines and drugs against tuberculosis. Improved understanding of the pathogenesis of tuberculosis and genetic determinants responsible for increased virulence in *M. tuberculosis* strains is highly needed to alleviate the problems. Recently, a set of genetic mutations have been identified in the genome of the hypervirulent *M. tuberculosis* strains isolated from tuberculous meningitis patients. These mutations were found to be associated with differentially elevated expression of the *phoP* gene in the hypervirulent *M. tuberculosis* strains but were absent in the low virulent *M. tuberculosis* strains of the same phylogenetic lineage. However, the causative role of these genetic factors in the development of tuberculous meningitis is still unknown. This thesis explains the findings of the study that help to bridge the existing research gap. This study has two objectives.

1)To construct a transformant *Mycobacterium marinum* (*M. marinum*) strain with enhanced expression of *phoP* gene of *M. tuberculosis.*

2) To elucidate the causative role of the enhanced expression of the *phoP* gene in mycobacterial virulence in causing tuberculous meningitis using zebrafish-*M. marinum* infection model.

In the first part of the study, the *phoP* gene and blue fluorescent protein (BFP) gene regions were amplified from the genome of *M. tuberculosis* H37Rv and the plasmid pME-loxP-mTagBFP2-stop-pA-loxP, respectively, and cloned into *Escherichia coli*-mycobacteria shuttle vector (pVV16). The recombinant *pVV16-phoP gene-BFP gene* plasmid was transferred into the *M. marinum* strain M/E11 using electroporation. To label the control *M. marinum* strain M/E11 with blue color, we also constructed a recombinant *pVV16-BFP gene* plasmid and transferred it into the mycobacterium using the same procedures. PCR and Sanger sequencing analyses and blue fluorescent transformants recovered from culture confirmed the presence of the target genes in the transformants. qPCR analysis of the transcription level of the *phoP* gene in the transformant transformed with *pVV16-phoP gene-BFP gene* plasmid indicated that the expression of the gene was increased about 3-fold relative to that of the control strain transformed with *pVV16-BFP gene* plasmid.

In the second part of the study, wild-type and a*bsolute* (*ednrba*^{b140}*;mitfa*^{b692}) (transparent) lines of zebrafish were injected with the transformant (*M. marinum*

strain M/E11) and control strain (*M. marinum* strain M/E11). The effects of the infection were examined in the brain of the zebrafish using bacteriological, histopathological, and immunohistochemistry analyses. Fluorescence microscopy was used for the detection and monitoring of blue fluorescent granuloma-like signals or aggregates in the body and brain region of the *M. marinum* E11 infected transparent zebrafish. Among the control strain-infected wild-type zebrafish, 6.25% (4/64) developed infection in their brains, whereas from those wild-type zebrafish infected with transformant, 28.13% (18/64) had brain infection (P=0.0018) with a higher bacillary load. Among the zebrafish that developed brain infection, 4 (3 from transformant-infected and one from control strain-infected) of them were from the *M. marinum* strain M-infected group. Notably, granuloma-like lesions were only observed in the brain of transformant-infected zebrafish. A lower survival rate (36.8%) was also observed in the transformant *M. marinum* E11 infected zebrafish relative to that of the control *M. marinum* E11 infected zebrafish (68.4%). Importantly, 47.37% (9/19) and 6.25% (1/16) of the wild-type zebrafish that died after being infected with the transformant and control strain, respectively, had brain infections. Among these transformant-infected zebrafish that developed brain infections, 77.8% (7/9) died within a week. In transparent live zebrafish, granuloma-like signals were also detected in the brain of 16.7% (2/12) and 41.7% (5/12) of the zebrafish injected with control and transformant *M. marinum* E11, respectively. Moreover, qPCR analysis showed a lower level of

tumor necrosis factor-alpha (TNF-α) in the brain of transformant-infected zebrafish than that of the control-infected zebrafish (P=0.2186). Taken together, our results indicated that the transformant *M. marinum* is more neurotropic and virulent than the control strain, reflecting the fact that differentially elevated expression of the *phoP* gene may enhance the virulence of mycobacteria in causing infection in the central nervous system. To our knowledge, this study is the first to validate the functional impacts of differentially expressed *phoP* gene on mycobacterial virulence in the development of tuberculous meningitis inside the host. Thus, the findings may provide a knowledge base for the development of novel and effective vaccines and drugs against tuberculosis particularly tuberculous meningitis.

PUBLICATION AND PRESENTATION

1. **Chala Chaburte GALATA**, Annie Wing-Tung LEE, Rahim RAJWANI, Xiangke CHEN, Lam-Kwong LEE, Kennth Siu Sing LEUNG, Wing Cheong YAM, Alvin Chun-Hang MA and **Gilman Kit-Hang SIU**. Determination of functional impacts of differentially expressed *phoP* gene on mycobacterial virulence in causing tuberculous meningitis (Submitted to mBio under review).
2. Rahim RAJWANI*, **Galata Chala Chaburte***, Pui-kin SO, Kenneth Siu Sing LEUNG, Kingsley King Gee TAM, Sheeba SHEHZAD, Timothy Ting Leung Ng, Li ZHUa, Annie Wing Tung LEE, Hiu Yin LAO, Chloe Toi-Mei CHAN, Jake Siu-Lun LEUNG, Lam-Kwong LEE, Kin Chung WONG, Wing Cheong YAM and **Gilman Kit-hang SIU**. A multi-omics investigation into mechanisms of hyper-virulence in a clinical strain of *Mycobacterium tuberculosis* (Published).
3. Zhu L, Lee AW, Wu KK, Gao P, Tam KK, Rajwani R, **Chaburte GC**, Ng TT, Chan CT, Lao HY, Yam WC, Kao RY, **Siu GKH**. Screening repurposed antiviral small molecules as antimycobacterial compounds by a lux-based *phoP* promoter-reporter platform. Antibiotics. 2022;11(3):369.

PRESENTATION

1. **Galata Chala Chaburte** and **Gilman Kit-hang SIU**. Determination of the functional impact of genetic markers specific to hypervirulent *Mycobacterium tuberculosis* in mycobacterial virulence using the zebrafish model. Oral presentation, Postgraduate Symposium organized by the Department of Health Technology and Informatics, June 23, 2021.
2. **Galata Chala Chaburte** and **Gilman Kit-hang SIU**. Determination of the functional impact of overexpressed *phoP* gene on mycobacterial virulence using the zebrafish model. Poster Presentation, 2021-14th International Conference on Research in Life-Sciences & Health care (ICRLSH), held from 10-11 September 2021, London, UK.

ACKNOWLEDGMENTS

I would like to express my deepest gratitude to my chief supervisor Dr Gilman SIU for providing me this wonderful opportunity, quality guidance, and his efforts in all aspects of my study. I appreciate your entertainment from the date I contacted you to join this PhD program and your unreserved encouragement throughout my PhD study. I say thank you again from the bottom of my heart.

I would also like to thank my Co-supervisor Professor Polly H.M. LEUNG for her constructive comments and encouragement to undertake my research.

I express my special thanks to all staff of the Department of Health Technology and Informatics, The Hong Kong Polytechnic University for all support and encouragement I have received.

My special thanks also go to the Research Grants Council (RGC) of Hong Kong for granting me The Hong Kong PhD Fellowship for my PhD study. Without their support, this research study would have been unthinkable.

I would also like to thank all Dr Gilman's team for supporting me in my research project. I also like to extend my gratitude to Dr Alvin MA for providing me zebrafish to carry out my experiments and his advice to shape my research work, and his team for supporting me in my research. I also extend my thanks to Dr Bojia Endebu, Mr Alemayehu Fanta and Dr Getachew Mulugeta for their advice to

continue my study to PhD level and their moral support. Thank you to all my colleagues and friends in CVMA, AAU for your advice and moral support.

I am very grateful to my brother Biru Chaburte, mother Side Adaru, and father for looking after my children, and moral support during this study.

Nama addaa, my lovely wife **Sukare Bekele**, I miss you, but you are always in my heart. Ati bu'ura waan hundaati kunis bu'aa hojii keetii keessa isa tokkodha. Waaqayyoon lubbuu tee Jannata keessatti bara baraan yaa qananiisu.

Above all, thanks to the almighty God for everything.

TABLE OF CONTENTS

CONTENTS ***PAGE***

LIST OF FIGURES

LIST OF TABLES

LIST OF ABBREVIATIONS

AFB	Acid-fast bacilli
ATCC	American Type of Culture Collection
BFP	Blue Fluorescence Protein
BSA	Bovine Serum Albumin
CNS	Central nervous system
DAB	Diaminobenzidine
DNA	Deoxyribonucleic Acid
EDTA	Ethylenediaminetetraacetic acid
HIV	Human Immunodeficiency virus
IS6110	Insertion Sequence 6110
LTB	Latent tuberculosis
LB	Luria-Bertani
LJ	Lowenstein–Jensen
OD	Optical Density
PBS	Phosphate-buffered saline
PCR	Polymerase Chain Reaction

qPCR	Quantitative polymerase-chain-reaction
RD	Region of Differences
RNA	Ribonucleic Acid
TB	Tuberculosis
TBM	Tuberculous meningitis
TBS	Tris-buffered saline
TST	Tuberculin skin test
WHO	World health organization

CHAPTER 1: INTRODUCTION

In this chapter, the background information and concepts related to tuberculosis and *Mycobacterium tuberculosis (M. tuberculosis)* are presented to conceptualize this study. In the first section, the chapter discusses what tuberculosis is, the history and global burden of tuberculosis, the causative agent of tuberculosis (*M. tuberculosis*), and its characteristics. The next sections explain the way of transmission of tuberculosis and its manifestations, strategies used by *M. tuberculosis* to manipulate the host immune response, and virulence-associated factors in *M. tuberculosis* strains. Then, it presents previous works done on hypervirulent *M. tuberculosis* strains, a vaccine against tuberculosis, and a zebrafish-*Mycobacterium marinum (M. marinum)* model for the study of tuberculosis. Finally, it describes the identified problems and why this study was conducted.

1.1 Tuberculosis and its global burden

Tuberculosis (TB) is an infectious disease caused mainly by *M. tuberculosis*. The disease predominantly affects the lungs where it is called pulmonary TB and it also affects other parts of the body such as lymph nodes, skin, intestine, central nervous system (CNS), bones, and genitourinary system of the host where it causes extra-pulmonary TB (1, 2).

TB has been the enemy of public health since the earliest time. The evidence collected by investigators from the corpse aged 4,000 years in Italy, Denmark, and the Middle East countries shows the existence of TB in that population at that time. The finding of the decay of skeleton because of TB (Pott's deformities) in the mummies aged more than 4,000 years ago in Egypt also indicates the dissemination of the disease in the population at that period (3, 4).

In Europe and America, TB also became a serious disease causing the death of one-seventh of the population between the 18^{th} and 19^{th} centuries (5). However, at the end of the 19^{th} century, the incidence of the disease radically decreased in these countries. This is for the reason that the development of effective antibiotics, improvement of the hygienic conditions, public health awareness in the population, and human resistance to the disease (6).

In the mid-1980s, the declining trend of the disease was ended, and new TB cases increased mainly as a result of increased homelessness and poverty, increased immigration from high TB prevalence countries, poor infrastructure for TB control programs, and the emergence of human immunodeficiency virus (HIV) in the developed world. Using huge expenses of money and human resources, especially

by directly monitoring antibiotics supply, the outbreak of these new TB cases was reversed in the United States and Europe (7, 8).

However, TB is still prevalent in developing countries. Even though it is hard to guess the TB burden in the first three-quarters of the 20thcentury, the available documents show that TB was not as widespread as it has been since the 1980s in developing countries (9). The disease burden started increasing following the emergence of HIV, and the development and widespread of drug-resistant strains of *M. tuberculosis.* According to the previous study, extra mortality because of HIV-TB co-infection was estimated between 120,000 and 150,000 in 1990 globally. Among these, 100,000-120,000 occurred in Africa (10). Besides, HIV disease has complicated the clinical properties of TB. In the case of co-infection, the chance of involvement of extrapulmonary TB is increased, often associated with pulmonary TB (11, 12). Furthermore, TB diagnosis has become challenging because of the increased number of HIV-affected individuals with false-negative smear and tuberculin skin tests (13, 14). By taking the crisis caused so far and is going to come about in the future due to TB into consideration, the disease was announced as a global emergency by the world health organization (WHO) in 1993. WHO also gave a warning that the disease will affect 30 million people if immediate actions are not taken to design better control strategies (15). As a result, different countries

have taken continuous measures to control the disease, and WHO started publishing the global TB report which includes updates on the prevalence, incidence, morbidity, and mortality of the disease at national, regional, and global levels every year since 1997. In 2001, the Stop TB Partnership was established with a target to reduce and reverse TB incidence. It launched three global plans to stop TB. The first plan was intended to cover from 2001-2005. In the plan, it delivered a coherent agenda to meeting important new partnerships, take forward research and development, and quick effect on TB in the regions where the disease is highly prevalent. Its attention was on the expansion of the DOTS (directly observed treatment short-course) strategy, and the evolving crisis from drug-resistant TB and HIV infection. The second strategy covers from 2006-2015 intending to reduce the TB incidence to half of its death and prevalence by 2015 compared with that of 1990 (16).

The third plan (updates from 2011-2015) showed what is required to be prepared to attain the 2015 targets. It concentrated on increasing the present interventions for TB diagnosis and treatment as well as establishing new technologies like new diagnostic tests. The 4th global plan covering from 2016-2020 is the end TB plan that represents a roadmap to speed up the impact on the TB epidemic and achieving

the targets of the WHO end TB strategy even though it was not successful in most countries (17).

Even though different prevention and control measures have been taken by the WHO and other stakeholders so far, the disease remains one of the most devastating health problems. It is the 13th leading cause of death and the second leading killer from infectious diseases next to coronavirus disease (COVID-19) globally (1). About 9.9 million people were sick, and 1.5 million deaths were recorded due to tuberculosis in 2020. Among these, 214,000 TB deaths were on HIV-positive individuals. Currently, about 2 billion people, one-quarter of the population in the world, are to be infected with the disease. Although the number of infected people is very high, only about 5-10% of the people are prone to develop active TB throughout their life (18).

All age groups of people are affected by TB. However, the largest proportion of the burden has so far occurred in adult men which accounts for 56%. The next highly affected age group is adult women (33%) followed by children (11%) (1). When the burden is geographically evaluated, an increased incidence of TB has occurred in Western Pacific (18%), South-East Asia (43%), and Africa (25%) **(Figure 1.1)**. Even though the number is smaller, the cases were also observed in the WHO's

eastern parts of the Mediterranean (8.3%), the Americans (3%), and Europe (2.3%). Two-thirds of the estimated global TB cases happened in 8 countries which include: Nigeria (4.6%), Indonesia (8.4%), Pakistan (5.8%), China (8.5%), India (26%), the Philippines (6%), South Africa (3.3%) and Bangladesh (3.6%)(1).

In Hong Kong, TB became one of the notifiable diseases in 1939 (19). According to the report of the Department of Health in 2021, the disease killed 193 individuals in 2020 in Hong Kong. The incidence of the disease is 3699 with the rate of 49 per 100,000 population in 2020, which dropped down from 697 per 100,000 population in 1952 (20). **Figure 1.2** indicates the overall declining trend of TB incidence rate from 1952 to 2020 in Hong Kong. The declining trend of disease notification is because of the continuous and effective actions taken in case finding, treatment, and control measures against the disease in the last 60 years. Starting from 2010, the incidence rate of the disease remains almost consistent indicating the need for more actions to eliminate the disease.

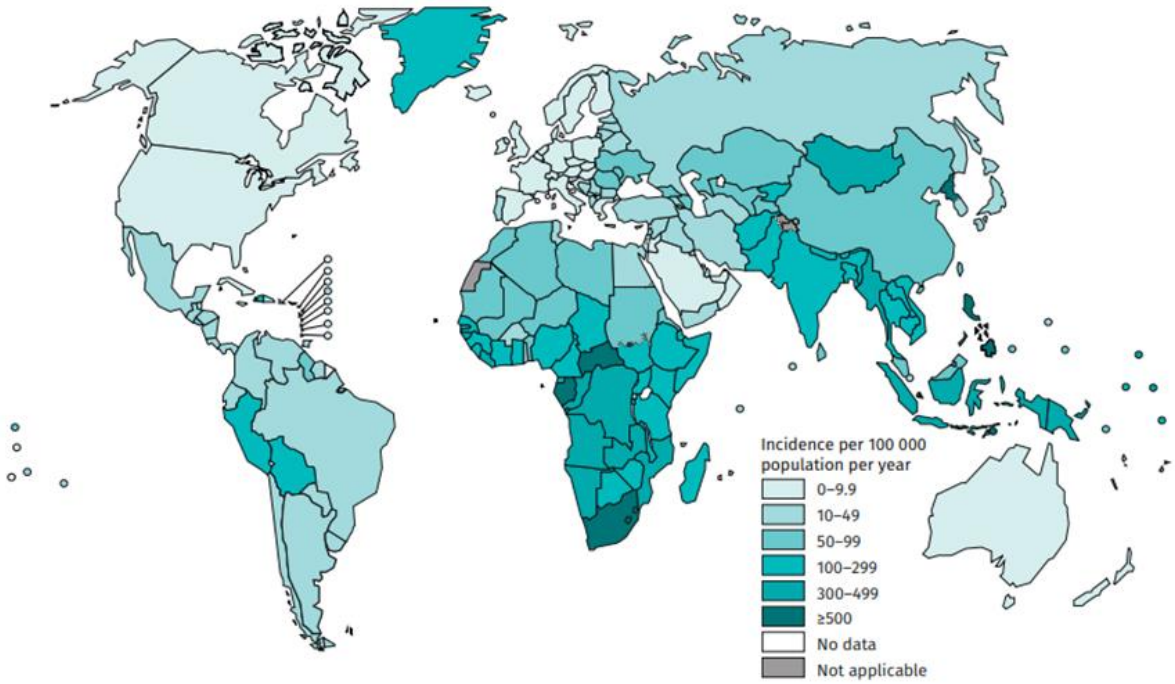

Figure 1. 1: Estimated incidence rates of global tuberculosis in 2020 (1).

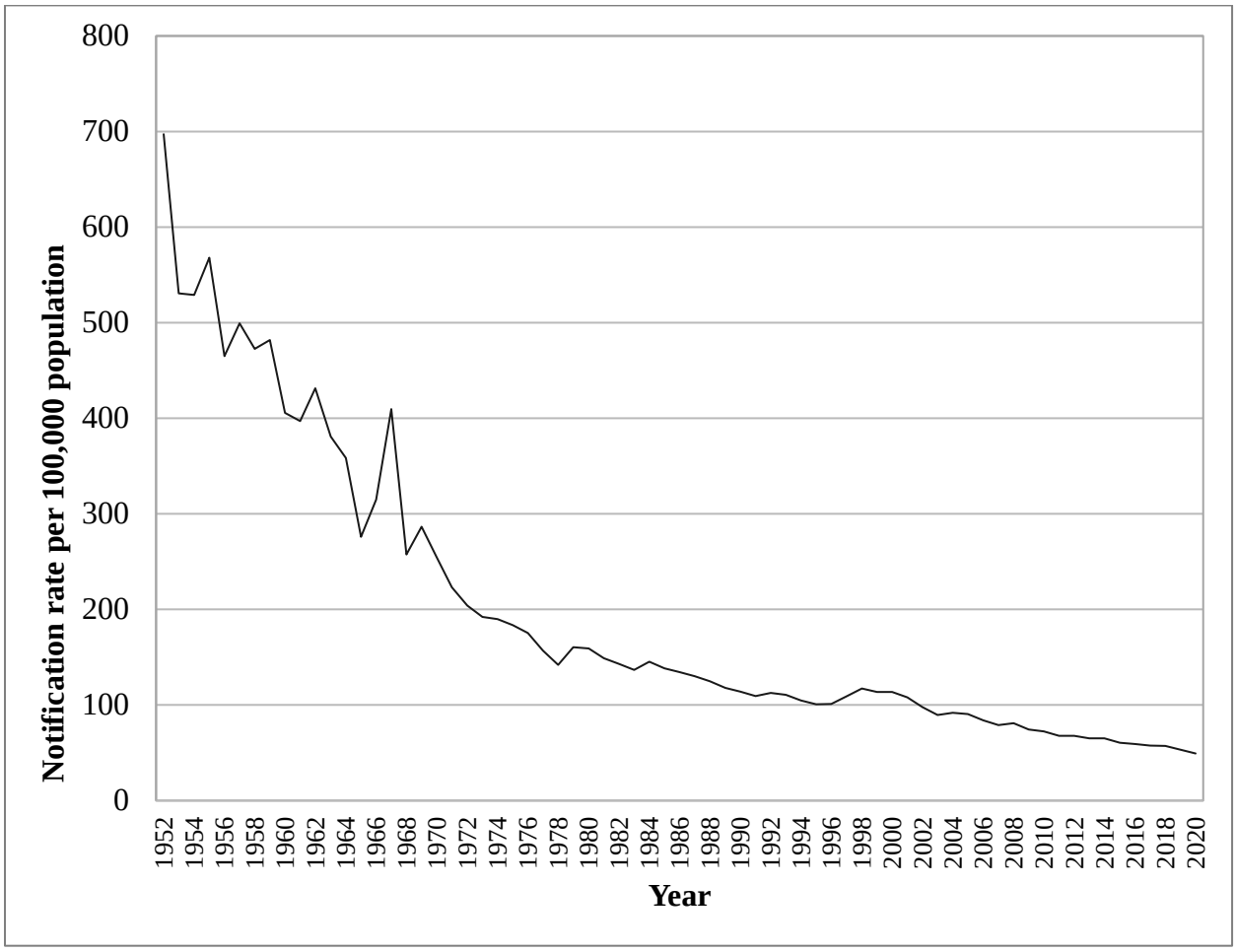

Figure 1. 2: Notification rate trend of tuberculosis in Hong Kong from 1952 to 2020. Source: Centre for Health Protection, Department of Health, 2021(21).

1.2 *M. tuberculosis* and its characteristics

1.2.1 Taxonomic characteristics

M. tuberculosis is the main cause of human TB, and it was discovered as the causative agent of TB in 1882 by Robert Koch (22). It is categorized under the class of Actinomycetes, order Actinomycetales, family Mycobacteriaceae and genus Mycobacterium (23). The genus mycobacterium is closely related to Corynebacterium and Nocardia. The name mycobacteria are meant fungus-like bacteria because they form pellicle-like structures when cultured in liquid media (24).

Under the genus mycobacteria, there are pathogenic and non-pathogenic species. Based on their growth, the species are also classified as slow-growing (needs more than 7 days) and fast-growing (needs less than 7 days) species (23, 25). Most of the fast-growing mycobacterial species are non-pathogenic and are isolated from soil and water (for example, *Mycobacterium smegmatis*). However, most of the slow-growing species are pathogenic. Currently, more than 170 mycobacterial species are available (26, 27). Among these, only a few are slow-growing such as *M. ulcerans* causes brulei ulcer which is considered as the 3rd most important disease of humans due to mycobacteria (28), *M. marinum* causes fish TB, *M. leprae* causes leprosy, *M. tuberculosis* causes human TB, and other TB causing species.

M. tuberculosis belongs to the member of *M. tuberculosis* complex (MTBC) which comprises *Mycobacterium africanum, Mycobacterium bovis, Mycobacterium mungi, M. tuberculosis, Mycobacterium microti, Mycobacterium pinnipedii, Mycobacterium caprae and Mycobacterium canettii.* These mycobacterial species have a similarity of 99.9% at the level of nucleotide and have an identical sequence of 16S rRNA (4, 29, 30). Among these species, *M. tuberculosis* is considered the most pathogenic and affects one-third of world people. It causes more than 95% of TB cases in humans (25, 31).

1.2.2 Growth characteristics of *M. tuberculosis*

M. tuberculosis is a rod-shaped, non-motile, non-capsulated, acid-fast because of its lipid-rich cell wall, non-spore-forming, aerobic or microaerophilic bacteria (7, 32). The bacteria have a length of 2-4µm and 0.2-0.5µm in width. It is a facultative intracellular parasite mostly of macrophages and grows slowly with its generation time of 15-20 hours which is too slow when compared with that of *Escherichia coli* which can double itself within 20min. *M. tuberculosis* grows on two commonly used media such as Lowenstein-Jensen (LJ) and Middlebrook's medium. To get visible colonies on these media, 4-6 weeks are required, and the colonies appear small, buff, irregular, granular, and rough on either of the medium as shown below

in **Figure 1.3** (31). When the smear of the colonies is stained with Ziehl-Neelsen staining and observed under the microscope, they form a special chain of cells called serpentine cords (33).

Figure 1. 3: *Mycobacterium tuberculosis* colonies on Lowenstein-Jensen medium (34).

1.3 Transmission of tuberculosis and risk factors

Transmission of TB is commonly through inhalation of small droplets containing tubercle bacilli produced by the infected individual who developed active tuberculosis. The droplets are discharged when the TB patient is talking, sneezing, and coughing nearby healthy people (35, 36). This occurs mostly in places that are devoid of air circulation such as in public gathering areas, prisons, and crowded transportation. The droplet nuclei have a diameter of about 10µm and may contain from one to ten bacilli. The infective droplets can be stayed airborne for a long time and spread in the buildings or rooms. The transmission of the disease is highly determined by the size of the droplets and the dose of the bacilli required for the development of infection. The droplet nuclei that are bigger than 10µm are usually attached in the upper respiratory tract (35), and those droplets less than or equal to 10µm can avoid mucous and ciliary system action and produce the port in alveoli and bronchioles. Usually, about 5 to 200 inhaled bacilli are needed for infection to be successful even though a single bacillus can lead to the establishment of the disease (37). TB can also be transmitted through close contact with infected animals (38) and ingestion of infected raw milk (39).

People who have prolonged contact with individuals that developed active TB are at high risk of acquiring the disease. Individuals that are living in TB endemic areas,

high congregate settings, and health care workers who handle serious TB cases are also at high risk to get infected by the disease(40). An individual patient suffering from active TB can disseminate a huge number of mycobacterial bacilli that infect so many people. Fortunately, all people who inhaled the bacilli do not develop TB. However, certain factors such as much consumption of alcohol, co-infection with HIV, malnutrition, cancer, smoking, diabetes, COVID-19, and other immune compromising agents enhance the chance of developing active TB (18, 41, 42).

1.4 Clinical manifestation of tuberculosis

TB is usually manifested in the form of pulmonary TB which is active infection of the lungs with *M. tuberculosis*. If the disease is left untreated, more than 50% of the infected individuals die. The majority of pulmonary TB cases are caused by post-primary infection with *M. tuberculosis*. This means that after the primary infection has healed, the granulomas that were formed in that process still contain the bacteria which can survive there for many years (43). If the immune system of the infected individual is compromised because of some reason, the bacilli can be reactivated and cause the disease again. At this point, the bacteria actively destroy the tissue surrounding the granuloma and result in massive destruction to the tissue. The lung tissue is a sponge-like thin structure and it is filled with air in the alveoli, where the exchange of oxygen between air and blood takes place. The affected

tissue of the lung becomes hard and makes an exchange of oxygen difficult and leads to fibrosis. Then, the cells that make up the tissue of the lung become die which is called necrosis. This necrotic tissue has the tendency to tear and break down resulting in the formation of cavitation in the lung. In the cavitation, the TB bacilli live in the center and gradually wipe out the tissues at the edges. Cavitation can be observed using an x-ray machine during the diagnosis of pulmonary TB. One milliliter of sputum in single cavitation contains about one million *M. tuberculosis*. In addition to the destruction of healthy lung tissue by cavitation, the damage continues and eventually reaches a part of the airways. Here, the bacilli destroy the airway's wall and create a link to the outside which speeds up their transportation into the trachea. When the infected person coughs, the bacilli can be transmitted to other people and establish a new infection for the development of the disease (44).

Destruction of the lung tissues and airways results in inflammation that is why individuals with pulmonary TB cough a lot to remove the inflammation-causing particles. In the beginning, the patient has a dry and persistent cough which is often worse at night. Such symptoms are observed in 85% of people with pulmonary TB. As the destruction of the tissue becomes worse, the coughed-up sputum starts to contain bloodstains. After the bacilli reach the airway from initial cavitation, they

can disseminate to other parts of the lungs by traveling up and down to find new places and form new cavitation. This is known as a bronchogenic spread. If the bacilli get access to the blood vessels, they can disseminate all over the lungs and other parts of the body forming disseminated TB or miliary TB which usually occurred when the immune system of the patient is compromised by HIV (44).

The infected individuals that developed an active form of the disease commonly show chest pain, fever, sweating, hemoptysis, coughing, and weight loss. In the case of tuberculous meningitis, the patient develops a headache, neck stiffness, and photophobia. The clinical signs observed when the disease affects other sites of the body usually depend on the affected parts (42, 45). In those people that have a strong immune system, the symptoms of the disease are not observed, and the infection develops to latent tuberculosis (LTB).

LTB is defined as the control of non-multiplying alive *M. tuberculosis* by the immune system of the infected individual without the manifestation of the symptoms of the disease (46). Most of the infection (90%) by *M. tuberculosis* leads to LTB. Currently, it is estimated that the prevalence of LTB is 23% (47). Individuals with LTB infection have *M. tuberculosis* inside their body but they do not have TB disease and, thus cannot transmit the disease to others. LTB infection

starts its process when the bacilli are engulfed by the macrophages and presented to other immune cells. This will initiate the immune cells and lead to the formation of a protective shelter called a granuloma. It is at this step that the LTB infection has been established. LTB can be diagnosed using an interferon-gamma release assay (IGRA) and tuberculin skin test (TST) (48). It takes 2 to 8 weeks after infection for the immune system to respond to tuberculin. The same time is taken for the infection to be diagnosed by TST. The TST is conducted by injecting purified protein derivatives (PPD) intra-dermally under the skin of the forearm and monitoring the induration size within 2-3days post-injection. If the size of induration is greater than 5mm, it indicates positive results (49, 50). The weakness of this test is it indicates similar results to infection with non-tuberculous mycobacteria and *M. bovis* making the prediction of recent TB infection difficult particularly in those individuals vaccinated with BCG (48). Interferon-gamma release assay (IGRA) is commercially available as T-spot or QuantiFERON TB which detects interferon-gamma released from T-cells presented with *M. tuberculosis*-specific antigens such as early secretory antigen target-6 (ESAT-6) and culture filtrate-protein-10 (CFP-10). Similar to TST, IGRA is not appropriate to test and predict a recent infection of TB (51).

1.5 Tuberculous meningitis

Tuberculous meningitis (TBM) is an inflammation of meningeal layers surrounding the central nervous system caused by infection with *M. tuberculosis* strains (52). Even though the main cause of TB in the CNS is *M. tuberculosis*, it can also be caused by non-tuberculous mycobacterium like *M. avium intracellularae*, particularly in patients with HIV(human immunodeficiency virus) (53). TBM is the most dangerous form of extrapulmonary TB and frequently occurred form of TB in the CNS (54). Every year, about 100,000 new TB cases which account for 1% of all TB cases, are TBM globally (18). The mortality rate of the disease is about 50% if the patient is co-infected with HIV, and it can also be 100% fatal if the patient has been infected with multi-drug resistant TB and left untreated (55, 56). Young children with primary TB infection and patients co-infected with HIV are at high risk of developing the TBM (57).

Similar to other forms of TB, primary infection with *M. tuberculosis* occurs in the lungs before the establishment of the disease in the CNS. From this initial site, the pathogens spread to the local lymph nodes leading to the development of miliary TB and followed by the migration of the bacilli to the brain via blood circulation. Then, the bacilli lodge themselves in the meninges, brain parenchyma, and adjacent tissues, creating small subpial or subependymal foci which are commonly known

as Rich's foci. The rupture of the Rich foci results in the dissemination of *M. tuberculosis* bacilli into cerebrospinal fluid in the subarachnoid space and initiates the infiltration of innate immune cells to the site and causes severe inflammation. Finally, it ends up with the development of the symptoms of TBM (58, 59).

1.5.1 Clinical signs and symptoms of tuberculous meningitis

TBM can present itself as the sole signs and symptoms of TB or simultaneously with other extrapulmonary and pulmonary infections (60, 61). It is commonly manifested by non-specific early signs that slowly lead to more noticeable symptoms such as fever, headache, vomiting, and stiffness of the neck. In children, it is usually presented with nausea, vomiting, and seizures. However, headache is less frequently observed in children (62). If the disease is left untreated, the symptoms become more dominant and consciousness falls (63). In more advanced cases, TBM is manifested as encephalitis (the increased volume of CSF in the space of the sub-ventricle) (62) and hyponatremia (lower level of sodium in the blood or an increase of sodium concentration in the plasma as a result of abnormal anti-diuretic hormone levels) (64).

1.5.2 Diagnosis of tuberculous meningitis

Diagnosis of TBM is still challenging despite several advanced new laboratory diagnostic tools being available (65). Detection of encephalitis needs more

advanced technologies like MRI (magnetic-resonance-imaging) and CT-Scan (computed tomography). The clinical symptoms of TBM are not specific and it shows similar features as that of cryptococcus meningitis and viral encephalitis. Therefore, the diagnosis that is only made based on clinical symptoms is not helpful to differentiate the disease. Before treatment, only 10% of all TBM cases are microbiologically confirmed and about 25% of them were confirmed using nucleic acid amplification tests. Even though it is not specific, the hematological and biochemical markers are important in collaboration with other findings such as increased content of protein (> 100mg/dl), 50% of CSF to plasma glucose ratio, and reduced white blood cells count in CSF with most proportion (>90%) is neutrophils (66). Although there is a problem of variability of reading of the results between the users, radiological findings are also useful.

1.5.3 Immune response to tuberculosis in the CNS

The main CNS cells infected with *M. tuberculosis* in cerebral parenchyma are microglia. Other cells like astrocytes and neurons are also involved in the process of the infection (67, 68). The pathogen is first detected by microglial cells through innate immune and neuron-specific receptors such as pattern recognition receptors. Among the pattern recognition receptors, toll-like receptors are very important in innate immunity. The process of *M. tuberculosis* internalization by microglial cells

is highly dependent on CD14 (cluster of differentiation 14) (a monocyte or macrophage differentiation antigen), which binds to lipopolysaccharide using toll-like receptor 4 (69). Like alveolar macrophage, microglial activation results in secretion of different cytokines such as IL-6, IFN-γ, IL-1β, TNF-α, CCL-5, CCL-2, CXCL-10, IL-1α and IL-12P40 (**Figure 1.4**) (70). Tumor necrosis factor-alpha (TNF-α) is generated by immune cells including infiltrating cells and non-immune cells of the CNS, and it plays a vital role in protecting against brain infection with *M. tuberculosis* (71).

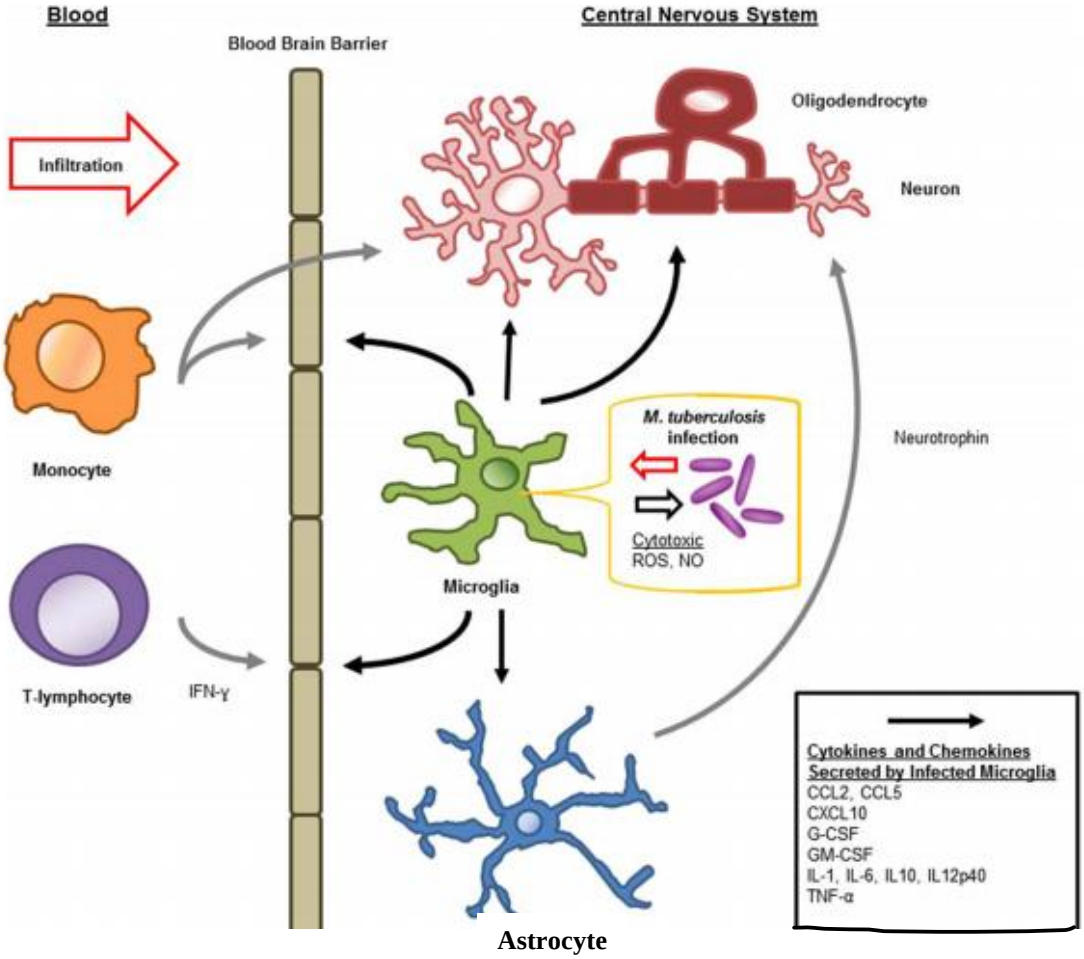

Figure 1. 4: Graphic presentation of microglial immune responses and interactions during infection with *Mycobacterium tuberculosis* in the CNS. Source (72).

1.6. Pathogenesis and survival strategies of *M. tuberculosis* in the host

Following the entrance of *M. tuberculosis* into the body of the host, the immune system can respond and destroy tubercle bacilli during the infection. However, *M. tuberculosis* has designed its survival strategies to react to the response of the host immune system and survive even multiply in the hostile environment established by the immune cells, particularly in the phagosome of macrophages (73). If the strategies used by *M. tuberculosis* are successful, the host becomes affected and develops the disease. Therefore, the pathogenesis of *M. tuberculosis* can be defined as the process by which the pathogen infects the host and causes the disease (4). *M. tuberculosis* uses different strategies and systems to defend the action of the host immune system and results in the development of TB.

1.6.1 Appropriate immune cell selection for initial infection

One of the strategies used by *M. tuberculosis* to escape from the action of the host immune system is selecting immune cells that are unable to eliminate the bacilli from its initial infection. Among the immune cells, macrophages are professional phagocytes that can engulf and digest invading pathogens (74). These macrophages are of various types and live in different organs of the body with different names. For example, microglial cells in the central nervous system, alveolar macrophages in the lung, osteoclasts in the bones, Kupffer cells in the liver, and histocytes in connective tissue (75, 76). The alveolar macrophages cannot efficiently eliminate

M. tuberculosis bacilli in the lungs, whereas those macrophages residing in the liver can successfully remove the infection from the site (77). Thus, the mycobacteria prefer the weaker macrophages to be used as an initial host cell for infection to attack its host.

Infection with *M. tuberculosis* is started when the bacilli in the droplets are inhaled and transported to the alveolar macrophages (78). After the bacilli arrive at the lower part of the respiratory tract, they are engulfed by alveolar macrophages, dendritic cells, epithelial cells, and neutrophils (78, 79), and the process is called phagocytosis which is the initial step for TB development in the host.

1.6.2 Living mechanism of *M. tuberculosis* inside the macrophages

The strategy that ensures the survival of *M. tuberculosis* in the macrophages is the way it arrests phagosome maturation and acidification in the immune cells. Once the bacillus is in the cytoplasm of the macrophage, it is forced to be placed inside the vesicle known as the phagosome. In the developmental processes of the phagosome, there are early and late markers. The appearance of the late marker on the phagosome facilitates the death of the pathogen in the macrophage. The early markers contain Rab5 and transferring whereas the late markers are Rab7 and lysosome-associated membrane glycoprotein 1. Under normal circumstances, at the

time of maturation of the phagosome, the early phagosome markers are excluded, and the late markers are acquired (80). The late phagosome and lysosome with lysosome-associated membrane protein initiate the release of many hydrolytic enzymes that are capable of killing the pathogen (80). When the phagosomes contain active *M. tuberculosis*, it is forced by the pathogen to retain the early markers. As a result, the phagosome cannot acquire the late markers (81, 82). *M. tuberculosis* inhibits this maturation process by producing glycolipids such as lipoarabinomannan (LAM), trehalose 6,6'-dimycolate (TDM) and sulphatides (83, 84). For example, the LAM (the trafficking toxin of *M. tuberculosis*) interferes with the production of phosphatidylinositol 3-phosphate (PI3P) pathways on the phagosomes by blocking the increase of cytosolic Ca^{+2}. This prevents late marker acquisition which leads to the inhibition of fusion of the phagosome with lysosome and ensures the residence of the bacilli in the infected macrophages for long period (83).

Maturation and acidification of the phagosome are also inhibited by the nature of the structural properties of *M. tuberculosis* and the composition of its mycelium. The pathogen protein which is ESAT 6 or CFP 10 and ATP1/2 (secretion ATPase1/2, secreted secA1/2 protein) decreases the PH in phagosome by inhibiting the availability of vacuolar ATP and GTP enzymes and impairs the ripening of

phagocyte. Tryptophan aspartate-rich coat protein, which is named coronin 1, is also recruited to phagosomes containing active bacilli but it is quickly released from phagosomes containing inactive mycobacterial bacilli (82). *M. tuberculosis* also inhibits lysosomal formation by intensifying the coronin 1 expression on the host phagocyte membrane (85, 86). Besides, interferon (IFN)-α hinders the maturation of phagosomes by triggering the synthesis of interleukin (IL)-10 in a STAT1-dependent manner. IL-10 declines extra IL-1β and hence overpowers the caspase1-dependent IL-1β maturation of pleural fluid mononuclear cells (87).

The phosphatidylinositol 3-phosphate (PI3P) is the macrophages' cell membrane component on the phagosome and surface of the early endosome (88). Following the infection with *M. tuberculosis*, lower biosynthesis of PI3P represses the fusion processes between lysosomes and phagosomes (89). The production of transcription factor NF-kB (nuclear factor kappa B), which is important for phagosome maturation and mycobacterial killing, is also suppressed following infection with pathogenic mycobacteria. Inhibition of NF-kappa B impairs the release of lysosomal enzymes to the phagosome. This reduces the killing of the engulfed *M. tuberculosis* (90). **Figure 1.5** indicates how *M. tuberculosis* inhibits the fusion of phagosome with lysosome and evades its host.

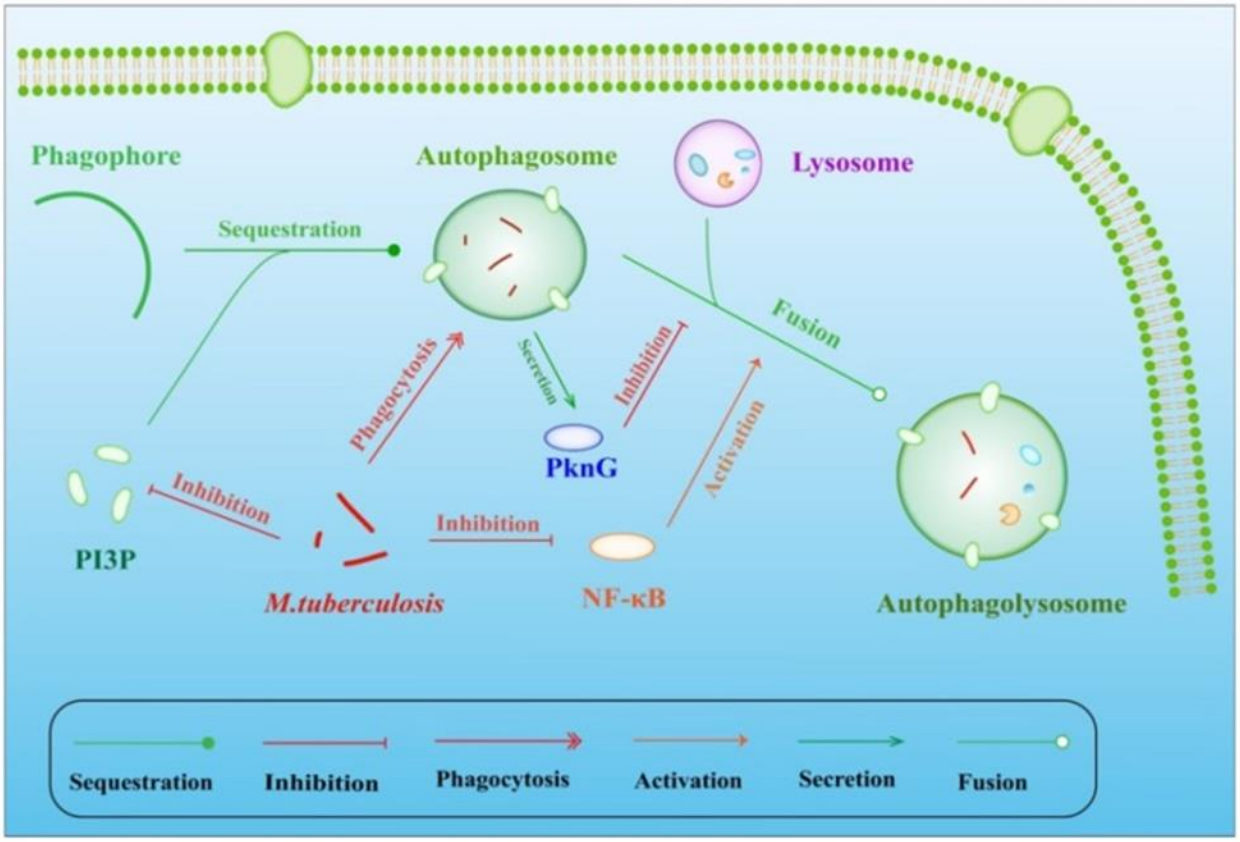

Figure 1. 5: *M. tuberculosis* evasion by inhibiting fusion of lysosomes with phagosomes.

Fusion of phagosomes with lysosomes is directly inhibited by the secretion of PknG (protein kinase G) produced by engulfed *M. tuberculosis.* Inhibition of NF-κB can also reduce the fusion. Phosphatidylinositol 3-phosphate (PI3P) is a vital component of the surface of the phagosome. Thus, higher hydrolysis and reduced biosynthesis of the PI3P also suppresses the fusion of phagosomes with lysosomes, facilitating the escaping route for *M. tuberculosis.* Source (88).

1.6.3 Developing resistance against nitrosative and oxidative stresses.

Inside the phagosome of the macrophage, the environment is too hostile due to the presence of excessive reactive oxygen and nitrogen species. Other bacterial species maintain their survival in the stresses using the redox-sensitive two-component systems (ArcAB) and transcription factors (FNR/SoxR) (91, 92). However, *M. tuberculosis* does not have these factors instead it designed strategies that facilitate its survival in the condition. It mitigates the pressure of this hostile condition by scavenging the radicals, inhibiting the production of the reactive radicals, and repairing the damaged DNA.

M. tuberculosis uses mainly its LAM to scavenge the reactive oxygen intermediates (ROIs) so that the bacterium is protected from the radicals (93). Other *M. tuberculosis* molecules such as phthiocol and mycothiol also scavenge the radicals and facilitate the way for the bacteria to resist the adverse conditions (94).

M. tuberculosis inhibits the synthesis of reactive oxygen intermediates in the macrophages using its sulphatides (86). The bacterium also produces powerful enzymes that neutralize the intracellular ROIs and reactive nitrogen intermediates (RNIs). These enzymes are catalase-peroxidase-peroxynitritase, dihydrolipoamide

dehydrogenase, alkyl hydroperoxide reductase (AhpC), and superoxide dismutase (94, 95). A recent study also showed that *M. tuberculosis* uses redox-sensitive transcription factors (WhiB3) to adapt to ROIs and RNIs stresses (96). It was also proved that *M. tuberculosis* has evolved a mechanism for DNA repairing mainly by base excision repair method to repair the damage of its DNA due to ROIs and RNIs (97, 98).

1.6.4 Management of scarcity of metal ions and nutrient

M. tuberculosis manages the scarcity of essential nutrients and metal ions in the phagosome of macrophages by using certain mechanisms. One of these is by changing the source of their carbon from carbohydrates to fatty acids (99). Like other living organisms, *M. tuberculosis* also needs metal ions as a co-factor for those enzymes that participate in critical cellular functions (100, 101). Since ferric ion (Fe+3) is poorly soluble at neutral PH and in the presence of oxygen, free iron (III) is not available in the mammalian host, but it is sequestered in complexes with iron-binding protein (102). Hence, to be successful in its infection, *M. tuberculosis* should have a mechanism to overcome the deficiency of iron ions caused by the host (103). This can be done by competing for metal ions with macrophage by using its divalent cation pump that works properly at the PH range of 5.5 to 6.5 (104) and ion-binding protein molecules including mycobactin and exochelins that play a role

in removing iron from ion-binding proteins (transferrin and lactoferrin) of the host (105-107).

1.6.5 Interference of the immune response of the infected individual by *M. tuberculosis*

Interfering the host immune response is also used by *M. tuberculosis* to survive inside the infected host. The host immune response is regulated by the components of the pathogen and the cytokines triggered by the pathogen. TNF-α is one of the pro-inflammatory cytokines used as a mediator to trigger cell-mediated immunity (CMI) to wipe out intracellular *M. tuberculosis* and protects the host (108, 109). However, this process is immediately inhibited by different mycobacterial components such as phenolic glycolipid (PGL), trehalose 6,6'-dimycolate (TDM), and 2,3,6,6' tetra acyl trehalose 2'-sulfate (SL) so that the generation of TNF-α from macrophage containing the pathogen is suppressed (110, 111). *M. tuberculosis* can also trigger cytokines such as transforming growth factor-beta and interleukin 10 (IL-10) to suppress the immune response of the host (112, 113). For instance, the LAM of *M. tuberculosis* is trimmed off from its cell wall and binds with dendritic cell-specific intercellular adhesion molecular-3 grasping non-integrin (DC-SIGN) to initiate the synthesis of IL-10. IL-10 is a common disabling cytokine that prevents different responses of the immune systems like the

generation of pro-inflammatory cytokines (TNF-α, IL-12), stimulation and proliferation of T-cell, and MHC class II molecules expression on dendritic cells (114, 115).

1.6.6 Tuberculous granuloma formation

Granuloma is a well-organized, compact, and nodular structure composed of aggregates of immune cells such as macrophages and epithelioid cells (modified form of macrophages), giant cells, and foamy macrophages surrounded by lymphocytes (**Figure 1.6**). It is considered as the characteristic feature that occurred in the *M. tuberculosis*-infected individuals and hence located in the center of the immunopathogenesis of tuberculosis (43, 116, 117). Granuloma is the result of complex processes. Once the tubercle bacillus is inhaled and transported into the lower respiratory tract crossing the lung epithelium, it is engulfed by either alveolar macrophage or dendritic cells. This infection leads to secretion of different cytokines (IL-1β and IL-α, IL-6 and IL-12), chemokines, lipoxins that may induce necrosis and contribute to immune protection, and prostaglandins that may provoke apoptosis (48).

Because of the influence of Il-12 and chemokines, the infected dendritic cells travel to the surrounding lymph nodes to initiate T-helper 1 (Th1) cells differentiation. Then, Th1 cells secrete interferon-gamma (IFN-γ) at the infection site and activate macrophages and dendritic cells to produce additional cytokines and antimicrobial factors that participate in the control of TB bacillus at the site (48). Finally, this process ends up with granuloma that becomes a protective shelter for *M. tuberculosis* and slows down its reproduction, and facilitates its latent infection.

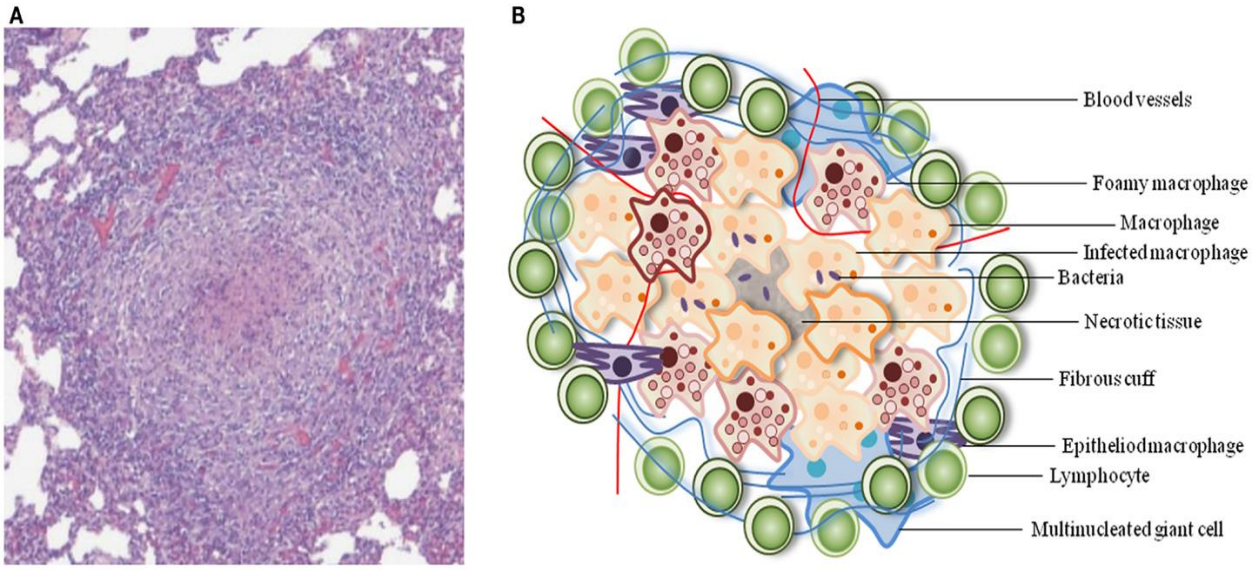

Figure 1. 6: Representative architecture of a TB granuloma. **(A)** Typical granuloma containing necrosis at the center from lung tissue of minipig. Histological samples were fixed with formalin, sectioned and stained with hematoxylin-eosin (118). **(B)** Graphic of the cellular components of a TB granuloma (116).

1.7 Virulence-associated factors of mycobacterium

Virulence is defined as the ability of a pathogen to infect its host and lead to the establishment of disease (119). It is used to distinguish pathogens from non-pathogens that are thought to be virulent and avirulent, respectively (120). *M. tuberculosis* complex members use different virulence factors that directly or indirectly strengthen their ability to respond against the immune response of an infected individual. These factors include cell wall, molecules, secretion systems, genes, and proteins.

1.7.1 Cell wall

The cell wall of *M. tuberculosis* is a remarkable structure that maintains the shape and integrity of the cell and thus it is important for the intracellular growth and survival of the pathogen (121). The cell wall is less permeable to several antibiotics and it supports the mycobacteria to survive in a harsh environment in the phagosome of the macrophages (122). It is made up of two layers which include the outer and the inner parts (**Figure 1.7**). The outer layer contains proteins and short and long lipids that are connected to a long chain of C_{60}-C_{90} mycolic acid (123). The lipomannan, transporter proteins, LAM, dimycolyl trehalose (cord factor), phosphatidylinositol mannosides and phthiocerol dimycocerosate containing lipids are distributed within the outer layer and remain connected to the mycolic acid (122). The inner layer of the cell wall is composed of mycolic acid

which is covalently linked to arabinogalactan (AG). The AG in turn attached to peptidoglycan (PG) creating mycolyl-arabinogalactan-peptidoglycan compound (124) and this complex serves as a pillar of the cell envelope and is highly important for *M. tuberculosis* in its survival, virulence, growth, and resistance to antibiotics (125).

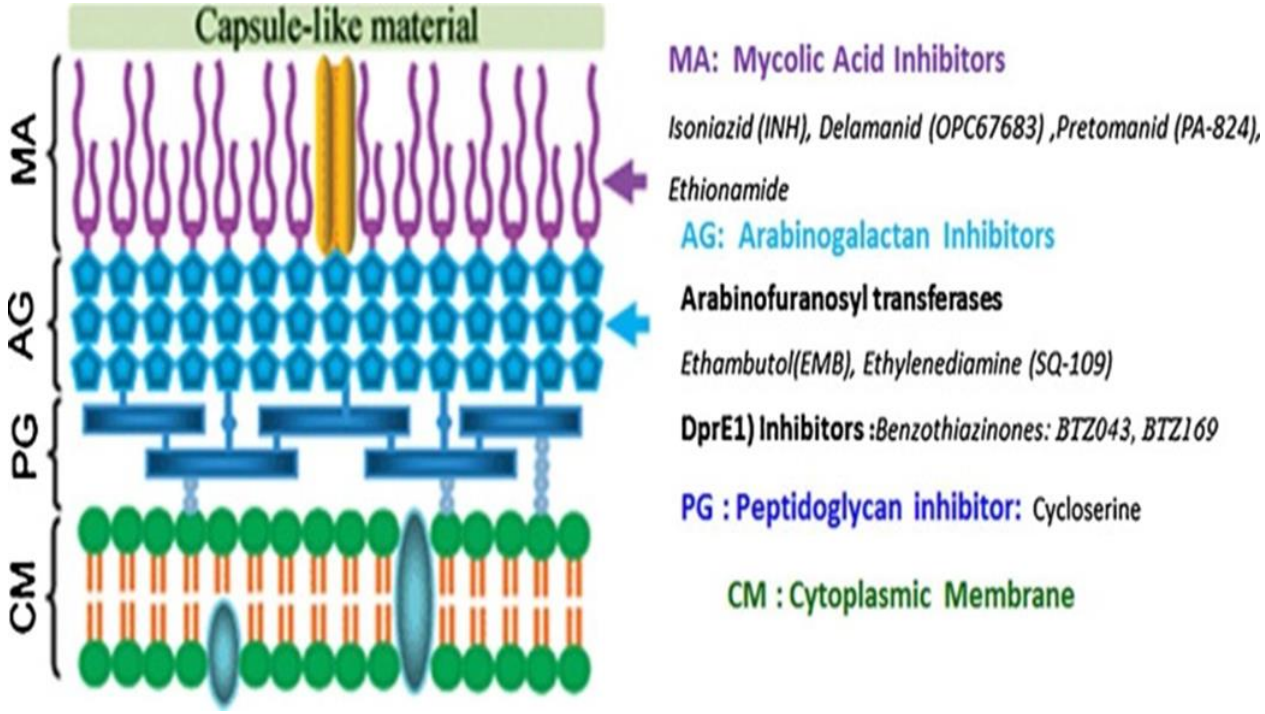

Figure 1. 7: Indicates the architecture of mycobacterial cell envelope and drug inhibitors (126).

More than sixty percent of the cell wall of mycobacteria is made up of lipid (34, 127). The lipid portion in the mycobacterial cell wall is composed of three main elements including cord factor, wax D, and mycolic acid. Among the three lipids, mycolic acid is exceptional alpha-branched lipid in the mycobacterial cell wall and accounts for 50% of the dry weight of the cell envelope of mycobacterium. It is a strong hydrophobic molecule surrounding the pathogen and affects the cell surface permeability. It is considered as the major determinant of virulence in *M. tuberculosis*. Because it provides protection for *M. tuberculosis* against the attack of lysozyme, cationic protein, and reactive oxygen radicals in the granule of phagocytes. It also protects extracellular mycobacteria from complement accumulation in serum (34).

The Wax-D lipid is the main element of Freund's complete adjuvant and contributes to the impermeability of the bacterial cell wall to dyes and staining. It gives the pathogen resistance to antibiotics and alkaline and acidic compounds. It also enables the bacteria to resist lethal oxidations, osmotic lysis via complement deposition, and ensures the survival of the bacteria inside the macrophages. Another element of the lipid part of the cell wall is the cord factor that plays a role in the formation of serpentine cords when the bacilli are stained with Ziehl-Neelsen staining. The cord factor is highly toxic to mammalian cells and inhibits the

migration of polymorphonuclear leukocytes. It is the most sufficiently produced lipid in virulent *M. tuberculosis* strains (34, 127).

1.7.2 Molecules

Some molecules are used by *M. tuberculosis* to inhabit its host at the level of the cell. One of these molecules is the secretory factor which is a key component of the armory of the bacteria that support it to pass the obstacles created by adaptive and innate immune responses produced in the host body. The second molecule is a membrane-associated component that assists the bacterium to adhere to and evade the host cells. The third molecule is the cytosolic factor which assists the pathogen to undergo rapid morphological, adaptive, physiological, and metabolic changes (119).

1.7.3 ESX secretion system

The pathogenicity of the bacteria is dependent on its capacity to produce virulence factors on the cell surfaces of the pathogen (128). Evidence indicated that *M. tuberculosis* has developed a novel and sophisticated type-VII secretion system encoded within five genomic-like loci (ESX1-5) to export a set of effector proteins that supports the pathogen to evade the immune response of the host. Among the

systems, ESX-1 and ESX-5 are engaged in virulence and they contribute to cell to cell migration of pathogenic mycobacteria (129).

ESX-1 system is the most characterized system of secretion. The ESX-1 secretion apparatus is a complex of protein with ATPase and transmembrane domains, encoded within eccA to eccE genes. Some proteins are synthesized through the ESX-1 system and encoded within the ESX-1 locus. These proteins are ESAT-6 and CFP-10. They are immune dominant antigens. ESAT-6 does not have any signal sequence for secretion. However, the CFP-10 consists of the C-terminal signal sequence and forms a heterodimer with the ESAT-6. The *Mycobacterium bovis* BCG vaccine strain has a deletion within the ESX-1 locus (region of difference-1). The attenuated virulence of the vaccine strain could be partly associated with the defect of the ESX-1 secretion system (130).

The ESX-1 secretion system of mycobacterium mediates lysis of the host cell via contact-dependent membrane disruptions which are structurally different from that of other bacterial species (131). The secretion system is also used as a means for the pathogen to cross the blood-brain barrier (BBB) membrane and create an infection in the CNS (132). Another key function of ESX-1 is causing rapture of phagosome which leads to the release of the bacilli or its products into the cytosolic compartment of the phagocytes of the host (133).

1.7.4 HigBA-a toxin-antitoxin system

In *M. tuberculosis*, the genes that encode HigBA are included in the operon formed by the genes from Rv1954-Rv1957 (134). Rv1955 encodes for HigB (toxin), Rv1956 encodes for HigA (antitoxin) and Rv1957 for *SecB*-like chaperone. Altogether, they make a tripartite toxin-antitoxin-chaperone (TAC) system. The complex made by the HigB toxin and HigA antitoxin is stabilized by the chaperone (135). TAC complex makes auto represses of its own transcription, which is rescued by a protease-mediated degradation of higA antitoxin leading to the unbound of endoribonuclease higB toxin (136). This unbound HigB toxin cleaves the mRNAs and facilitates growth restriction and increases the survival time of the pathogen in stressful condition (134). The higBA locus is initiated in the situation of heat shock, DNA damage, growth, and hypoxia in activated macrophages (137). A study showed that the production of HigB toxin in the absence of HigA affects the growth and triggers cell death in *M. tuberculosis.* The HigB toxin also lowers the quantity of IdeR (for iron import) and Zur (for zinc import) regulated mRNAs and cleaves tmRNA in the pathogen (134). This shows that the importance of the HigBA toxin-antitoxin system for the survival of the pathogen under stress faced at the time of infection (137).

1.7.5 RD4

Regions of difference 4(RD4) include Rv1506c-1516c in *M. tuberculosis* H37Rv and participated in the synthesis of trehalose-containing glycolipids. But it is

lacking in *M. bovis* and *M. bovis* Bacille Calmette-Guerin (BCG) (138). It was indicated that there is an expanded RD4 (more than 40 genes) in *M. marinum* and participated in the biosynthesis of lipo-oligosaccharides (139). RD4 plays a great role in the virulence of mycobacteria and improves the potential of BCG strains (140). To assess its role in virulence, one study was done by introducing the entire genes (Rv1501 -1516c) and partial (Rv1501-1508c) RD4 into *M. bovis* BCG and *M. marinum* using mice and zebrafish infection model, respectively. The result showed that *M. marinum* holding the whole RD4 was more infectious than the wild-type strain. The BCG strains that contain the whole RD4 also showed better protection of zebrafish against *M. mariunum* (140).

1.7.6 Exported repetitive protein (Erp)

One of the extracellular proteins specific to the mycobacterial family is exported repetitive protein (Erp) (141). This protein plays a role in *M. tuberculosis* pathogenesis and other pathogenic mycobacterial species. The study conducted using the frog and zebrafish embryo model confirmed that Erp is also important for the growth and survival of *M. tuberculosis* in both in vivo and in vitro conditions (142). The protein performs its function in *M. tuberculosis* by interacting with another protein called Rv2212 which is an adenylyl cyclase and producing cyclic

AMP (cAMP). This cAMP is a second messenger that regulates the intracellular survival of *M. tuberculosis* (143).

1.7.7 Proline proline glutamic acid/Proline glutamic acid (PPE/ PE)

PPE/PE are proteins that are exclusively found in mycobacteria and contribute to the enhancement of mycobacterial virulence and survival in the host. It accounts for about 10% of the genome encoding capability of *M. tuberculosis* (144, 145). These proteins are characterized by the conserved PPE and PE domains at N-termini such as 69 PPE genes and 99 PE genes in *M. tuberculosis* H37Rv strains. They are important for facilitating the way for the pathogen to escape from the attack of the immune system (146). The genes of PE/PPE are relatively fewer in non-pathogenic mycobacteria. The proteins are highly polymorphic and selectively available at the time of infection, and they are secreted by the type-VII ESX secretion system. For example, ESX-1 is important for the PPE68 secretion in *M. marinum* (146), and ESX-3 secrets PE15-PPE20 and PE5-PPE4 (147).

1.7.8 Sigma factors

Sigma factors are also virulence factors that *M. tuberculosis* uses to adapt and survive in a hostile environment. For the effectiveness of the survival process, proper regulation of gene expression is crucial. In the genome of *M. tuberculosis*, there are certain sigma factors important for the regulation of gene expression (148).

For example, Sigma factor A (Sig A) is a constitutively expressed factor used for transcription regulation of various housekeeping genes in *M. tuberculosis* and it is also important for the growth of the bacterium in both in vivo and in-vitro conditions. It was identified that the enhanced expression of the mRNA of SigA increased the intracellular growth of the hypervirulent *M. tuberculosis* strain TB294 in the macrophage. This is partly linked to the gene functionally found downstream to the SigA called enhanced intracellular survival (*eis*) gene (149, 150).

Sigma factor B is also important for mycobacterial survival. It is initiated when *M. tuberculosis* is in stress conditions like exposure to heat shock, sodium dodecyl sulfate, and low aeration (151). Another sigma factor is SigC which is important in the survival and pathogenesis of mycobacterium within the granuloma. For example, the SigC mutant produced smaller and fewer spleen and lung granulomas compared to the parental *M. tuberculosis* H37Rv. In the strain of CDC1551 *M. tuberculosis* background, the SigC mutation considerably decreased the reproduction of the mycobacterial bacilli in the lungs of infected guinea pigs (152). It also regulates the expression of many important virulence-related factors such as crystallin homolog *hspX*, a two-component response regulator *mtrAr*, and a two-component sensor kinase *senX3* as reviewed by Forrellad and his colleagues (25).

1.7.9 PhoPR

The PhopR is one of the functional two-component systems that are highly conserved signal transduction pathways in prokaryotes (153). PhopR (rv0757-rv0758) is considered as a virulence regulating factor in *M. tuberculosis*. It consists of a histidine kinase (PhoR) which is used as a sensor and PhoP (a response regulator) as the effector. The PhoR is often associated with a membrane and used for detecting extracellular stimuli. Once it detects the signal, it autophosphorylates itself and transfers its phosphate to the PhoP (response regulator). Then, the PhoP changes its conformation and regulates gene expression through DNA binding (153, 154). **Figure 1.8** describes how *M. tuberculosis* that contains a functional PhoR can sense its cognate stimulus and subsequently phosphorylate PhoP (153). The post-translational stimulation of the PhoP leads to the activation of transcription of at least 30 genes (155). It coordinates various types of functions in the virulence and persistence of *M. tuberculosis* (156, 157). The results of integrated proteomic and transcriptomic laboratory analysis indicated that PhoP regulates different vital processes such as metabolism of respiratory, major T-cell antigen ESAT-6 secretion, stress response, generation of pathogenic lipids, response to hypoxia via dormancy survival regulator (DosR) cross-talking, and persistence of *M. tuberculosis* through transcriptional regulation of isocitrate lyase (**Figure 1.9**) (158). The same study demonstrated that *M. tuberculosis phoP* mutant SO2 shows an antigenic capability that is similar to that of the BCG vaccine. It was also

indicated that the mutation in the *phoP* gene results in the avirulence of *M. tuberculosis*. For example, the attenuation of H37Ra has occurred as a result of the amino acid change from serine to leucine. This happened through a strategy that negatively affects the secretion of the major T-cell antigen ESAT-6 (159, 160). On the other hand, the mutation that happened in a promoter associated with elevated expression of *phoP* was observed in the outbreak of *M. bovis* strains (161).

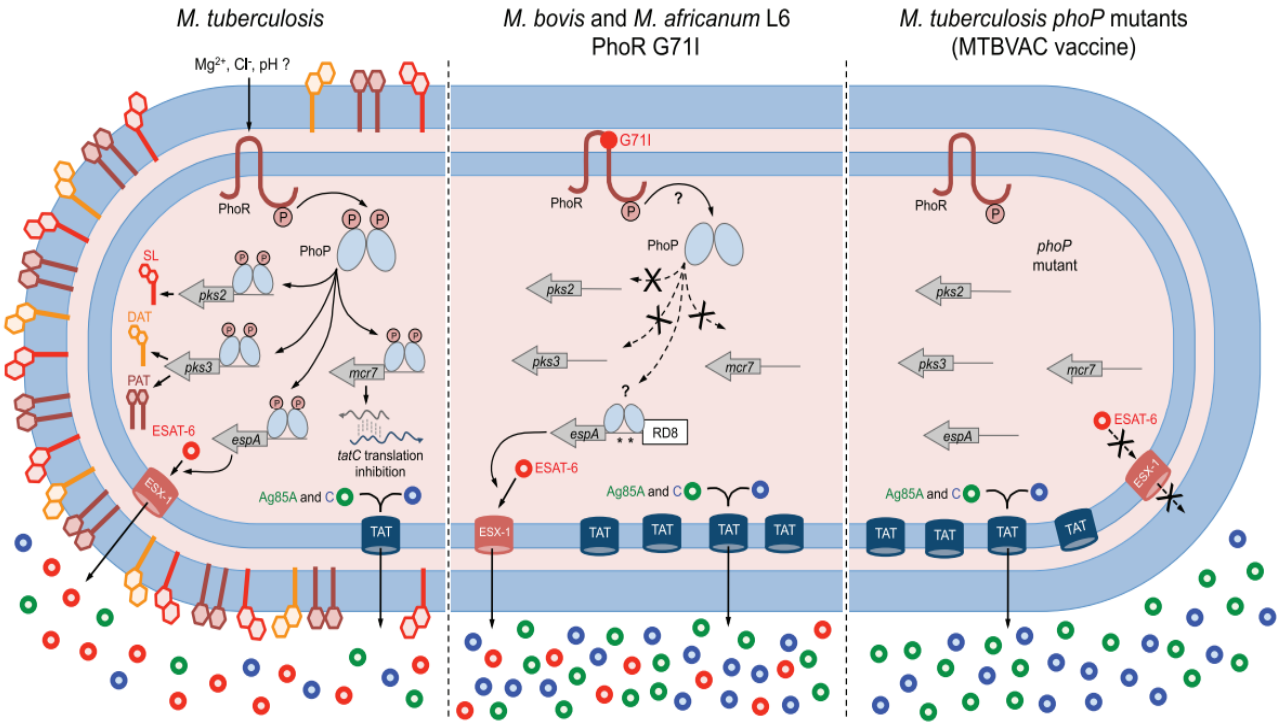

Figure 1. 8: Comparative illustration of PhoPR-regulated phenotypes in *M. bovis*, *M. africanum* L6, *M. tuberculosis phoP* mutant, and *M. tuberculosis*. Source (153).

The details in **figure 1.8** are summarized as follows: *M. tuberculosis* can sense extracellular stimuli through its PhoR and then phosphorylate PhoP. The phosphorylated PhoP regulates biosynthesis of sulfolipid (SL), diacyltrehalose (DAT) and polyacyltrehalose (PAT) via *pks2* and *pks3* genes, ESAT-6 secretion through *espA*, and post-transcription of *tatC* via *mcr7* non-coding RNA. The *M. africanum* L6 and *M. bovis*, containing malfunctioning PhoR G71I allele, are supposed to have deficiencies in phosphorylation of PhoP. As a result, the strains lack biosynthesis of DAT, SL, and PAT. But the secretion of ESAT-6 is restored in the strains by compensatory mutations such as RD8 deletion and species-specific polymorphisms (asterisks

in the figure) in the espACD promotor region. On the other hand, *M. tuberculosis* PhoP mutants lack the above-mentioned phenotypes regulated by PhoP, and this leads to the absence of DAT, SL, and PAT biosynthesis or secretion of ESAT-6 in the PhoP mutant strains. They also have a decontrolled twin-arginine translation (TAT) system and as a result, secrete more TAT substrates such as antigens Ag85A and Ag85C. Subsequently, sufficiently attenuated *M. tuberculosis* PhoP-based vaccine strains (MTBVAC), are supposed to stimulate better and long-lasting immunogenicity relative to that of BCG in clinical trials (153).

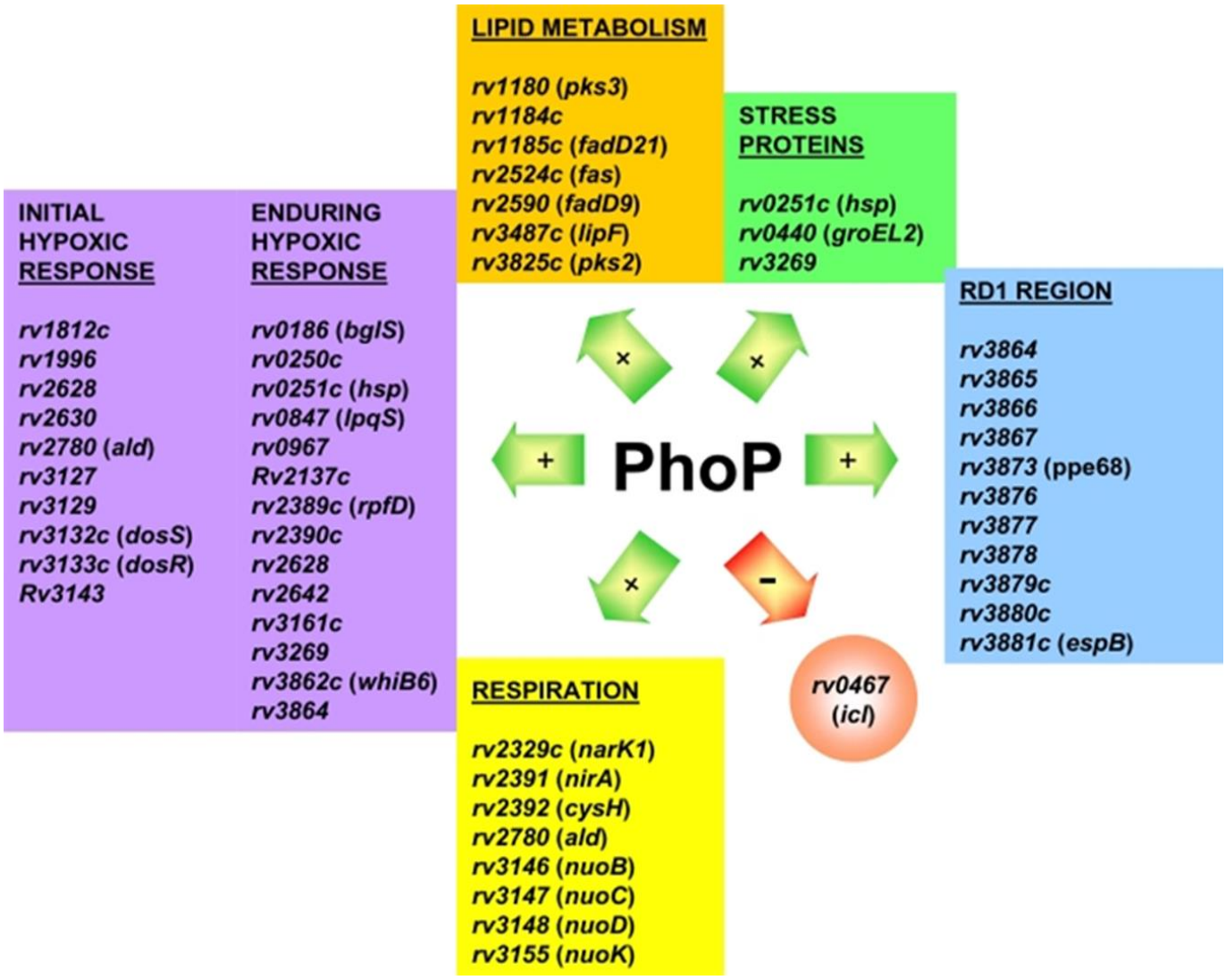

Figure 1. 9: "The *M. tuberculosis* PhoP regulon. The PhoP regulon was identified by comparing transcriptional profiles of the *M. tuberculosis* wild-type and the PhoP mutant using DNA microarrays. Some of the more related genes to virulence and intracellular survival are listed and grouped by function. Red and green arrows indicate genes whose expression is negatively or positively regulated by PhoP, respectively" (158).

1.8 Our previous works on hypervirulent *M. tuberculosis* strains

Infection with *M. tuberculosis* manifests itself in the range of asymptomatic (latent) to the severe and life-threatening form of tuberculosis (TBM). The causes of the differences in disease spectrum among TB patients had not been identified for a long time. Our study is one of the pioneer studies that tried to identify whether the cause of the differences is associated with the genetic diversity between the strains of *M. tuberculosis.* The first study was the study done on the molecular characterization of 125 clinical isolates of *M. tuberculosis* collected from Shanghai and Hong Kong over two years. The number of strains collected from pulmonary and extrapulmonary was almost proportional. The strains of extrapulmonary were collected from urine, cerebrospinal fluid, stool, biopsy specimen, wound, and others. The IS6110 typing analysis of the 125 strains identified more than 100 different patterns, indicating the presence of genetic diversity among the strains, and 71 of the strains belonged to the Beijing family (162). The study also measured the intracellular growth of the strains using human macrophages. After incubating all the strains for 10 days, three strains showed significantly increased intracellular growth, but the other strains including *M. tuberculosis* H37Ra did not show intracellular survival. The growth of the three strains and *M. tuberculosis* H37Rv strain was increased by 2 to 4-fold in their colony-forming unit showing the differences in virulence among the strains (162). Because of this, the three strains were named hypervirulent *M. tuberculosis* strains. When the background of the

hypervirulent strains was investigated, they were isolated from TBM patients. Among the clinical isolates, the H112 strain of *M. tuberculosis* showed the intracellular growth of 3 to 4 folds higher than the other clinical isolates including the *M. tuberculosis* H37Rv (162). The hypervirulent H112 strain also stimulated a lower level of TNF-α in infected macrophages whereas the other strains induced an excess amount of TNF-α in the macrophages. It was believed that the strategies used by the H112 strain to escape from the immune response of the host could be a possible means for its increased growth and survival in the macrophages and the establishment of the severe form of tuberculosis.

Later on, our group selected the hypervirulent *M. tuberculosis* H112 strain and conducted further research to determine the genetic determinants of the enhanced virulence in the strain. They reassessed and compared the intracellular growth of the H112 strain with that of low virulent strain (H54) which belongs to the same phylogenetic lineage of H112, and virulent reference strain H37Rv using macrophages. Subsequently, it was observed that H112 demonstrated significantly higher intracellular survivability and rapid growth than the H37Rv and H54 strains. Using whole-genome sequencing, the study also found genetic mutations in the H112 strain which are lacking in the H54 strain. In the H112 strain, seventeen genetic mutations (12 single nucleotide polymorphisms (SNPs) (**Table 1.1**) and five structural variations (SVs) (**Table 1.2**) were identified and these mutations

were also found common to the hypervirulent strains of *M. tuberculosis* previously identified from Hong Kong and other parts of the world (163).

The effects of the identified mutations on neighboring genes that encode for virulence-associated transcriptional regulators such as *phoP* and *higB* genes were also confirmed (163). One of the mutations occurred due to 2 base pair (bp) deletion in the intergenic region *rv0759c-rv0760c* of H112 genome downstream to the virulence-associated PhoPR operon as indicated in **Figure 1.10.** As a result of the mutation, the *phoP* gene expression was differentially increased in the hypervirulent *M. tuberculosis* H112 strain.

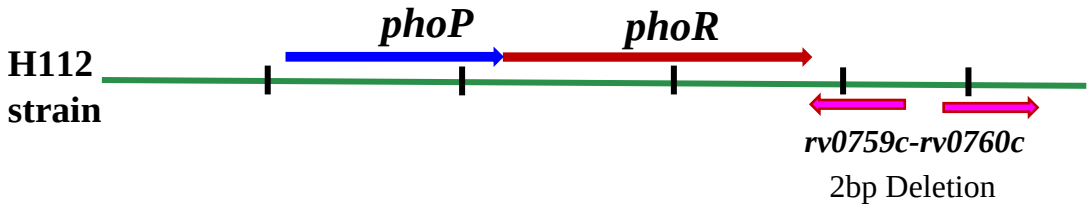

Figure 1.10: The location of mutation that occurred in the genome of the H112 strain and resulted in differential expression of the phoP gene. The mutation was present between the rv0759c and rv0760c.

Table 1.1: Single nucleotide polymorphisms common to H112-clade.

Position (NC_000962.3)	**Nucleotide change**	**Gene**	**Type**	**Amino acid change**	**SIFT prediction**
209387	T>G	*rv0178*	Non-synonymous	D150E	Deleterious
3865243	G>T	*eccC4*	Non-synonymous	A999D	Tolerated
3012950	G>T	*rv2696c*	Non-synonymous	A220E	Tolerated
249350	G>A	*rv0209*	Non-synonymous	A105T	Tolerated
3785898	G>A	*rv3371*	Non-synonymous	A323T	Tolerated
2201808	C>G	*higB*	Non-synonymous	D30E	Tolerated
3301648	T>G	*fadD29*	Non-synonymous	M270L	Tolerated
1622580	C>A	*rv1443c*	Non-synonymous	R38L	Tolerated
3569220	G>A	*uvrD2*	Synonymous	A664A	Tolerated
752134	C>T	*mkl*	Synonymous	206I	Tolerated
3476350	G>A	*agpS*	Synonymous	S204S	Tolerated
295746	C> T	*fadE5-rv0245*	Intergenic	-	-

Source (163). (SIFT: Sorting Intolerant from Tolerant).

Table 1.2 : Structural variation common to H112-clade.

Start (NC_000962.3)	End (NC_000962.3)	Size (bp)	Type	Annotation
730085	730094	9	Deletion	The deletion was within coding
854259	854261	2	Deletion	Intergenic:*rv0759c-rv0760c*. The deletion was present near *phoP*.
937115	937115	1,358	Insertion	The insertion was within coding sequence proline immunopeptidase (*pip).* This insertion event was mediated by *IS6110* element. *Pip* belongs to the intermediary metabolism and respiration functional category.
2431514	2431515	1	Deletion	Intergenic:*rv2168c-rv2169c*
2559504	2559504	1,358	Insertion	The insertion is within *rv2286c* which encodes a conserved hypothetical protein. This insertion was mediated by *IS6110* element.

Source (163).

In an evolutionary context, the *phoP* gene in the H112 and H37Rv is similar in their genetic sequence. However, the *phoP* gene in H112 showed differentially increased expression due to the mutation that occurred at around 400 bp downstream to the operon PhoPR (163). In the *phoP* gene in the H37Ra strain, the mutation occurred at Ser219Leu and resulted in the down-regulation of the gene expression and contributed to the avirulence of the *M. tuberculosis* H37Ra strain (160).

The differentially increased expression of the *phoP* gene in the H112 strain resulted in the strong repression of at least 14 genes' products controlled by the PhoP including pks2, and pks3 which are important for the biosynthesis of sulfolipids and polyacyltrehalose lipids. Loss of the biosynthesis of sulfolipid facilitates the growth of *M. tuberculosis* in the macrophage (163). **Figure 1.11** indicates how the overexpressed *phoP* gene affects other genes' functions and **Figure 1.12** represents the summary of our previous studies

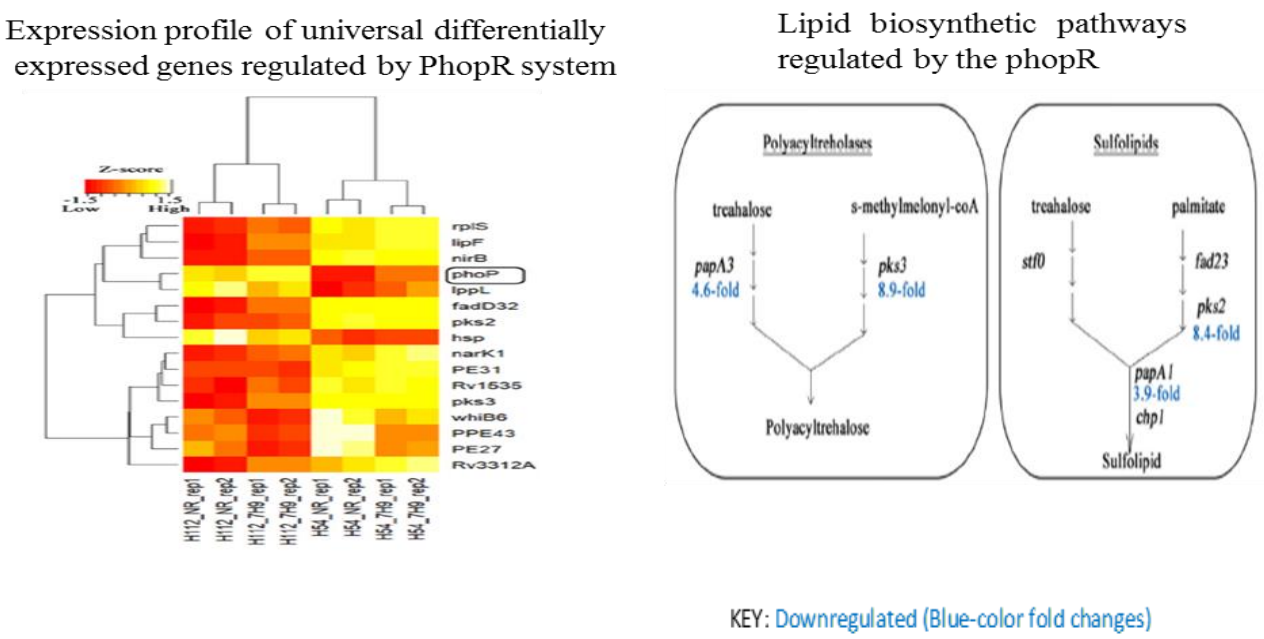

Figure 1. 11: The expression profile of the PhoPR virulence system and associated pathways (164).

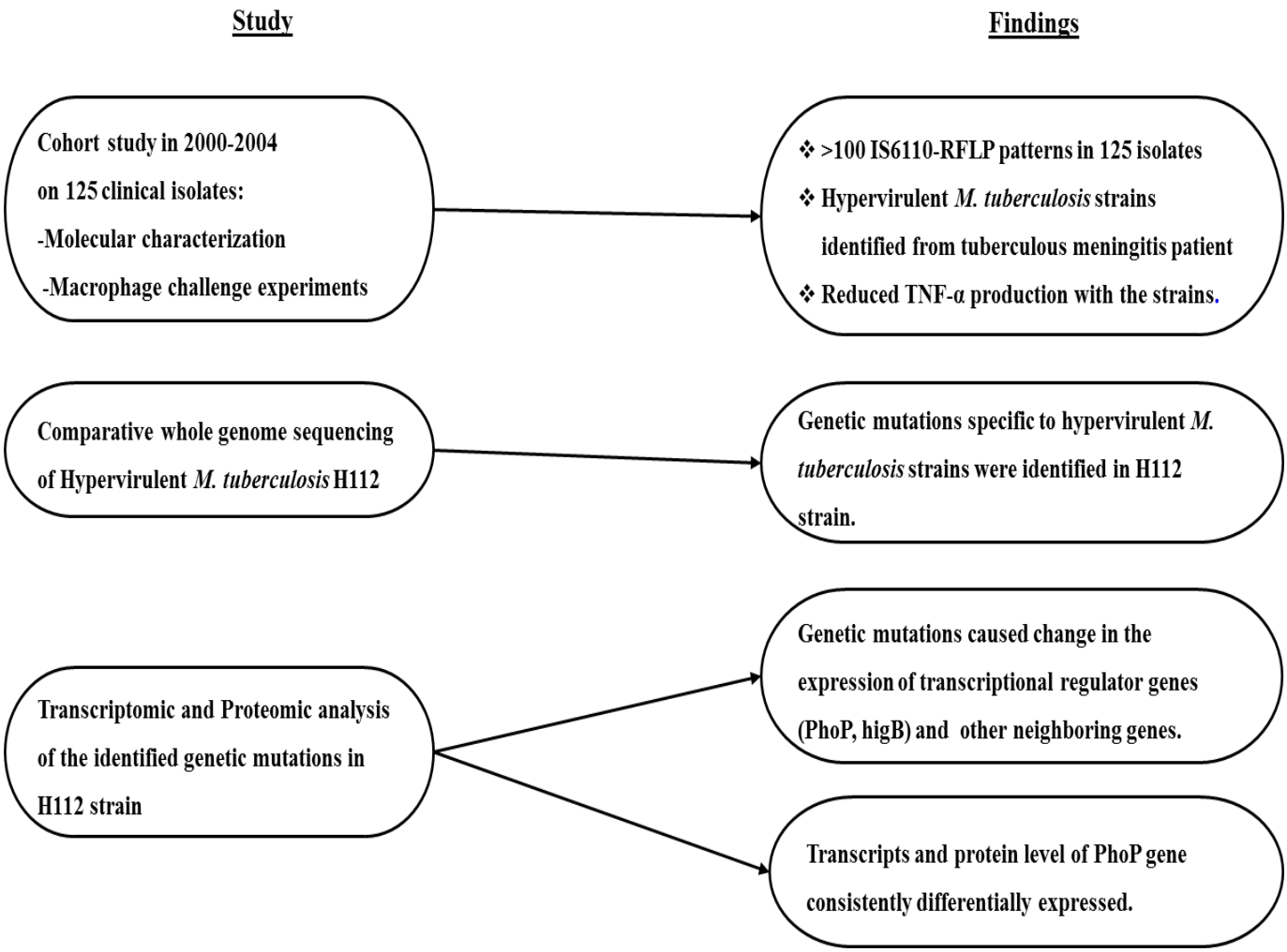

Figure 1. 12: Summary of our previous works on hypervirulent *M. tuberculosis*.

1.9 Vaccine against tuberculosis

The currently available and widely used vaccine against TB is Bacillus Calmette Guerin (BCG) vaccine. It is given to more than 85% of infants in countries using it as part of their national childhood immunization program. Many BCG strains are recommended for use across the world. But no evidence shows whether safety and efficacy differ among the strains (18). The result of one meta-analysis study showed that BCG protects infants and young children against meningeal or miliary TB (165). Neonatal BCG may decrease the de novo infection with *M. tuberculosis* in infants and young children. However, there is no reliable evidence that indicates the protection against active TB after 10 years of post-vaccination of infants in tropical climates (165, 166). Studies also show that the BCG vaccine cannot prevent the establishment of the reactivation of pulmonary and latent TB in adolescent and adult people. Because of this, it cannot be used as a booster dose for adults that are previously induced by vaccination with BCG or LTB or exposure to mycobacteria from the environment (167, 168). Therefore, more immunogenic and full protective new vaccines for both children and adult age groups are needed. To produce such kinds of vaccines, an extensive study of the pathogenesis of *M. tuberculosis* using appropriate animal models is crucial.

1.10. Zebrafish-*Mycobacterium marinum* model for the study of tuberculosis

This model consists of zebrafish and *Mycobacterium marinum (M. marinum).*

1.10.1 Zebrafish

Zebrafish is one of the tropical freshwater fish belonging to the Cyprinidae family. It differs from other fish in that it maintains a diploid state. The other fish can be triploid or tetraploid which makes their genetic analysis difficult (169). Zebrafish have become a major animal model used in biomedical research to study human diseases (170). The use of this animal as a research organism has been started since 1960. However, it has been well known as a model organism after George Streisinger developed procedures to facilitate genetic analysis in zebrafish at the beginning of 1980 (171).

Animal models that recapitulate all or some of the detected pathological features of the disease in humans are highly needed to study the nature of the disease. Because it enables insight into the genetic basis of the disease and the phenotypical outcomes (172). Nowadays, zebrafish are used as animal model to study many human diseases such as skin cancer, blood diseases, tuberculosis, and obesity. This animal model has many advantages over other models. For example, it has high fecundity, external development of embryos, small size, and rapid development (173). Another important feature of this animal is its transparency which helps to examine

the process of disease development using non-invasive imaging and tracking of protein or cell markers in both disease and biological processes (174). The anatomy and function of the blood-brain barrier (BBB) of zebrafish are also very similar to the BBB of humans. After three days of post-fertilization, the BBB of zebrafish is functional and prevents large molecule exchange between the blood and brain (175). More interestingly, the transparency of the body of the zebrafish combined with different fluorescent tools provides a good opportunity to examine the interaction between host and pathogen in real-time (176).

1.10.2 *Mycobacterium marinum*

M. marinum is atypical mycobacteria that cause tuberculosis in zebrafish and other amphibians. It also causes opportunistic infections in humans (177). The bacterium was first identified in marine fish by Von Betegh in 1910 (178) and was isolated for the first time by Aronson in 1926 (179). This bacterium grows well at an optimum temperature of 30^{o}C. Its generation time (4-6hr) is very short when compared with that of *M. tuberculosis* which takes about 20hr. It is a non-motile, aerobic waterborne, acid-fast bacillus, non-spore-forming, and photochromogenic mycobacterial species, and produces pigment like the yellow color at the time exposed to light (180, 181).

M. marinum commonly infects the fish through the oral cavity when the fish consume contaminated dead bodies of other fish and contact with the skin of the fish infected with the bacteria. The bacteria can also get inside the fish through gills and other openings (182). The common clinical symptoms observed in diseased fish are abdominal swelling, uncoordinated swimming, weight loss, skin ulceration, and white nodule in the liver and spleen (182, 183). It also causes a granuloma-like structure inside the brain of the zebrafish (184, 185).

M. marinum is closely related to the *M. tuberculosis* complex with 99.3% 16S rRNA sequence homology. The genome of *M. marinum* is 85% identical to the orthologous regions in the genome of *M. tuberculosis* and its orthologous coding sequences share an average amino acid identity of 85% with that of *M. tuberculosis.* Moreover, *M. marinum* shares the strategies of *M. tuberculosis* that are important for intracellular growth and survival in their hosts. For example, they share many common important virulence factors such as ESAT-6, CFP-10, ESPA, ESX-1, etc. The virulence factors are directly or indirectly regulated by the *phoP* gene. The *phoP* gene in *M. marinum* has a genetic similarity of 85% with that of *M. tuberculosis*. The genes of *M. marinum* can usually complement mutations in *M. tuberculosis* orthologs and vice versa (157, 186, 187). Therefore, *M. marinum* is anticipated to be used as a model organism for the study of the pathogenesis of *M. tuberculosis* (188).

1.11 Summary of the chapter and identified research gap

From this brief review of the previous works, it may be concluded that TB is still one of the most devastating health problems globally. One of the major factors contributing to the high morbidity and mortality rate of the disease is the enhanced virulence of *M. tuberculosis* strains. Even though the host immune system can effectively react to the mycobacterial infection, *M. tuberculosis* strains devise mechanisms that help them to tolerate the hostile environment in the immune cells and become hypervirulent and establish the most severe form of the disease. The genetic markers specific to the hypervirulent *M. tuberculosis* strains and their effects on neighboring genes and virulence-related transcriptional regulators were recently well identified. It was also determined that among those affected genes, the *phoP* gene was the one its RNA transcript and protein level were consistently differentially elevated in the hypervirulent strains using multi-omics analysis. However, the functional impacts of this differentially expressed *phoP* gene on mycobacterial virulence were not confirmed. To bridge the existing research gap, determination of the causative role of the elevated expression of the gene in mycobacterial virulence in causing TBM is needed. This can be done by manipulating the orthologous region of the *phoP* gene specific to the hypervirulent *M. tuberculosis* in *M. marinum* and validating its effects in the zebrafish animal model. If the causative role of this genetic marker is confirmed, it will be used for tracing the hypervirulent *M. tuberculosis* strains in case of outbreaks and it would

also be used as a knowledge base for new and effective vaccine and drug development against TB.

1.12 Aims of the project

This study aimed to examine the causative role of differentially expressed *phoP* gene specific to the hypervirulent strains of *M. tuberculosis* in mycobacterial virulence using zebrafish model approach.

Specifically, this study aims:

1. To construct a transformant *M. marinum* strain by using the *phoP* gene of *M. tuberculosis*.

This objective was achieved by amplifying the *phoP* gene region from the genome of *M. tuberculosis* H37Rv and cloning it into pVV16 mycobacterial vector and transferring it to *M. marinum* through transformation by electroporation.

2. To examine and compare the bacteriological and pathological features of infection caused by wild-type and transformant *M. marinum* strains in the brain of zebrafish.

This objective was attained by injecting the mycobacterial suspension into zebrafish and examining the mycobacterial load, and the number and size of granulomas-like features of transformant *M. marinum* in the zebrafish brain and comparing it with that of the wild-type strains. Detection and monitoring of blue fluorescent granuloma-like signals or aggregates in the body and brain region of infected transparent zebrafish were also performed to achieve the objective.

CHAPTER 2: METHODS AND MATERIALS

Following the summary of the previous works and development of the conceptual framework in the preceding chapter, this chapter explains the methods used to achieve the objectives of the study. It starts with the animal model and the mycobacterial strains used to study the impacts of differentially expressed *phoP* gene on the virulence of mycobacteria and continues by discussing how the plasmid was constructed for the transformation of the *M. marinum* strains used in this study. Then, it explains the transformation of *M. marinum* strains by electroporation, preparation of the mycobacterial strains, and how the infection of zebrafish with the strains was performed. Finally, it highlights different methods used to examine the effects of the infection on the infected zebrafish and how the assessed data were analyzed. The workflow of the major methods is presented in **Figure 2.1.**

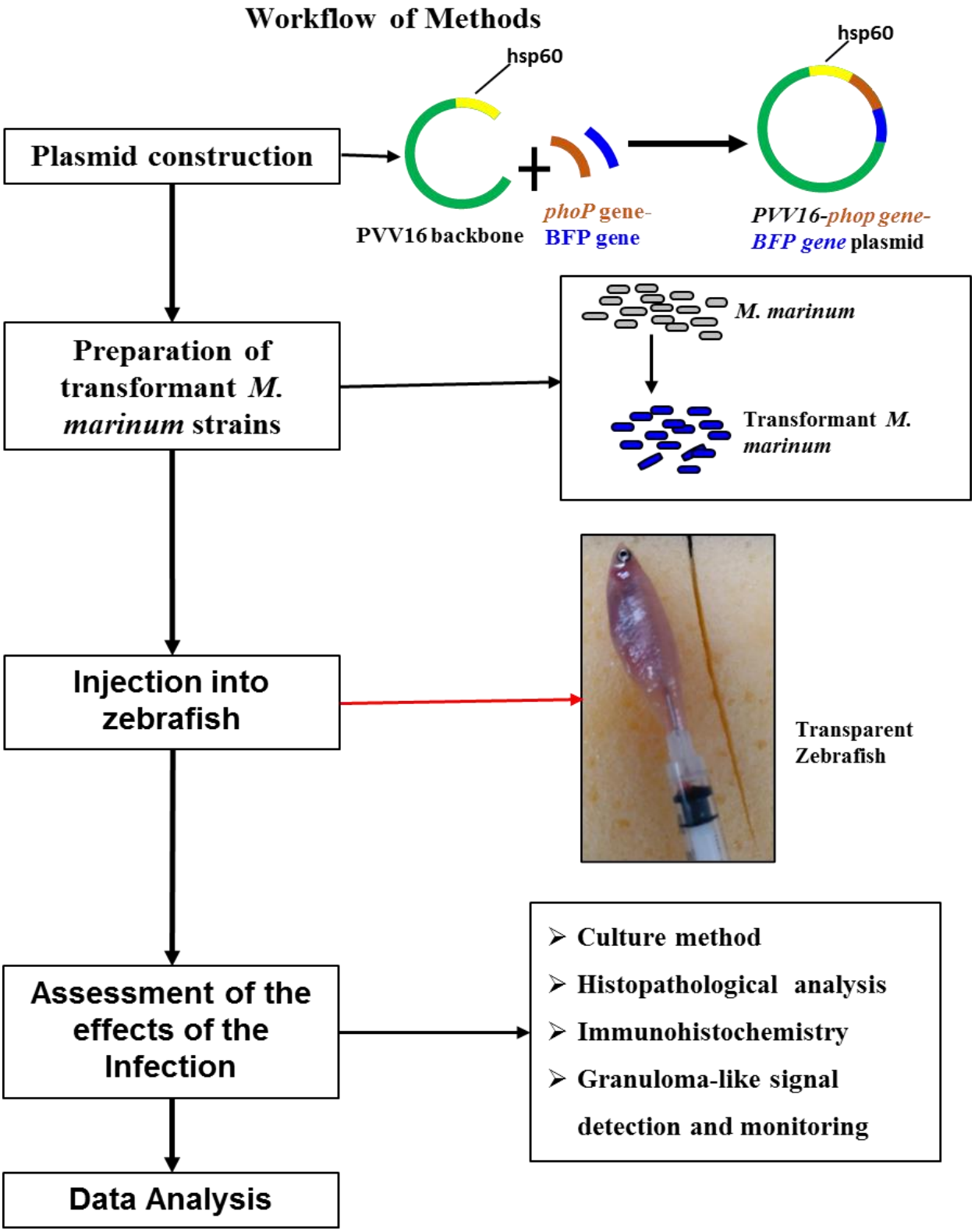

Figure 2.1: Workflow of major methods used in the study. (BFP: blue fluorescent protein).

2.1 Zebrafish-*Mycobacterium marinum* model

In this study, zebrafish-*M. marinum* infection model was used and the model consists of zebrafish and *M. marinum*. The model is used to study how *M. tuberculosis* establishes infection in the body of the host, particularly in the CNS, and leads to the development of TBM in humans. The zebrafish model mimics similar features of human TB in the formation of granulomas-like lesions and establishment of either acute or chronic infection based on the number of bacilli involved in the infection when infected with *M. marinum* **(Figure 2.2)** (189, 190). In this study, *M. marinum* strain M (ATCC BAA-535), an isolate originally from human patients with fish tank granulomas (191), which was purchased from The American Type of Culture Collection (ATCC), and *M. marinum* E11, a sea bass isolate of *M. marinum* (192), were used. *M. marinum* M and strain E11 cause acute and chronic disease, respectively, in zebrafish (192). Infection of adult zebrafish with the strains also results in TBM with granuloma formation in the brain and meninges (184, 185).

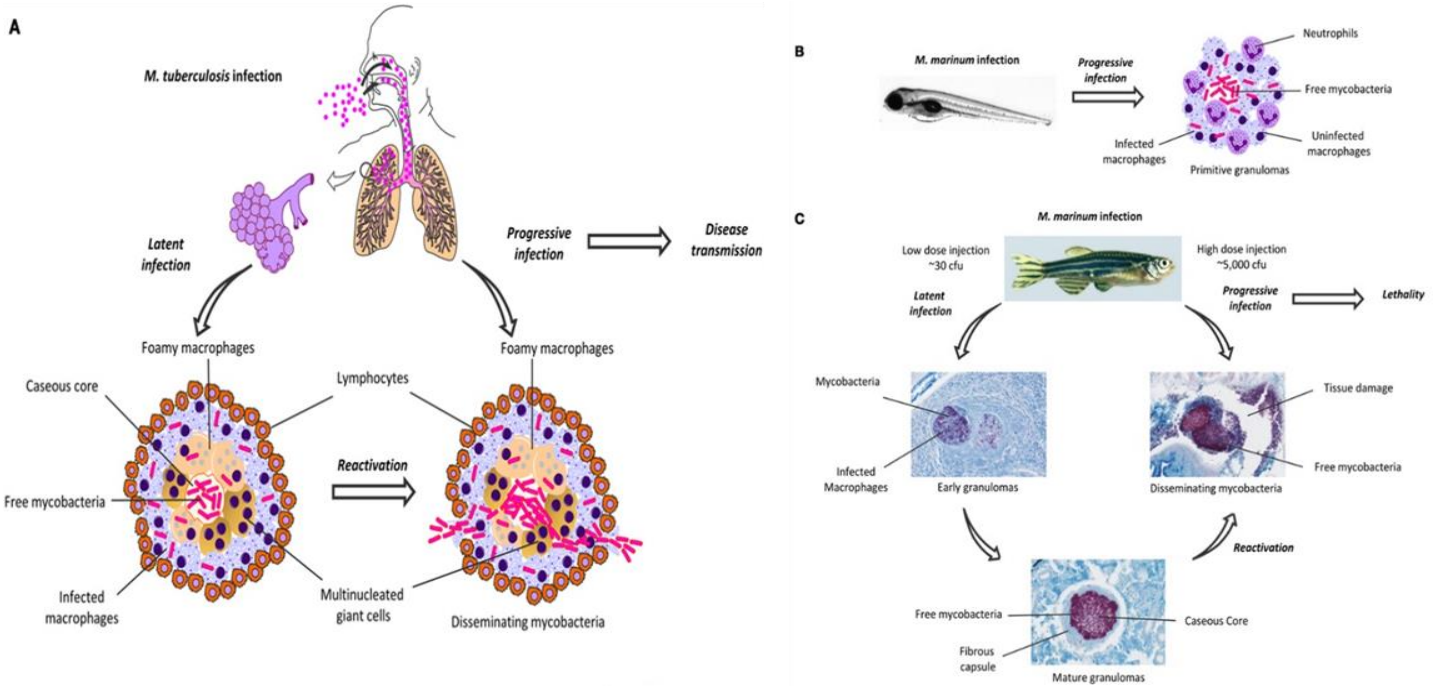

Figure 2.2: Formation of granuloma in *M. tuberculosis*-infected human (**A**) and in zebrafish infected with *M. marinum* (**B**) (190).

2.1.1 Zebrafish lines and Husbandry

Two different lines of adult zebrafish were used for these experiments. These are the wild type and absolute (*ednrba*^{b140}*;mitfa*^{b692}) (transparent) lines. The wild-type zebrafish were obtained from zebrafish breeding facilities in our university and the transparent zebrafish were purchased from Zebrafish International Resource Center, University of Oregon, USA. The transparent zebrafish is the one that has a mutation in *ednrba* gene at the b692 allele contains a single T to G point mutation that resulted in the substitution of isoleucine by serine at position 215. The gene is involved in the production of pigment and the mutation in the gene resulted in optically transparent fish. The zebrafish were maintained under a standard condition of 14:10hr light: dark cycle and fed with living brine shrimp two times a day. The transparent fish were allowed to stay in the breeding room for one month after their arrival in Hong Kong to exclude health problems related to transportation stress. Before injection was performed, the fish were transferred to the experiment room with similar conditions (water quality, PH, light, temperature) as that of the breeding room and kept there for a minimum of 10 days. The fish were injected either with mycobacterial suspension or phosphate-buffered saline (PBS) and housed in 8 per tank water at 28^{o}C. Each animal experiment was conducted following the protocol approved by the Animal Subjects Ethics Sub-Committee ASESC case No.: 19-20/64-HTI-R-GRF) of the Hong Kong Polytechnic University.

2.2 Construction of plasmids

For the construction of recombinant plasmid used for transferring the genes needed for the transformation of *M. marinum*, components like pVV16 mycobacterial plasmid, blue fluorescence protein gene, and *phoP* gene were used. Two types of recombinant plasmids were constructed for this study. These are the following:

1. Recombinant pVV16 plasmid that only ligated to blue fluorescent protein (BFP) gene.
2. Recombinant pVV16 plasmid ligated to both the *phoP* gene and blue fluorescent protein gene.

The construction processes of the recombinant plasmids are described in the next subsections.

2.2.1 Plasmid DNA extraction from *Escherichia coli*

To obtain the BFP gene, tagbfp, which is found in plasmid pME-loxP-mTagBFP2-stop-pA-loxP (Addgene) (**Figure 2.3**), plasmid DNA was extracted from *Escherichia coli (E.coli)* after incubating the bacteria overnight in Luria Bertani (LB) broth medium containing kanamycin sulfate at 50µg/ml. The plasmid DNA was isolated by using the QIAprep Spin Miniprep Kit (Qiagen, USA). Briefly, the cells were first harvested by centrifugation of the culture at 8000 rpm for 3min. The pellet was re-suspended in 250µl P1 buffer and transferred into a microcentrifuge tube. A total of 250µl P2 buffer was added to the solution and mixed thoroughly

until it turned blue. After adding 350µl neutralization buffer (N3), the mixture was spun for 10 min at 13,000 rpm in a microcentrifuge. About 800µl supernatant was added to the QIAPrep 2.0 spin column and spun for 1min. The flow-through was discarded and 0.5ml PB buffer was added. The solution was centrifuged for 1min and the flow-through was removed. The QIAPrep 2.0 spin column was washed by adding 0.75ml PE buffer and spun for 1min. The column was transferred to the new collection tube and centrifuged for 1min to remove the residual of the washing buffer. The spin column was taken to a clean 1.5 microcentrifuge and 35µl of nuclease-free water was added at the center of the spin column to elute the plasmid DNA. Then, the tube was allowed to stand for a minute and followed by centrifugation for 1min. The plasmid DNA was collected and kept at -20^{o}C until use.

Figure 2.3: Depicts the location of TagBFP (blue fluorescence protein) insert in the plasmid pME-loxP-mTagBFP2-stop-pA-loxP(Addgene) (193).

2.2.2 Amplification of blue fluorescence gene from extracted plasmid DNA

To amplify the BFP gene from the plasmid pME-loxP-mTagBFP2-stop-pA-loxP or pVV16 vector, polymerase chain reactions (PCR) were conducted. The gene was amplified from the extracted plasmid DNA using the designed cloning primers with the Nde I and Hind III restriction sites. The sequences of the primers used for the gene amplification are indicated below. The underlined parts in the sequence of the primers indicate the restriction sites of the enzymes.

Forward primer: 5' TATAACATATG AGCGAGCTGATTAAGGAGAACA3'

Reverse primer: 5' TATAA AAGCTTTTAATTAAGCTTGTGCCCCAGT3'

Note: the underlined sequences are restriction sites of Nde I and Hind III.

To amplify the gene, PCR was performed using a total volume of 50µl reaction consisted of 25µl of high-fidelity 2x PCR master mix,1µl of 10mM forward primer, 1µl of 10mM reverse primer, 18µl of nuclease-free water, and 5µl of DNA. The cycling conditions for the PCR included initial activation of 1 cycle at 98^{o}C for 2 min, denaturation of 35 cycles at 98^{o}C for 20 seconds, annealing of 35 cycles at 55^{o}C for 30 seconds, 35 cycles elongation at 72^{o}C for 30 seconds, and followed by a final extension at 72^{o}C for 2 min.

2.2.3 Agarose gel electrophoresis

The size of the gene of interest in the PCR products was determined by mixing 5µl of the products with 2µl of 6X DNA loading dye and running it for 1hr using 1.5% agarose gel (Vivantis Agarose Molecular Biology Grade) in 1X Tris-Borate EDTA

(1X TBE) buffer with RedSafeTM Nucleic Acid Staining Solution (iNtRON Biotechnology). The PCR products were run using gel electrophoresis. Then, imaging was performed under UV transillumination (Bio-Rad), and the product size of the amplified gene was determined by using the 100bp ladder.

2.2.4 Purification of inserts

After the insert (BFP gene) was amplified from its source, it was purified following PCR Purification Kit protocol (QIAGEN, USA). The purification process was performed as follows: the PCR product was mixed with buffer PB in the proportion of one volume DNA to five volume buffer solution. The mixture was added to the MinElute column placed in a 2ml collection tube and spun at 13,000 rpm for one minute. The flow-through was discarded and 750µl of buffer PE was added to the column and centrifuged for 1min. To completely remove the remained ethanol, additional centrifugation was performed for 1min. The column was placed in a clean 1.5ml tube and 10µl of buffer EB was added to elute the DNA. Then, the column was allowed to stand for 1min at room temperature and centrifugated at 13,000 rpm for 1min. Finally, the DNA was collected in the microcentrifuge tube and stored at -20^{o}C.

2.2.5 Digestion of pVV16 plasmid and purified insert

The plasmid (*E. coli*-mycobacterial shuttle pVV16 vector (**Figure 2.4**)) and the purified PCR products of BFP gene were digested using Nde I and Hind III restriction enzymes. A total of 50µl of the reaction volume consisting of 5µl of 10x

NEBuffer 2, 1µl of 20U/µl Nde I, 1µl of 20U/µl Hind III, 2µg of insert or pVV16 plasmid DNA and nuclease-free water was used for the double enzymatic digestion. The solution was incubated overnight at 37^{o}C and followed by purification using the same protocol as performed for the insert in section **2.2.4** above.

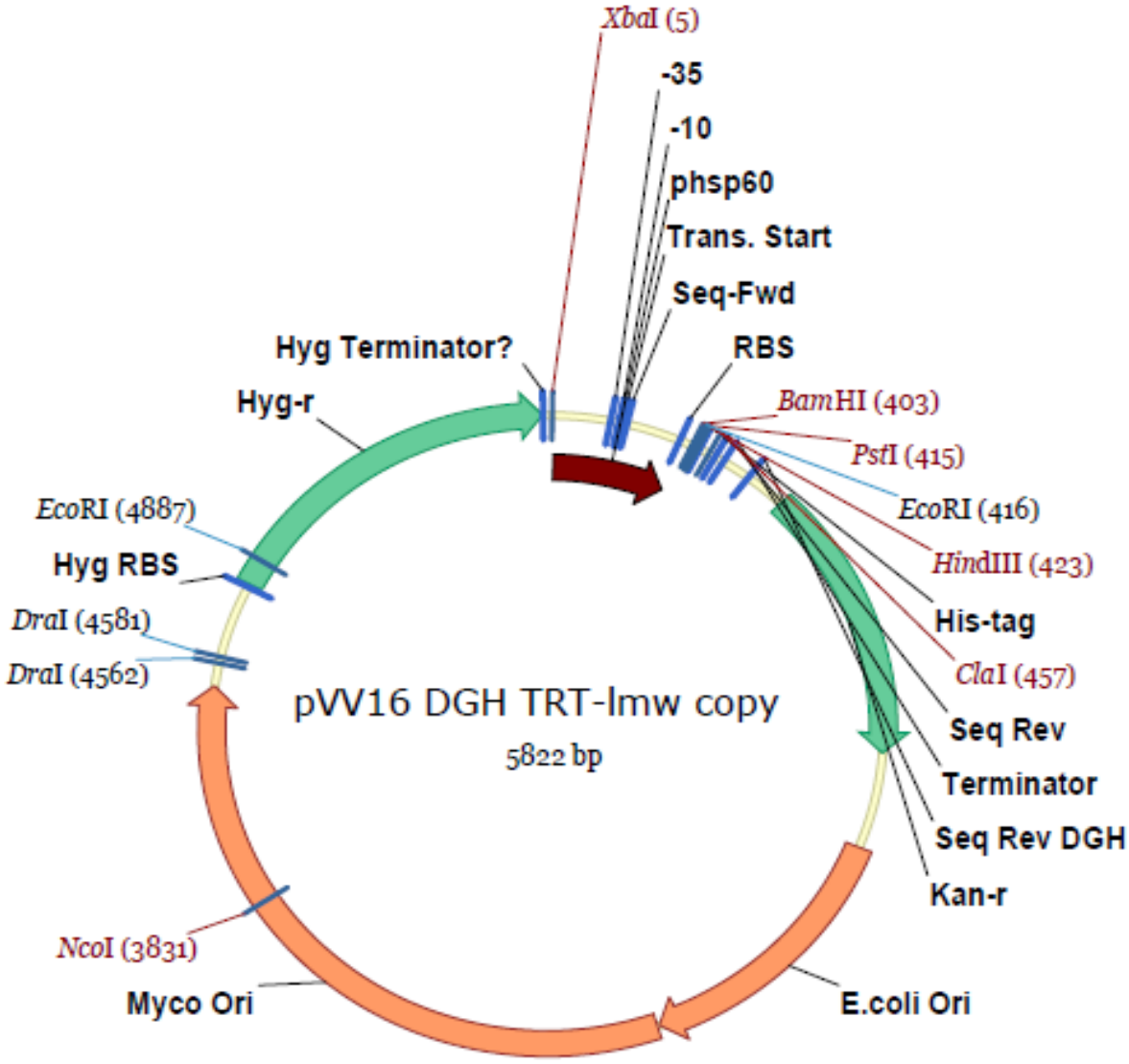

Figure 2.4: Indicates the plasmid map of *E. coli*-mycobacterial shuttle pVV16 vector (Addgene) (194).

2.2.6 Construction of recombinant *pVV16-BFP gene* plasmid

To construct the recombinant plasmid *pVV16-BFP gene,* the purified BFP gene was ligated with the pVV16 vector by using the following components and procedures. The components include a 1X T4 DNA ligase reaction buffer (New England Biolabs), 400 units of T4 DNA ligase (New England Biolabs), insert, pVV16 vector, and nuclease-free water. To perform the ligation process, the enzyme and the reaction buffer were first allowed to thaw on ice. After the insert and pVV16 were incubated in the water bath at 45^{o}C for 5min, they were put on ice and spun down. The reaction volume consisted of 1µl of 1x T4 DNA ligase reaction buffer, 2µl of pVV16, 3µl of insert, 3µl of water, and 1µl of T4 DNA ligase. The concentration of the insert and pVV16 plasmid was calculated using the following formula:

$$\text{Amount of insert (ng)} = \text{Amount of pVV16 (ng)} \times \frac{\text{insert size (bp)}}{\text{pVV16 size (bp)}} \times \text{insert: vector}$$

$$= (100) \times \frac{(\text{product size of insert-13})}{(5{,}822)} \times (3)$$

Then, the mixture was incubated overnight at room temperature and stored at -20^{o}C until use.

2.2.7 Construction of recombinant *pVV16-phoP gene-BFP gene* plasmid

To prepare the transformant *M. marinum* strains, a recombinant pVV16 plasmid was constructed by ligating the *phoP* gene, BFP gene, and pVV16 together. The *phoP* gene and the BFP gene were amplified from *M. tuberculosis* H37Rv genomic DNA and pME-loxP-mTagBFP2-stop-pA-loxP plasmid, respectively, using PCR.

The primers used for the amplification of the two DNA fragments were designed using Vazyme Software (CE Design: http://www.vazyme.com) as indicated in **Table 2.1**. The restriction sites of the Nde I and Hind III enzymes were included at the 5' termini of amplified DNA fragments on the right and left regions. The amplification of the genes was performed using a total volume of 25µl reaction containing 12.5µl Q5 hot start high-fidelity 2X master mix (New England Biolabs), 1.25µl of 10µM forward primer, 1.25µl of 10µM reverse primer, 5µl of template DNA, and 5µl of nuclease-free water. The conditions of the PCR were initial activation of 1cycle at 98^{o}C for 30 seconds, denaturation of 35 cycles at 98^{o}C for 10 seconds, annealing of 35 cycles at 56^{o}C for 30 seconds, 35 cycles elongation at 72^{o}C for 30 seconds, and a final extension at 72^{o}C for 2min.

Table 2.1: Primers used for the amplification of *phoP* gene and BFP gene from *M. tuberculosis* H37Rv and plasmid pME-loxP-mTagBFP2-stop-pA-loxP, respectively, for multi-fragment assembly.

Primer name	Sequence (5'->3')	Length	Tm
phoP MTB F	cggaggaatcacttccatatgATGCGGAAAGGGGTTGATCT	41	60.8
phoP MTB R	tcagctcgctcatTCATCGAGGCTCCCGCAG	31	62.4
BFP F	tcgatgaATGAGCGAGCTGATTAAGGAGAA	30	60.4
BFP R	gtggtggtggtggtgaagcttTAATTAAGCTTGTGCCCCAGTTT	44	60.4

Note: The underlined regions in the sequence of primers are the restriction sites for the enzymes. F: forward, R: Reverse, Tm: Melting temperature, MTB: *Mycobacterium tuberculosis.*

The pVV16 vector was digested and linearized using the Nde I and Hind III restriction enzymes. The PCR products of the two genes and the linearized pVV16 vector were purified by using the protocol of the PCR Purification Kit used in **section 2.2.4**. After the purified inserts and vector were mixed in the appropriate ratio, the recombinant pVV16 plasmid was constructed using the ClonEXpress Ultra-One Step Cloning Kit (Vazyme Biotech Co. Ltd, China) with a little modification. The appropriate volumes of the linearized pVV16 and inserts were determined by using the formula given in the manual of the ClonExpress Ultra-One Step Cloning Kit. The concentration and volume of each insert and linearized vector are mentioned below in **Table 2.2.**

Table 2.2: Amounts of inserts and linearized vector used for the construction of the recombinant plasmid.

Component	Recombination	Negative control 1	Negative control 2
Linearized vector Pvv16	2µl	2µl	0µl
Insert(N=2),1µl each	2µl	0µl	2µl
2XClonExpress Mix	5µl	0µl	0µl
ddH_2O	1µl	8µl	8µl
Total	10µl	10µl	10µl

After adding the components in a single tube, the reaction was mixed and incubated at 50^oC for 50 min and then kept at -20^oC until use.

2.3 Preparation of competent cells of *E. coli* DH5α

Before the pVV16 plasmid containing the gene of interest was introduced into *M. marinum*, it was transferred into the competent cells of *E. coli* strain DH5α using chemical transformation. A plasmid-free *E. coli* strain DH5α strain was used to amplify the pVV16 plasmid ligated with the gene of interest. Therefore, to make the *E. coli* DH5α cells competent to take the plasmid DNA, it was first cultured at 37^{o}C overnight in 5ml of LB broth medium. Then, the whole 5ml culture was subcultured in 200ml LB at 37^{o}C with shaking at 250rpm until its optical density (OD) at 600nm reached 0.6. After the desired OD was reached, the cells were collected by centrifugation at 3000xg for 10 min at 4^{o}C. The pellet was mixed with 50ml $CaCl_2$ and kept on ice for 4hrs. The solution was spun at 3000xg for 10 min and the supernatant was discarded. The pellet was re-suspended in 4ml of 15% glycerol $CaCl_2$ solution and aliquoted in 200µl into the 1.5ml centrifuge tube and kept in -80^{o}C until use.

2.4 Transformation of *E. coli* DH5α cells with recombinant pVV16

After the amplified gene (either BFP or BFP and *phoP*) was digested using restriction enzymes and purified, it was cloned into an expressive *E. coli*-Mycobacteria shuttle vector (pVV16) (194) extracted from *E. coli*. The ligated vector was introduced into *E. coli* Dh5α strain by using the chemical transformation

method (New England Biolabs) to completely seal the gap between the insert and the plasmid sequences. The process was undertaken as follows: first, competent cells (DH5α) and the purified plasmid ligated with the gene of interest (pVV16) were thawed on ice for 30 min. Next, 2µl of the plasmid DNA was mixed with 100µl of the competent cell suspension, and the mixture was incubated in the water bath at 42^{o}C for 1min. After putting the mixture on ice for 2min, 1ml LB broth without antibiotics was added immediately and suspended. Then, the solution was incubated in a shaker at 37^{o}C for 1hour and spun at 5000rpm for 2min. From the supernatant, approximately 50-100µl was used to re-suspend the pellet. The suspension was spread on LB agar media mixed with kanamycin sulfate at 25µg/ml. To confirm the success of the transformation, PCR was performed from the colonies that appeared on the medium. To check the absence of mutation in the inserts, the segment was amplified by PCR and sequenced using the Sanger sequencing method. The primers used for the amplification of the regions and sequencing are presented in **Table 2.3.** Then, the plasmid was extracted from the colonies and purified to be transferred into the competent cells of *M. marinum* by electroporation.

Table 2.3: Primers used for PCR and sequencing of the overlapping regions from recombinant *pVV16-phoP gene-BFP gene* plasmid.

Primer name	Sequence	No. of bases	Tm	Product length
BP1 F	GCAGCGAGGACAACTTGAGC	20	61.91	236
BP1 R	AGGCTCACCGACAGCAGTTC	20	62.44	
BP2 F	TAAGAACCTCAAGATGCCTGG	21	57.37	261
BP2 R	CCAGTCTTTCGACTGAGCC	19	57.87	

Tm: melting temperature

2.5 Preparation of *Mycobacterium marinum* competent cells

Initially, the competent cells of *M. marinum* were prepared by growing them in Middlebrook 7H9 broth (Becton Dickinson) enriched with 10% albumin- dextrose catalase (ADC enrichment, Becton Dickinson), 0.05% Tween 80 and 0.2% glycerol at 30^{o}C with shaking at 250 rpm until the OD at 600nm reached 0.8-1. Then, the culture was kept on ice for 1.5hr and centrifuged at 300xg for 10 min. The pellet was washed three times with ice-cooled 10% glycerol. The first wash was performed with 20ml of 10% glycerol for 10 min. The second wash was done with 10ml 10% glycerol and the last wash was done with 5ml 10% glycerol. The pellet was then suspended in 1: 10 with ice-cooled 10% glycerol in sterile PBS and aliquoted in100µl into a 1.5ml microcentrifuge tube and stored at -80^{o}C. The cells were harvested by centrifugation and re-suspended with fresh 10% glycerol before use in the next step.

2.6 Labeling of wild-type *Mycobacterium marinum*

To visualize the *M. marinum* clearly inside the body and brain of transparent zebrafish, the bacterium was labeled with blue fluorescence. The pVV16 plasmid containing BFP gene was transferred into the competent cells of *M. marinum* using transformation by electroporation. Transformation in the genus mycobacterium is very difficult because of the thick and waxy nature of its cell wall (195).

Electroporation is the most successful means of introducing the genetic materials into the mycobacterial species by generating pores with a high voltage pulse (195, 196). Therefore, we used transformation by electroporation to transfer the plasmid ligated to the gene of interest in the *M. marinum* following the protocol described previously (195). Briefly, 100ng of ligated and purified plasmid was thawed and mixed with 100µl competent cells of *M. marinum*. The mixture was transferred to a 0.2cm gap cuvette (BioRad, USA) pre-cooled on ice and electroporated at 2.5KV, 25MF, 200Ω in a Gene Pulser (BioRad, USA). Immediately after electroporation was performed, 1ml of Middlebrook 7H9 without antibiotics was added and incubated at 30^{o}C and 200 rpm shaking incubator for 2hr. The cells were harvested after centrifugation of the mixture at 13,000 rpm for 3 min. Using 100µl of the supernatant, the pellet was re-suspended and 50-100µl of the solution was inoculated on the Middlebrook 7H10 agar medium containing kanamycin at 50µg/ml and incubated at 30^{o}C for 5 to 7 days.

To confirm the success of the transformation, PCR was performed to amplify the gene of interest from the DNA of the bacterial colonies recovered on the medium. The smear and suspension of the colonies were also examined under the confocal microscope for the detection of blue fluorescent *M. marinum*. Moreover, Sanger sequencing was performed on the DNA of the BFP gene extracted from the colonies

of the bacterium to check the absence of mutation in the sequence of the gene of interest. Those colonies that contain blue fluorescent *M. marinum* were preserved and kept under -80^{o}C for further use.

2.7 Preparation of transformant *Mycobacterium marinum*

Gene functionality can be examined by constructing a mutant or overexpression of the gene and this helps to evaluate the function of the wild-type of the gene of interest in the bacterium (197). Therefore, to measure the effects of the *phoP* gene on the virulence of *M. marinum*, the overexpression method was used. To achieve this, the pVV16 ligated to both BFP and *phoP* genes was transferred into the competent cell of *M. marinum* using electroporation by following similar procedures performed in **section 2.6**. Then, the presence of the two genes in the transformants was confirmed by growing the transformants on Middlebrook 7H10 agar medium containing kanamycin sulfate at 50µg/ml, and by performing PCR on the *pVV16+phoP gene* segment, and *BFP gene+pVV16* overlapping region at upstream and downstream of the insert, respectively. The total length of the insert consisted of the DNA segments of both genes were also checked using PCR. Blue fluorescent *M. marinum* was detected in the recovered colonies using confocal microscope.

2.8. DNA Extraction from *Mycobacterium marinum*

The DNA of *M. marinum* was extracted using Roche diagnostics which is commonly known as an AMPLICOR Respiratory specimen preparation Kit. The colonies of *M. marinum* were collected from agar plate in a microcentrifuge and mixed with 500µl of washing buffer (RW). After the mixture was centrifuged for 10 min at 14,000 rpm, the supernatant was removed and 100µl lysis buffer (RL) was used to resuspend the pellet and incubated at 60^{o}C for 45 min in a water bath. Then, the mixture was spun down and 100µl neutralization buffer (RN) was added and vortexed to mix the solution well. The solution was again spun for 10 min at 14,000 rpm and the supernatant containing the DNA was collected in a new 1.5ml Eppendorf tube and kept at -20^{o}C until use in the next step.

2.9 Sanger sequencing method

The *phoP* gene was sequenced before and after transformation by electroporation in *M. marinum* to check if there is a mutation in the sequence of the gene. It was performed following the protocol previously described. Briefly, the insert was amplified from the DNA extracted from the transformant *M. marinum* using PCR and was purified with exonuclease I and shrimp alkaline phosphatase (ExoSAP). A volume of 5µl of PCR product was mixed with 2µl of ExoSAP. Then, cleaning was performed at 37^{o}C for 15 min and 80^{o}C for 15 min for 1 cycle in the thermal cycler.

Two-cycle sequencing reactions, one forward and one reverse reaction were set up in a total volume of 20µl for each reaction using 1µl of BigDye terminator V 1.1Mix (life technologies, Part no.4337455), 3.5µl of 5x sequencing buffer, lµl of 3.2µM forward primer, lµl of 3.2µM reverse primer, 2µl of the ExoSAP purified PCR product and nuclease-free water. The cycle sequencing was performed following BigDye_kit_std* in the ABI Verti program such as at 96^{o}C for 1min of one cycle, 96^{o}C for 10sec of 25 cycles,58^{o}C for 5sec of 25 cycles and 60^{o}C for 4min of 25 cycles. Then, the product was purified using 75% isopropanol. After the sequencing product was re-suspended in 12µl of Hi-Di formamide, it was analyzed using ABI Genetic analyzer 3130. Finally, the sequencing data analysis was performed.

2.10 Determination of the differential expression of *phoP* gene in *M. marinum*

2.10.1 RNA Extraction from *M. marinum*

To determine the expression level of the *phoP* gene, total RNA was extracted from the transformants (*M. marinum* containing recombinant *pVV16-phoP gene-BFP gene* plasmid), and wild-type (*M. marinum* containing recombinant *pVV16-BFP gene* plasmid) following Quick-start protocol (RNeasy Plus Mini Kit, Qiagen). Briefly, the bacterial cells were harvested from broth culture at its logarithmic phase (OD=1) and suspended in 1ml of autoclaved PBS. The suspension was transferred to a 1.5ml tube and spun at 6000g for 5min and the PBS was removed using a pipette. A total volume of 100µl of lysozyme was added and incubated for 15 min with a vortex at

room temperature. Then, 500µl RLT plus was added to the solution and homogenized with a 5ml syringe for about 15 times. The solution was centrifuged at 14,000 rpm for 3min and 500µl of the supernatant was saved. The saved supernatant was well mixed with one volume (500µl) of seventy percent ethanol. From the solution, 700µl was added to the RNeasy spin column and centrifuged for 30sec at 8000g. About 700µl wash buffer (RW) was added and allowed to stand for 5min, and then centrifuged for 30sec at 8000g. Then, 500µl RPE buffer was added and centrifuged at 8000g for 30sec. This step was repeated and centrifuged for 1min. The spin column was placed in a new 2ml collection tube and spun for 2min at 8000g. The spin column was placed in a new 1.5ml tube and 35µl RNase-free water was used to elute the DNA. After allowing it to stand for 5min, centrifugation for 1min at 8000g was performed. Finally, the RNA was stored in a -80^{o}C fridge for future use.

2.10.2 Digestion of DNA

To remove the genomic DNA from the extracted total RNA, treatment of the RNA solution was performed by using DNase I enzyme according to the manufacturer's instructions. In brief, a volume of 10µl containing 8µl of total RNA, 1µl of DNase I (Sigma Aldrich), and 1µl of DNase buffer, was incubated at 37^{o}C for 30 min. Then, the solution was mixed with 1µl EDTA to stop the reaction. Before the use

of the treated RNA for the synthesis of cDNA, the absence of the genomic DNA in the solution was checked by running agarose gel electrophoresis.

2.10.3 Complementary DNA (cDNA) Synthesis

The synthesis of cDNA was conducted using reverse transcriptase. A mixture of 1µl 50µM random hexamers (New England Biolabs),1µl of 10mM dNTP mix and 11µl of RNA and 1µl of nuclease-free water, was incubated for 5min at 65^{o}C and then put on ice. Then, 4µl RT reaction (5XSS IV buffer), 1µl of 100mM Dithiothreitol, and 1µl of superscript IV reverse transcriptase (Invitrogen, USA) were added to the mixture making a total volume of 20µl. After the reaction was mixed gently, it was incubated in a Verti Thermal Cycler (Applied Biosystems, USA) with the condition of 1cycle at 23^{o}C for 10min, 1 cycle at 50^{o}C for 10min, and then inactivated at 80^{o}C for 10min. Finally, the solution was kept in a fridge at -20^{o}C until used for quantitative polymerase-chain-reaction (qPCR).

2.10.4 Quantitative real-time PCR

After the cDNA was prepared, it was used as a template for the qPCR reaction. The quantitative real-time PCR was used to quantify the mRNA level of *phoP* gene expression in the transformant *M. marinum*. Real-time PCR has become essential for the quantification of nucleic acid because of its incomparable sensitivity (198). It also gives accurate and kinetic quantification allowing data analysis in the only

log-linear phase at which the amplification efficiency of each reaction is constant (199). A singleplex PCR reaction was set up in a 96-well plate. A total volume of 25µl consisted of 12.5µl of SyBer Green master mix, 10.5µl of nuclease-free water, 1µl of the cDNA, and 1µl primer mix (forward and reverse primers) was used for the PCR reaction. The primers used for the qPCR are indicated below (**Table 2.4**). After transferring the PCR reactions to Roche LightCycler 480 real time PCR machine (Roche), it was performed with the condition of 1 cycle of initial enzyme activation at 95^{o}C for 2min, 40cycles of denaturation at 95^{o}C for 15sec and real-time quantification for 10 min at 60^{o}C. The threshold cycle (Ct) values were normalized to the reference gene *rrs* and the $2^{-\Delta\Delta CT}$ comparative method was used to determine the fold changes (200).

Table 2.4: Primers used for real-time quantitative PCR

Gene	**Name of primer**	**Primer sequence (5'-3')**	Length	Tm
phoP	Qmmm1 PhoP F	GACACGTAGGACTCGACGAC	20	59.91
gene	Qmmm1 PhoP R	ACCTTGTTGCGCTATTTCGTG	21	59.80
rrs gene	rrs F	TTCACGGGGTCGAGTTGCAG	20	62.71
	rrs R	GTCCAGGGCTTCACACATGCT	21	62.94

Tm: melting temperature

2.11 In vitro growth of wild-type and transformant strains of *M. marinum*

To determine the effect of the differentially expressed *phoP* gene on the growth of *M. marinum*, in vitro growth of transformant *M. marinum* was performed and compared with that of wild-type strains. A loopful of the two strains were inoculated in Middlebrook 7H9 broth enriched with antibiotics, 0.2% glycerol, 10% ADC, and 0.05% Tween 80, and incubated at 30^{o}C without shaking for 8 days. The optical density (OD) of the bacterial suspension was measured every 24hr for 7 consecutive days.

2.12 Preparation of single cell for *Mycobacterium marinum*

M. marinum tends to come together and form various sizes of clumps in its culture. Because of this, the processing of the culture is essential to produce homogenous and single-cell preparation for consistent infection dosing and injections (201). The bacterial suspension for injection was prepared following the protocol described by Bernard and his colleagues (202). In brief, the *M. marinum* strain was allowed to grow on Middlebrook 7H10 agar (Becton Dickinson) supplemented with 0.5% glycerol, 10% oleic acid-albumin-dextrose-catalase (OADC) (Becton Dickinson), and kanamycin sulfate in 50µg/ml. The colony of *M. marinum* was picked from the colonies that had been confirmed for the presence of pVV16 plasmid containing our genes of interest and suspended in 7H9 broth enriched with 0.2% glycerol, 0.05%

Tween 80 (Sigma-Aldrich),10% ADC and kanamycin sulfate in 50µg/ml. The bacteria were allowed to grow at 28.5^{o}C until the optical density (OD) at 600nm is 0.8-1. After the bacterial cell was harvested by centrifugation, the sediment was washed three times in sterile PBS. Then, the pellet was re-suspended and repeatedly passed through a 27-gauge needle to reduce the size and abundance of aggregates of the bacteria, and at the same time generating a single cell bacteria. The OD of the re-suspended solution was measured again, and the desired concentration was prepared. To aid the visualization of the process of injection in zebrafish, 0.085% of phenol red (Sigma-Aldrich) was used. Then, the bacterial suspension was either directly used for injection or stored in sterile 20% glycerol in PBS at -80^{o}C until use.

2.13 Infection of zebrafish with *Mycobacterium marinum*

Before injection of zebrafish was performed, the dose of the bacteria was determined based on the optical density of the prepared bacterial suspension and colony-forming unit (c.f.u) recovered from serial dilutions after culturing on the medium containing kanamycin sulfate at 50µg/ml. After the fish was anesthetized in tricaine solution for 3 to 5 min, an injection was performed either through the caudal vein or peritoneal cavity of the zebrafish. About 10^4 c.f.u. of mycobacterial suspension containing either wild-type or transformant strains of *M. marinum* was

injected into a single fish via peritoneum (203) and $5x10^3$ c.f.u through the caudal vein (**Figure 2.5)**. To estimate the number of bacteria injected into the fish, the same volume of the injected bacterial suspension was inoculated on the 7H10 agar medium mixed with kanamycin sulfate at 50µg/ml.

Figure 2.5: Caudal vein injection of transparent zebrafish.

2.14 Assessment of the effects of infection in Zebrafish

After injection with the bacterial suspension was performed, all the injected zebrafish were monitored daily for the presence of signs and symptoms of the disease. Besides, for those injected transparent zebrafish, monitoring of blue fluorescent granuloma signals in the body of alive fish was conducted every two days using a fluorescence microscope. After the infected zebrafish died or were sacrificed, bacteriological and histopathological analysis**,** immunohistochemistry, and culture methods were used to assess directly or indirectly the effect of the infection on the brain tissue.

2.14.1 Histopathological analysis

To examine the presence of mycobacterial infection and pathological changes in the brain of infected zebrafish, the brain tissue was processed and stained. After the infected fish was died or euthanized using an overdose of tricaine solution, the head was cut and cleaned with 70% of alcohol and saline water and preserved in 10% of neutral buffered formalin for 24 hrs. Then, the tissue was rinsed two times in saline water to remove excess formalin and put into 0.5M EDTA for 7 days (204). Then, the tissue was rinsed in saline water again and put into the tissue processor machine (Thermo Scientific Excelsior As Tissue processor). The following subsections explain how the tissue was processed and prepared for observation.

2.14.1.1 Tissue processing

In the tissue processor, different steps such as dehydration, clearing, and wax infiltration were performed. In the dehydration step, the water in the tissue was replaced with alcohol after immersing the tissue in a series of ethanol solutions of increasing concentration (70%, 90% 100%) until water-free alcohol was attained. The next step is the clearing step in which the ethanol in the tissue was replaced with xylene after multiple changes. Then, the tissue was infiltrated with paraffin wax using infiltration sequences.

2.14.1.2 Embedding

After the process of replacing the formalin and water with paraffin wax in the tissue was completed, the embedding of the tissue was performed using a mold. The mold was filled with molten wax and the head, or the brain tissue was carefully placed into it with the desired orientation. The cassette was put on the top of the mold and more molten wax was added to it. Finally, it was solidified on the cold plate and the block with the cassette was removed and kept at $4^{o}C$ until sectioning was done.

2.14.1.3 Tissue sectioning

Sectioning of the embedded tissue was done using a rotary microtome set to the thickness of 4µm and transferred on the microscope slide in the water at $41^{o}C$. After drying the slides, the consecutive tissue sections were stained using Ziehl–Neelsen, hematoxylin and eosin, and immunohistochemical staining techniques to examine

the presence of *M. marinum* bacilli, structural changes, and detection of blue fluorescence protein, respectively, in the tissue.

2.14.1.4 Tissue staining using Ziehl–Neelsen staining

After the tissue sections of the brain of each infected fish were prepared and mounted on the slides, it was stained with Ziehl-Neelsen staining techniques to examine the presence of acid-fast bacilli in the tissue. The tissue staining was performed by using the procedures described previously (205, 206). In short, the tissue sections were first deparaffinized thoroughly in three changes of xylene for 3min each and followed by hydration through dipping the slides 10 times in two changes of each 100% and 95% ethyl alcohols. After the slides were washed well in distilled water and heat dried, it was stained with carbol fuchsin stain for 15 min. The stained slides were rinsed in running tap water for 3min and decolorized in 1% acid alcohol until the color no longer runs off the slides by performing 7 rapid dips. The slides were washed in running water for 3min and rinsed in distilled water. Then, it was counterstained with 0.14% methylene blue stain which was alcoholic, and rinsed in distilled water for 1min. Finally, the slides were dehydrated in two changes of each of 95% and 100% ethyl alcohol and cleared in three changes of xylene by dipping 10 times in each, and a coverslip was applied with LAMB DPX mounting medium (Thermo Scientific).

2.14.1.5 Hematoxylin and eosin staining

To evaluate the pathological changes in the brain tissue of the fish that developed infection in the brain, the tissue section was stained using hematoxylin and eosin staining solution. The tissue section was first deparaffinized by immersing in two xylene changes for 3 and 5min, respectively, and then, put into 100% and 95 % ethanol for 2min each. The slides were washed in running water for 1min and put into Harris hematoxylin for 3min. The slides were washed in water for 1min and decolorized in 1% acid alcohol for 1min. The slides were washed again in water and put in Scott's tap water for 1min each. After washing the slides in water for 1min, they were put in working alcoholic eosin for 30 sec. Then, slides were dipped in 70%, 95 %, and 100% ethanol for 1min each. Finally, the slides were cleaned with two changes of xylene, and the coverslip was applied with the mounting medium to be examined by the microscope.

2.14.2 Immunohistochemistry Analysis

Immunohistochemistry was performed to examine the presence of BFP in the brain tissue sections of those fish positive for the *M. marinum* bacilli in their brain. It was also performed to identify whether the mass of aggregation of cells in the brain and other tissues of the infected fish is leukocytes or not. The immunohistochemical staining of the brain tissue section was performed following the manufacturer's

protocol (Abcam). First, deparaffinization of the tissue section and antigen retrieval methods were performed, and then, followed by the immunohistochemical staining of the tissue.

2.14.2.1 Deparaffinization

Deparaffinization was performed to remove the paraffin in the tissue sections. The slides with tissue sections were allowed to stay in two xylene changes for 3min each and then in xylene 1:1 with 100% ethanol for 3min. After the slides were put in 95% ethanol for 3min, it was cleaned in 75% ethanol and 50% ethanol for 3min each. Finally, the slides were rinsed in running cold tap water and kept in distilled water until the antigen retrieval process was performed.

2.14.2.2 Antigen retrieval

To retrieve the antigen in the tissue sections, a heat-induced epitope retrieval method using a scientific microwave was performed. The deparaffinized and rehydrated sections of the tissues on the slides were put in the microwavable vessel containing Tris-EDTA buffer (10mM Tris Base, 1mM EDTA solution, 0.05% Tween 20, pH 9.0) and placed in a microwave set at 98^{o}C for 20 min. Then, cold tap water was run into the vessel for 10 min to cool the slides.

2.14.2.3 Immunohistochemical staining

After the antigen retrieval process was performed, the slides with the tissue sections were washed two times for 5min each in tris-buffered saline (TBS) plus 0.025% Triton X-100 with gentle agitation. The slides were blocked in 10% fetal bovine serum (FBS) with 1% bovine serum albumin (BSA) in TBS for 2 hours at room temperature. After the slides were drained for a few seconds and the places around the sections were wiped with tissue paper, the primary antibody diluted in TBS with 1% BSA was applied and incubated at 4^{o}C overnight. On the following day, the slides were rinsed two times for 5min in TBS 0.025% Triton with gentle agitation and then incubated in 0.3% H_2O_2 in TBS for 15 min. The secondary antibody diluted in TBS with 1% BSA was applied to the slides and incubated for 1hr at room temperature. Then, the slides were rinsed 3 times in TBS for 5min and

flooded with 3,3' diaminobenzidine (DAB) chromogen for 10 min at room temperature. After the slides were rinsed in running tap water for 5min, it was counterstained using hematoxylin for 20 sec and washed in water for 10 sec. Finally, the slides were dehydrated and cleaned with xylene to be mounted and examined under the microscope.

2.14.3 Bacteriological analysis

2.14.3.1 Brain tissue culture

To examine the presence of *M. marinum* strains in the brain of infected zebrafish, brain tissue was cultured. After the euthanized fish was cleaned three times in saline and disinfected with 70% alcohol, the brain tissue was carefully extracted with hygiene. Then, the tissue was well homogenized in 200µl sterile PBS and 50µl of the mixture was inoculated on the Middlebrook 7H10 agar medium with kanamycin sulfate at 50µg/ml. The culture was incubated for 7-10 days in the incubator at 30^{o}C to observe the growth of the bacteria. DNA was extracted from the recovered colonies, and the presence of BFP and *phoP* genes was confirmed by using PCR in the bacteria.

2.14.3.2 Internal organs culture

After the infected fish were euthanized and cleaned with saline and 70% alcohol, the whole internal organs were collected and homogenized in 1ml PBS. Then, serial dilution was performed from the solution and cultured on the Middle Brook 7H10 agar medium containing kanamycin sulfate at 50µg/ml to estimate the bacterial load in the internal organs. The number of recovered colony-forming bacteria was counted and compared among the treatment and control groups.

2.14.4 Monitoring of granuloma-like signals in alive zebrafish

Two groups of transparent zebrafish were injected with about $5X10^3$ c.f.u of the suspension of either wild-type or transformant strains of *M. marinum* into the caudal vein. After two days of post-infection, fluorescent aggregates of infected immune cells or granuloma-like signals in the body of fish were monitored every 2 days. To observe the signals in the body and brain region, the fish was first anesthetized in tricaine solution and examined under a stereomicroscope as described previously (202).

2.15 RNA extraction from Brain Tissue of Zebrafish

After the brain tissue was carefully isolated from the infected zebrafish, RNA was extracted using the RNeasy Mini Kit (cat. nos. 74104 and 74106, Qiagen) protocol. Briefly, the brain tissue was mixed with 350µl buffer RLT and homogenized using tissueRuptor. The mixture was centrifuged for 3min at 14,000rpm and the supernatant was removed and well mixed with 350µl 70% ethanol. Using the RNeasy Mini spin column, 700 µl of the mixture was centrifuged for 15sec at 8000 x g. About 700µl Buffer RW1 was added to the spin column and centrifuged at 8000 x g for 15 sec. Buffer RPE (500µl) was added to the spin column and centrifuged again at the same condition. Then, the same amount of the Buffer RPE was added to the spin column and spun for 2min at 8000 x g. To dry the membrane, the spin column was centrifuged for 1min at full speed. Finally, the spin column was put in a new 1.5ml tube and 40µl RNase-free water was added to the spin column and centrifugated at 8000 x g for 1min to elute the RNA.

2.15.1 Removal of genomic DNA from RNA

To remove the genomic DNA from the total RNA, a mixture containing 1µg total RNA, 1µL of 10X reaction buffer with $MgCl_2$, 1µL DNase I, and nuclease-free water was incubated at 37^{o}C for 30 min. To terminate the reaction, 1µL of 50mM EDTA was added to the solution and incubated for 10 min at 65°C.

2.15.2 First-strand cDNA synthesis

The first stranded DNA was generated by using the protocol in the kit of the RevertAid First Strand cDNA Synthesis (Thermo Fisher, K1621). Briefly, a total volume of 12µL containing 40ng of RNA, 1µL of primer Oligo (dT)18, and nuclease-free water was first mixed and incubated at 65°C for 5min and then chilled on ice. After 4 µL 5X reaction buffer, 1µL RiboLock RNase inhibitor (20 U/µL), 2µL 10 mM dNTP Mix and 1µL RevertAid M-MuLV RT (200 U/µL) were added to the mixture, the solution was mixed gently and incubated for 60 min at 42°C. The reaction was terminated by incubating at 70°C for 5min and stored at -20°C until used for qPCR analysis.

2.15.3 qPCR Analysis

The ViiA 7 Real-time PCR System (Applied Biosystems) was used to analyze the expression level of the pro-inflammatory cytokines (TNF-α, IL-1ß) in the brain tissue of wild-type, treatment and control groups of zebrafish following the manufacturer's protocol. A total volume of 10µl reaction containing,5µl of power Track SyBR Green master mix, 1µl of DNA, 0.5µl of forward and reverse primers, and 3.4µl of nuclease-free water was used. The qPCR was performed with the conditions of an initial incubation at 50^{o}C for 2min, 1cycle enzyme activation at 95^{o}C for 2min, 40 cycles of 95^{o}C for 15 sec followed by incubation at 60^{o}C for

1minute. The primers we used for the PCR were listed below in **Table 2.5.** The expression levels of the TNF-α and IL-1ß between the zebrafish infected with wild-type and the zebrafish infected with the transformant *M. marinum* were determined. The fold changes were computed using the $2^{-\Delta\Delta CT}$ (207). The Ct value of each gene was calculated using ß-actin as a reference gene.

Table 2.5: List of target genes and primers used for qPCR analysis.

Gene	Primer name	Primer sequence (5'-3')	Length	Tm
TNF-α	TNF	GGTGTCTAGGAGGAAAGCTGG	21	59.79
	TNR	CCTGGGTCTTATGGAGCGTG	20	60.18
ß-actin	ß-acF	CACTGAGGCTCCCCTGAATC	20	59.82
	ß-acR	CGTACAGAGAGAGCACAGCC	20	60.18
IL-1ß	IL-1F	GGCATGCGGGCAATATGAAG	20	60.04
	IL-1R	TGTAGCTCATTGCAAGCGGA	20	60.04

Tm: melting temperature, F: forward, R: reverse

2.16 Data Analysis

The gene expression data from RT-qPCR were analyzed using GraphPad Prism 8 Software (GraphPad Software Inc., La Jolla, CA, USA) and were presented as means ± standard deviation (SD). The fold changes in the expression level of the target gene and the mean OD at 600nm were compared between the wild-type and transformant *M. marinum* strains using a t-test. The t-test was also used to compare the bacillary load differences in the brain and internal organs culture of wild-type-infected zebrafish and transformants-infected zebrafish. A Chi-square test was used to compare the survival rates between the zebrafish infected with wild-type and transformants-infected zebrafish. Fisher's exact test was used to compare the differences between the infectivity of wild-type and transformant *M. marinum* in the zebrafish. The differences were considered statistically significant if a *P*-value <0.05.

CHAPTER 3: RESULTS

This chapter presents the findings obtained from the conducted experiments in the preceding chapter. The first section of the chapter presents cloning and transformation results, differential expression of the *phoP* gene in the transformant *M. marinum*, and its effect on the growth rate of the mycobacterium. The second section describes the effects of transformant *M. marinum* on the survival rates of infected zebrafish, and the bacteriological and pathological feature differences between the transformant and control strains in the brain of the zebrafish. The third section explains the association of brain infection with the death of zebrafish. Lastly, it demonstrates the results of detection and monitoring of blue fluorescent granuloma-like signals or aggregates in the body and brain of transparent zebrafish models, and the proinflammatory cytokines (TNF-α and IL-1β) level differences in the brain of the control-infected zebrafish and transformant-infected group.

3.1 Cloning of *phoP* gene and blue fluorescence protein gene into pVV16 mycobacterial plasmid

To obtain the target genes, the DNA regions corresponding to the *phoP* gene (744bp) and blue fluorescent protein gene (702bp) were amplified from the genome of *M. tuberculosis* H37Rv and plasmid pME-loxP-mTagBFP2-stop-pA-loxP, respectively, using PCR. Gel electrophoresis of the PCR products showed the presence of the target DNA segments in the products using the 100bp marker ladder (**Figure 3.1**). Following the purification of the PCR products, the inserts (*phoP* and BFP gene) and pVV16 plasmid were separately digested using the Hind III and Nde I restriction enzymes. After the digestion products were purified, the BFP gene was successfully cloned to the pVV16 plasmid. Both the *phoP* and BFP gene segments were also successfully cloned into a single pVV16 plasmid. To seal the gaps (nick) between the plasmids and the inserts, and to get a high copy number of the plasmids, the recombinant plasmids were transferred into the competent cells of *E. coli* Dh5α using chemical transformation. The growth of the transformant *E. coli* Dh5α on the Luria-Bertani (LB) agar medium with kanamycin sulfate (**Figure 3.2**) and the colony PCR (**Figures 3.3 A and B)** showed the presence of the recombinant pVV16 inside the transformants.

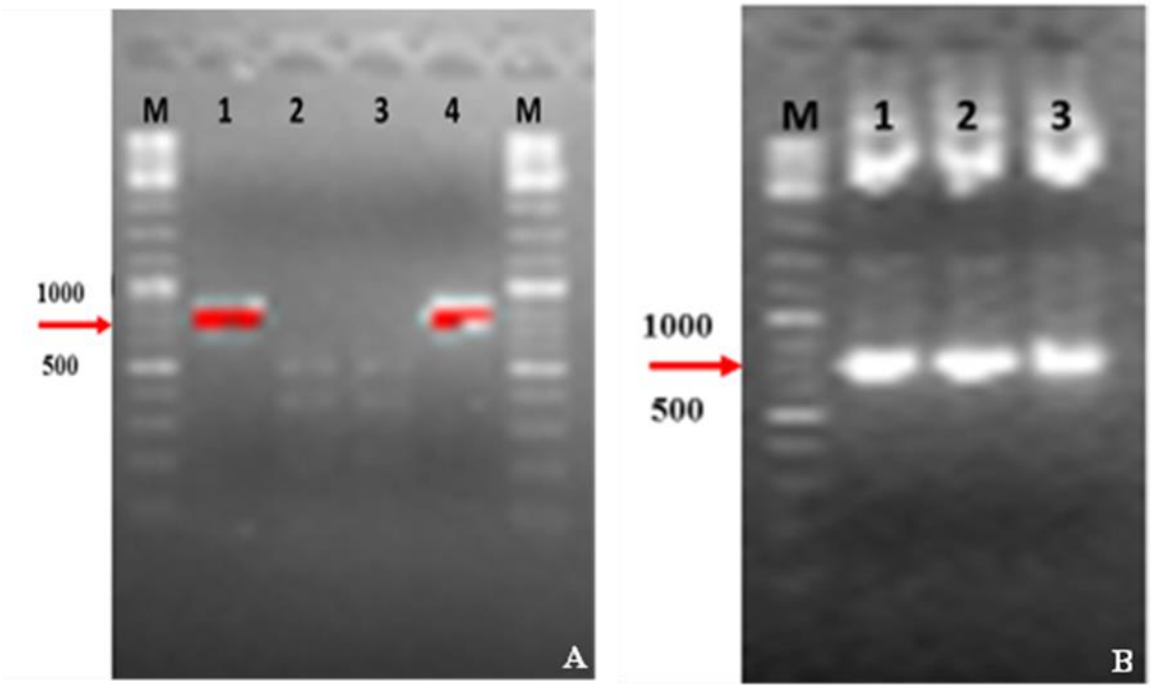

Figure 3. 1:The presence of product size of the *phoP* gene and BFP gene in the PCR products. In picture **A**, lane M represents the 100bp ladder. Lanes 1 and 4 show the bands corresponding to the product size (744bp) of the *phoP* gene; **B**, Lanes 1, 2, and 3 indicate the bands representing the product size (702bp) of the BFP gene.

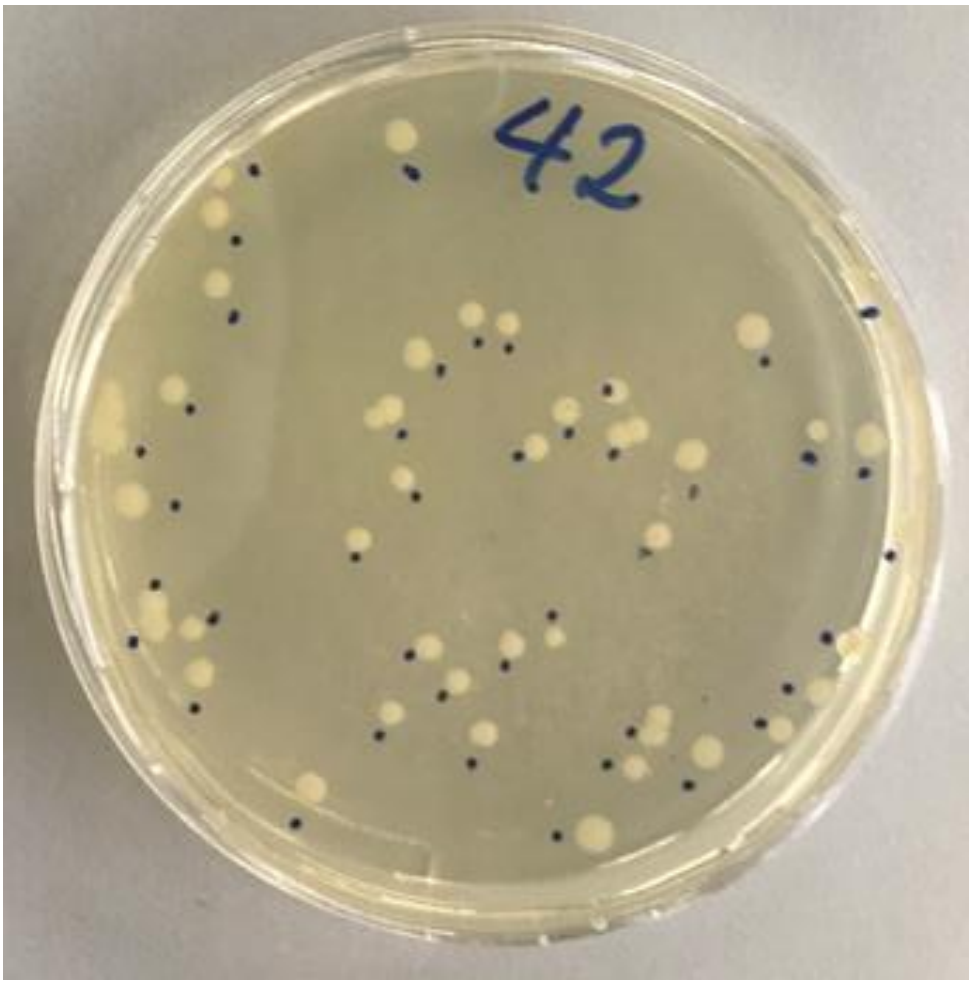

Figure 3. 2: Colonies of *E. coli* appeared on Luria-Bertani agar medium containing kanamycin sulfate after chemical transformation of *E. coli* Dh5α with recombinant pVV16-*phoP* gene-BFP gene plasmid.

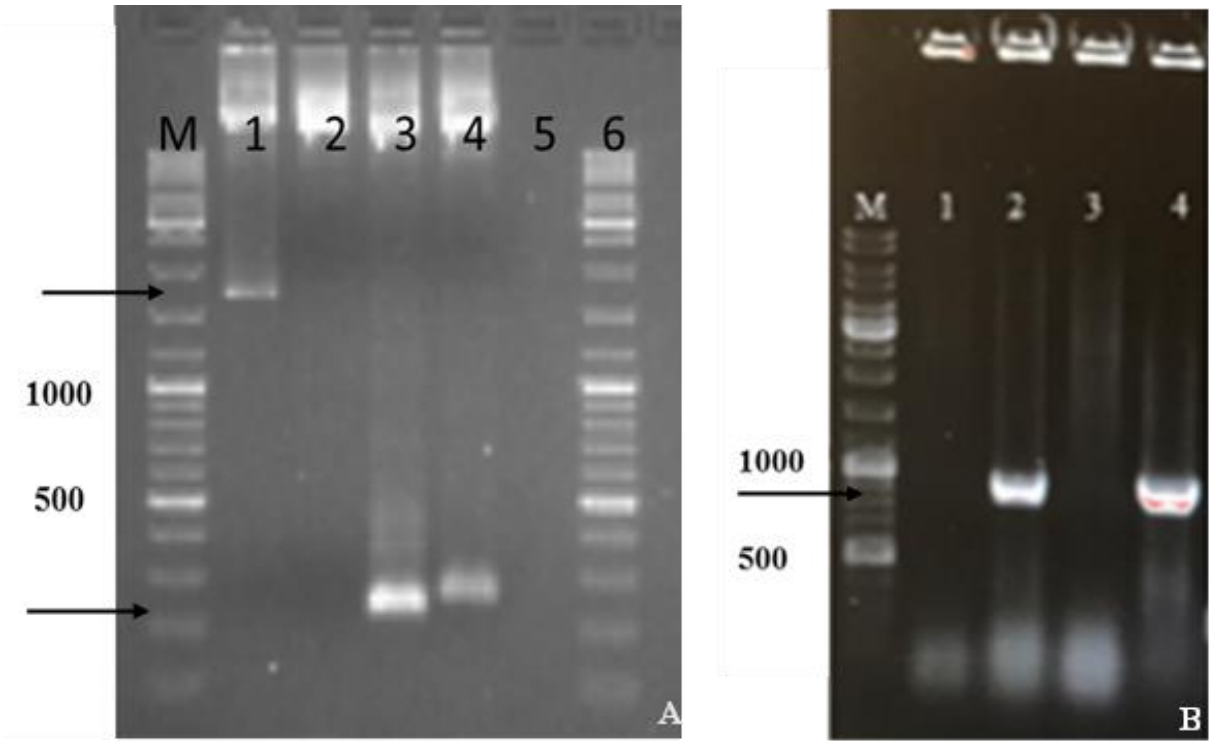

Figure 3. 3: Gel electrophoresis of PCR products from recovered transformant *E.coli* on the culture plate showing the presence of recombinant pVV16-*phoP* gene-BFP gene plasmid in the bacteria. **A**, Lane 1 represents the *phoP* gene+BFP gene segment in the pVV16 plasmid, lane 3 represents the pVV16+*phoP* gene overlap region (left side) (236bp), and lane 4 indicates the BFP gene +pVV16 plasmid overlap region (right side) (261bp). **B** shows the presence of blue fluorescent protein gene product size in the PCR products. Lanes 2 and 4 in picture B show the band related to the size (702bp) of the blue fluorescent protein gene.

3.2 Transformation of *M. marinum* with recombinant *pVV16-BFP gene* plasmid

Transformation by electroporation was performed on the competent cells of *M. marinum* to transfer the blue fluorescent protein gene that ligated to the pVV16 vector into *M. marinum.* Consequently, the transformant *M. marinum* was able to grow on Middlebrook 7H10 agar medium mixed with kanamycin sulfate (**Figure 3.4A**). The blue fluorescent *M. marinum* was also detected in the recovered colonies under the Leica TCS-SPE confocal microscope (**Figure 3.4B**). Moreover, the PCR products amplified from the recovered colonies of transformants confirmed the presence of the BFP gene in the transformants (**Figure 3.4C**). These show that the recombinant *pVV16-BFP gene* plasmid was successfully transferred to the *M. marinum.*

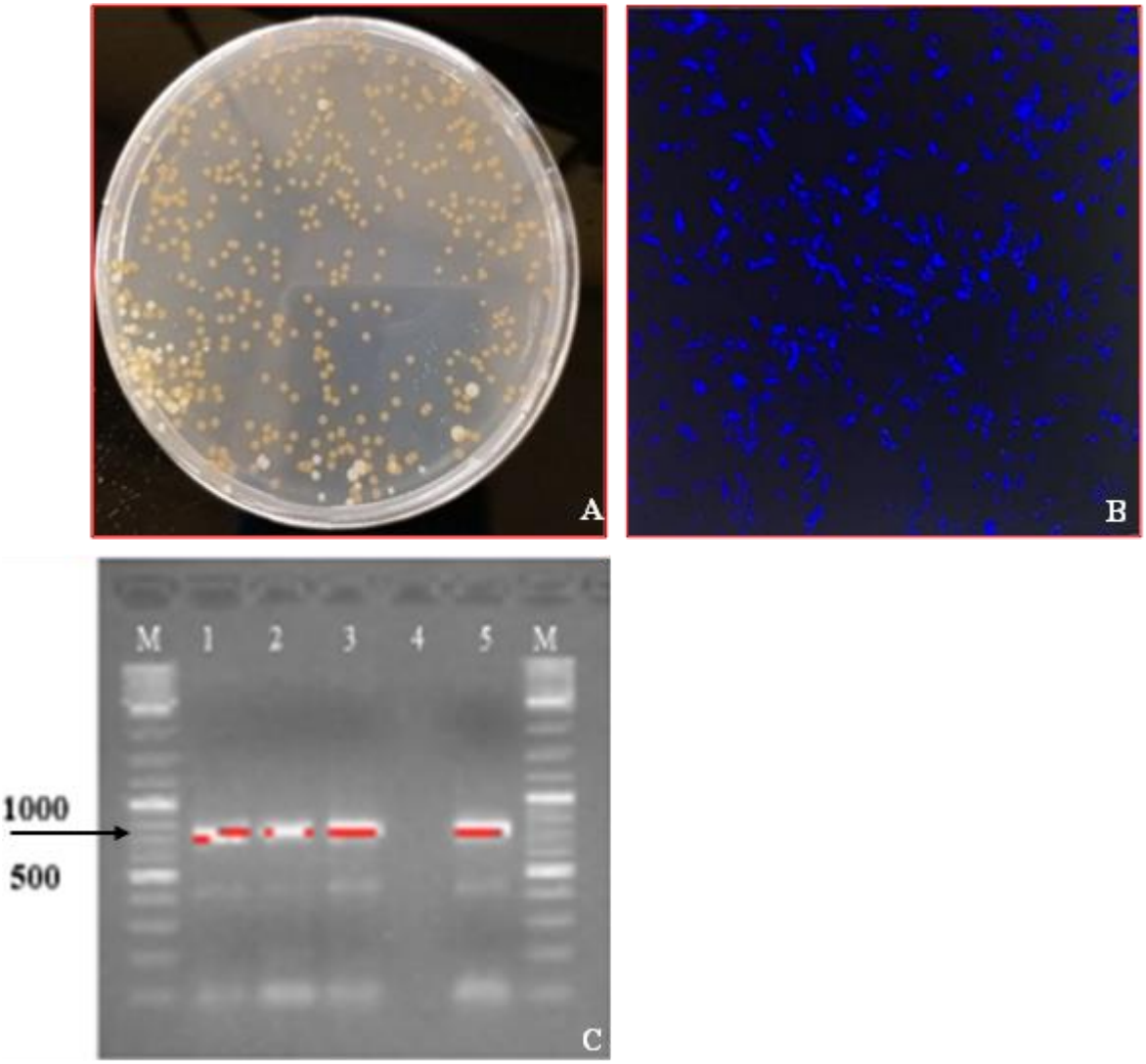

Figure 3. 4: Successful transformation of *M. marinum* with recombinant pVV16-BFP gene plasmid. **A** shows colonies of *M. marinum*; **B** indicates the blue fluorescent *M. marinum* in the recovered colonies under the confocal microscope(63X). In picture **C**, lanes 1, 2, and 3 represent the band corresponding to BFP gene size (702bp), lanes 4 and 5 represent negative (distilled water) and positive (BFP gene from its source) control, respectively.

3.3 Transformation of *M. marinum* with recombinant *pVV16-phoP gene-BFP gene* plasmid

Blue fluorescent, *phoP*-overexpressed *M. marinum* mutant (transformant) was constructed by transferring the recombinant *pVV16-phoP gene-BFP gene* plasmid into the *M. marium* using electroporation. Colonies of the recovered transformants appeared on the medium containing kanamycin sulfate (**Figure 3.5A).** PCR was performed on the DNA extracted from the recovered colonies and showed the presence of both genes in the transformants (**Figure 3.6A and B).** Sanger sequencing analysis confirmed the absence of mutation in the inserted gene (**Figure 3.7**) and confocal microscopy validated the expression of BFP in the transformants (**Figure 3.5B**).

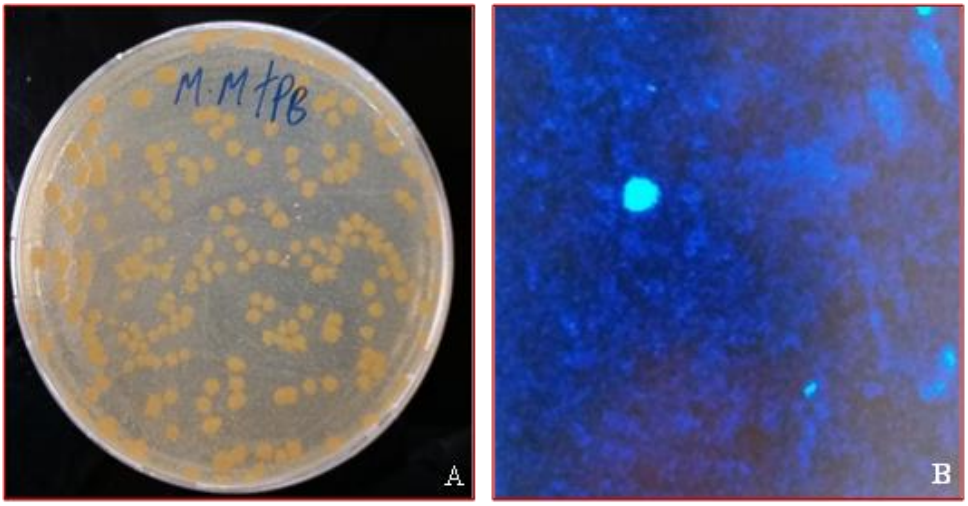

Figure 3. 5: Transformation of *M. marinum* with recombinant pVV16-*phoP* gene-BFP gene plasmid. **A** shows colonies of transformant *M. marinum*. **B** depicts blue fluorescent, transformant *M. marinum* from the recovered colonies indicating the presence of the plasmid pVV16 with *phoP* and BFP genes inside the transformants.

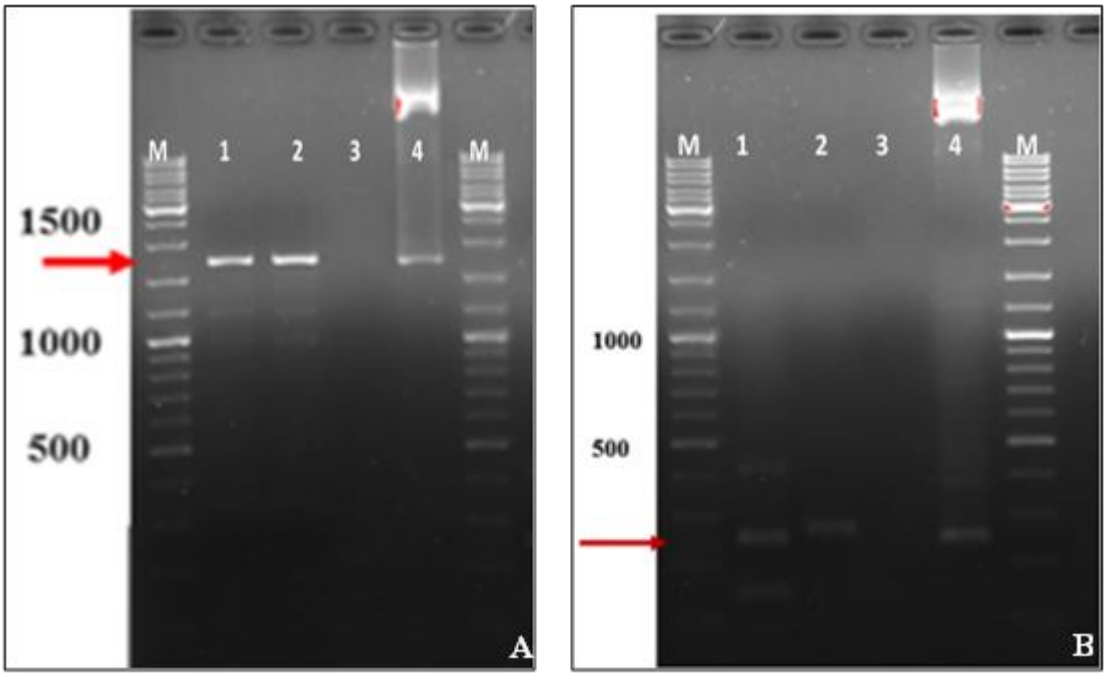

Figure 3. 6: The gel electrophoresis of PCR products performed on DNA extracted from colonies of transformants. **A**, Lanes 1 and 2 show positive bands representing the product size of the insert consisting of BFP and phoP genes together. Lanes 3 and 4 indicate negative (water) and positive control(PCR product contains the inserts that were amplified from the plasmid before the plasmid transferred into the *M. marinum*), respectively; **B**, Lane 1 represents the plasmid pVV16 + *phoP* gene overlap region (236bp) on the left side and lane 2 represents the BFP gene segment + pVV16 plasmid overlap region on the right side (261bp). Lanes 3 and 4 represent negative (water)and positive(PCR product contains the same length of DNA) control, respectively.

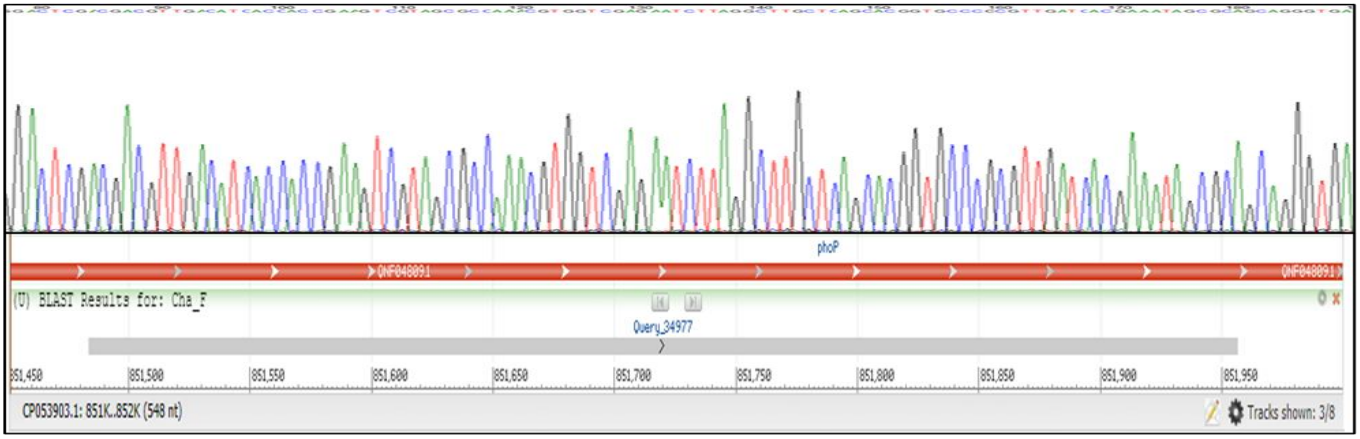

Figure 3. 7: Sanger sequencing analysis of the DNA segment of the *phoP* gene in the colonies of recovered transformant *M. marinum* and BLAST alignment with the target region of the gene in the genome of *M. tuberculosis* H37Rv strain. (BLAST: Basic Local Alignment Search Tool).

3.4 *phoP* gene was differentially expressed in transformant *M. marinum*

Both control and transformant strains of *M. marinum* were allowed to grow in the 7H9 broth medium mixed with kanamycin sulfate at 50µg/ml until its logarithmic phase. To determine the mRNA level of the *phoP* gene in the transformants, RNA was extracted from the broth culture of both strains and analyzed using qPCR. The results showed that the expression level of the *phoP* gene in the transformant strain was about 3-fold increased relative to that of the wild-type strain (P=0.0241) (**Figure 3.8**).

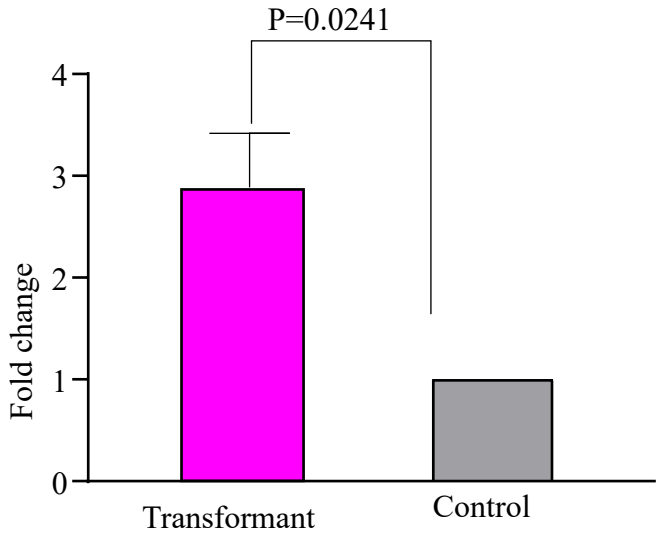

Figure 3. 8: The quantitative real-time PCR analysis of the phoP gene expression level of transformant compared to that of the control strain (n=3).

3.5 Differentially expressed *phoP* gene increases the in-vitro growth of *M. marinum*

Growth curve experiments were conducted for control and transformant *M. marinum* strains to determine the effects of the differentially expressed *phoP* gene on the in-vitro growth of *M. marinum*. Both strains were allowed to grow in 7H9 mixed with kanamycin sulfate under similar conditions. The culture optical density was measured every day for seven consecutive days, and the results indicated that the growth of the transformant strain was more rapid than that of the control strain (P=0.0712) (**Figure 3.9)**, suggesting the presence of physiological differences between the two strains.

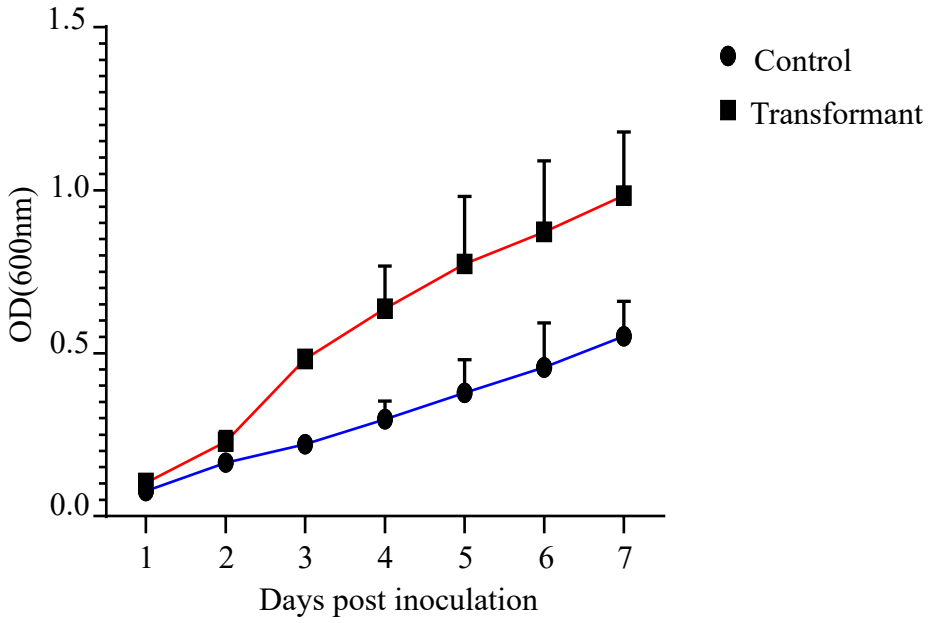

Figure 3. 9:The in-vitro growth differences between the control and transformant strains of *M. marinum* (P=0.0712). (OD: Optical density).

3.6 Transformant *M. marinum* infection reduced the survival rate of zebrafish

Three groups of zebrafish were injected with the transformant *M. marinum* strain (n=19), control strain (n=19), and uninfected (n=19), and followed for 15 days to compare the virulence of the infections based on the survival rate of zebrafish. The result indicated that transformant-infected zebrafish showed a lower survival rate (36.8%) than that of the control strain infected zebrafish (68.4%) though the discrepancy did not reach the statistically significant level (P=0.0809) as indicated in **Figure 3.10**.

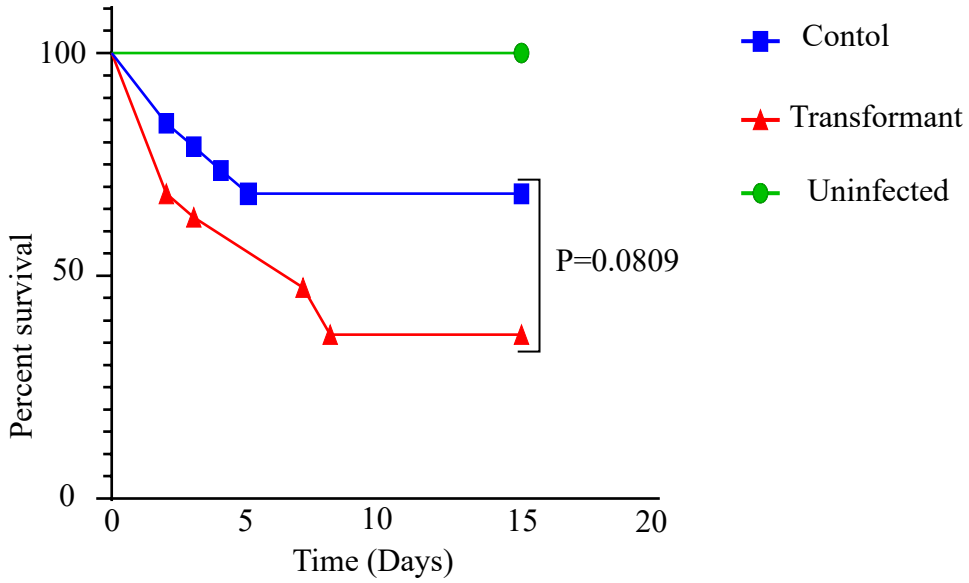

Figure 3. 10: The survival rate differences between zebrafish infected with transformant and control strains of *M. marinum*. The green line in the graph represents the survival rate of uninfected zebrafish. The blue and red lines represent the survival rate of those zebrafish infected with control strain and transformant, respectively.

3.7 Transformant *M. marinum* was more infective than the control strain in the brain of zebrafish

In the bacteriological study, groups of zebrafish were infected with transformant strain (n=64), control strain (n=64), and uninfected (n=58). Fifty seven and 7 zebrafish were infected with *M. marinum* E11 and *M. marinum* strain M, respectively, in both transformant and control infected groups. Brain tissue was removed when zebrafish died or on day 30 after infection and histopathologically analyzed for acid-fast bacilli (AFB) microscopic examination (n=52 which includes 19 zebrafish for which survival rate was determined and 33 zebrafish that were not included in the survival rate evaluation), and bacteriological culture (n=12) for each transformant and control strain.

By using AFB microscopy, bacilli were detected in the processed, sectioned, and Ziehl–Neelsen stained brain tissue of 23.1% (12/52) and 5.8% (3/52) zebrafish infected with transformant *M. marinum* E11 and control *M. marinum* E11, respectively. From the results, it is observed that some zebrafish developed brain infections and most of the fish did not in both strains infected groups. This might be related to the biological and physiological system differences among the fish, the ability of the bacterial strains to evade the host immune system and cross the blood-brain barrier membrane, and environmental factors. As it is observed from

the visual comparison of microscopic images below, the number of bacilli in the brain tissue of the transformant-infected zebrafish was more abundant than that of the control group (**Figure 3.11 a and b**). The bacillary load detected in the brain tissue of each zebrafish was measured by using the semi-quantitative grading system described previously (208). The bacillary load detected in the brain of transformant *M.marinum* E11 infected zebrafish ranged from few (2+) to numerous(4+) whereas it was limited to rare(1+) and moderate(3+) for zebrafish infected with control *M. Marinum* E11(**Table 3.1)**.

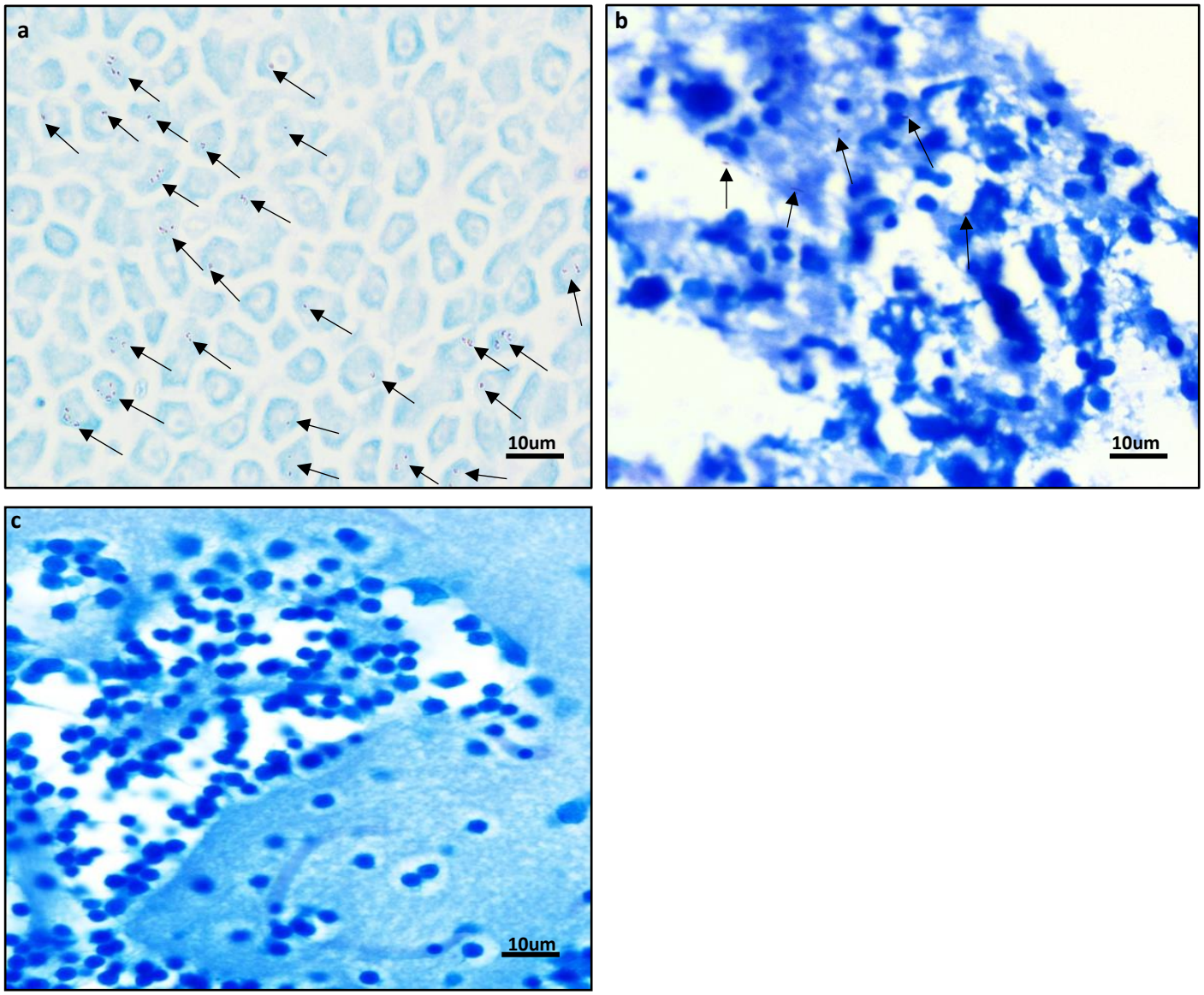

Figure 3. 11: The presence of bacilli in the brain tissue of zebrafish injected with transformant and control strains of *M. marinum* E11. Picture **a** is a representative image containing numerous Ziehl-Neelsen stained bacilli (black arrows) in the brain tissue section of zebrafish that were euthanized 30 days post-infection with the transformant strain; **b** indicates the bacilli (black arrows) in the brain tissue section of zebrafish euthanized at 30 days after infection with control strain; **c** shows the stained brain tissue section taken from uninfected zebrafish (100X).

Table 3. 1: The grade of mycobacterial load detected in the brain tissue section of infected zebrafish.

Infection agent	Total fish developed infection	Mycobacterial load grade and number of fish affected			
		Rare(1+)	Few(2+)	Moderate(3+)	Numerous(4+)
Control	3	1	-	2	-
M. marinum					
Transformant	12	-	3	5	4
M. marinum					

Note: Rare: 1-9 bacilli per 100 fields; Few: 1-9 bacilli per 10 fields; Moderate: 1-9 bacilli per field; Numerous: >9 bacilli per field (208).

AFB culture was also done for the brain tissues collected from a subset of 12 zebrafish of each group. For the control group, only 8.33% (1/12) of zebrafish infected with *M. marinum* strain M was culture positive with the bacterial load of 8 c.f.u, whereas 50% (6/12) of the transformant group was positive with the bacterial load ranging from 8–192 c.f.u **(Figure 3.12).** Among the culture-positive cases under the transformant-infected group, 3 fish with c.f.u of 8, 8, and 36 were from *M. marinum* strain M infected and the other 3 with the c.f.u of 44,160, and 192 were from E11 infected group. The brain tissue of all the zebrafish was extracted 30 days post-infection. The number of mycobacteria recovered from the brain culture of the transformant-infected zebrafish was higher than that of the control strain infected zebrafish (P=0.0706). No growth was seen from the uninfected group.

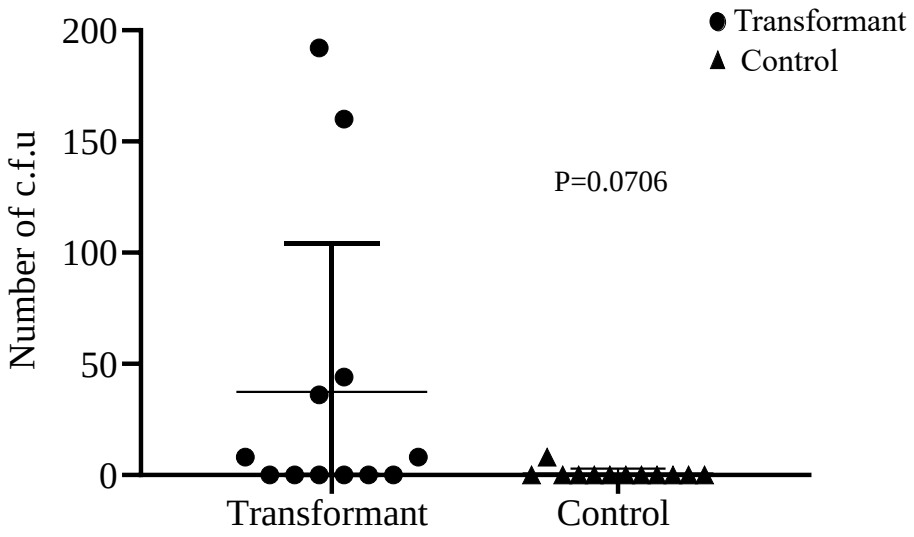

Figure 3. 12: The bacillary load in the brain tissue of zebrafish infected with the control strain (n=12) and transformant (n=12). The brain tissue was extracted from all zebrafish 30 days post-infection. Three zebrafish were culture positive from each group of zebrafish infected with transformant *M. marinum* strain M (n=7) and E11(n=5). Only one was culture positive from zebrafish infected with the control *M. marinum* strain M. The black dot represents the individual zebrafish infected with the respective strain. (c.f.u: colony-forming unit).

AFB were detected in the colonies recovered from the brain culture using Ziehl-Neelsen staining. The presence of the *phoP* gene and blue fluorescent protein gene was also confirmed in the colony PCR of acid-fast bacilli positive brain culture **(Figure 3.13)**. Moreover, blue fluorescent *M. marinum* strains were observed in the recovered colonies under confocal microscopy.

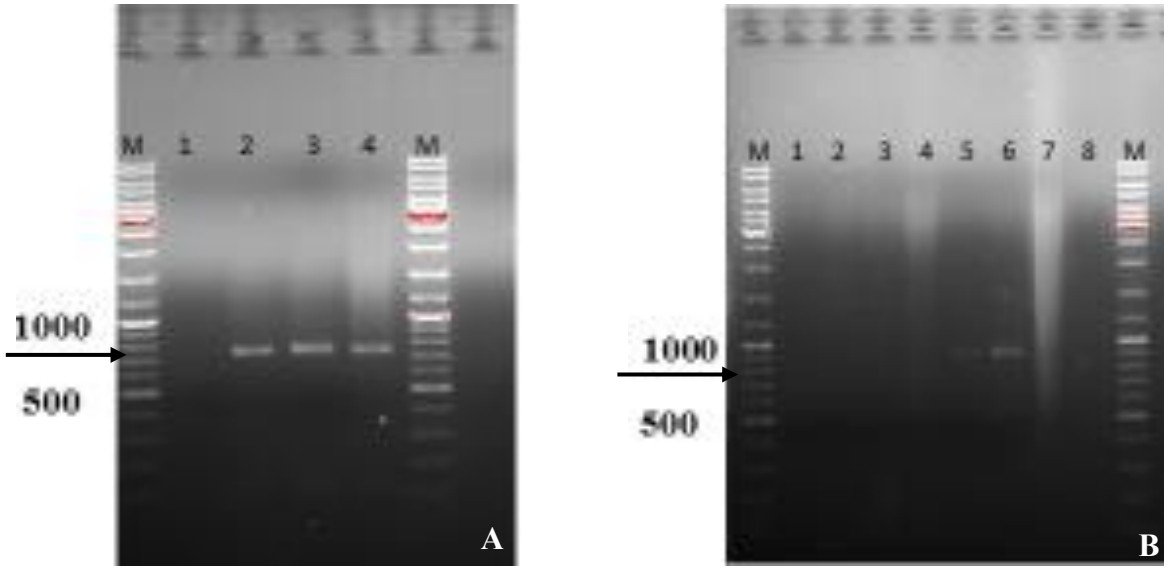

Figure 3. 13: Gel electrophoresis of PCR products amplified from colonies recovered from brain culture of zebrafish. **A** shows the presence of the blue fluorescent protein (BFP) gene in the colonies of *M. marinum*. Lane 2, 3, and 4 represent positive bands for BFP gene (702bp) and were obtained from the brain of the zebrafish infected with the transformant strain of *M. marinum* E11. Lane 1 shows a negative result for the BFP gene in colony PCR. In picture **B**, lanes 5 and 6 represent positive bands for the *phoP* gene(744bp) indicating the presence of the transformant with the target genes. The other lanes show negative results in colony PCR products.

By combining the AFB microscopy and brain culture results, 6.25% (4/64) of zebrafish infected with the control *M. marinum* developed brain infection, whereas 28.13% (18/64) of infected zebrafish in the transformant *M. marinum* group had brain infection (P=0.0018), showing that the transformant *M. marinum* with overexpressed *phoP* gene is significantly more neurotropic than the control strain **(Figure 3.14).** The combination of the results was based on the presence or absence of the bacilli in the brain of the infected zebrafish.

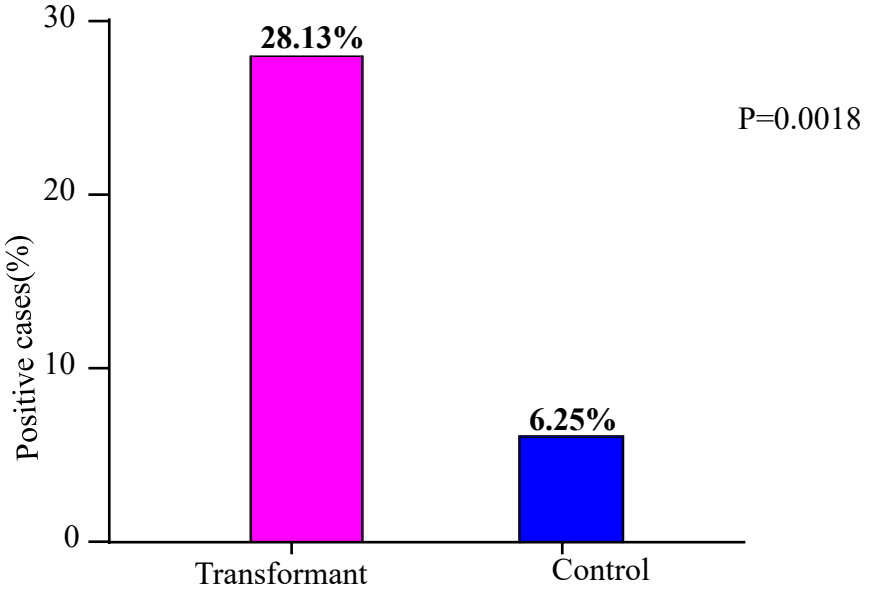

Figure 3. 14:The proportion of zebrafish that developed infection in their brain tissues after injection with transformant strain of *M. marinum* relative to that of the control-injected zebrafish**.**

Moreover, the internal organ culture of some of the zebrafish infected with the control strains (n=22) and transformant strains (n=22) was performed on the Middlebrook 7H10 agar medium containing kanamycin sulfate to evaluate the mycobacterial load difference in the zebrafish body between the two strains. Of the control-infected zebrafish, the internal organs of 59.1%(13/22) were positive for the bacilli with the bacterial load ranging from 10^2-5.4X10^5c.f.u., whereas 59.1%(13/22) of transformant-infected zebrafish were positive for *M. marinum* with the mycobacterial burden ranging from 20 to 1.4X10^6 c.f.u. (P=0.2753) **(Figure 3.15).** No growth was seen for the uninfected group.

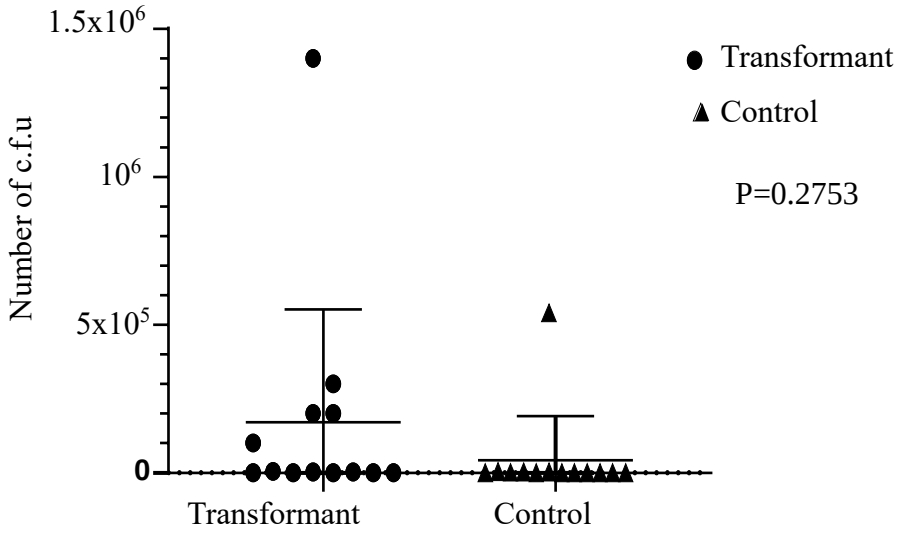

Figure 3. 15: Bacillary load in the internal organs of zebrafish infected with control and transformant strains. The black symbol represents the individual zebrafish.

3.8 The pathological features of transformant *M. marinum* E11 infected zebrafish

Examination of the brain tissue sections stained with hematoxylin and eosin was performed for all acid-fast bacilli-positive brain tissues in Ziehl-Neelsen stained tissue sections. The result showed the presence of granuloma-like lesions or aggregates of immune cells (n=11) in transformant *M.marinum* E11 infected zebrafish (n=4) but not in those control strain infected zebrafish (**Figure 3.16**). In addition to the brain infection, the transformant strains were also found in the tissue adjacent to the brain and resulted in the infiltration of distorted cells in the tissue (**Figure 3.17b and c**)**.** Conversely, no structural changes were observed in similar regions in the control strain infected zebrafish (**Figure 3.17e and f**).

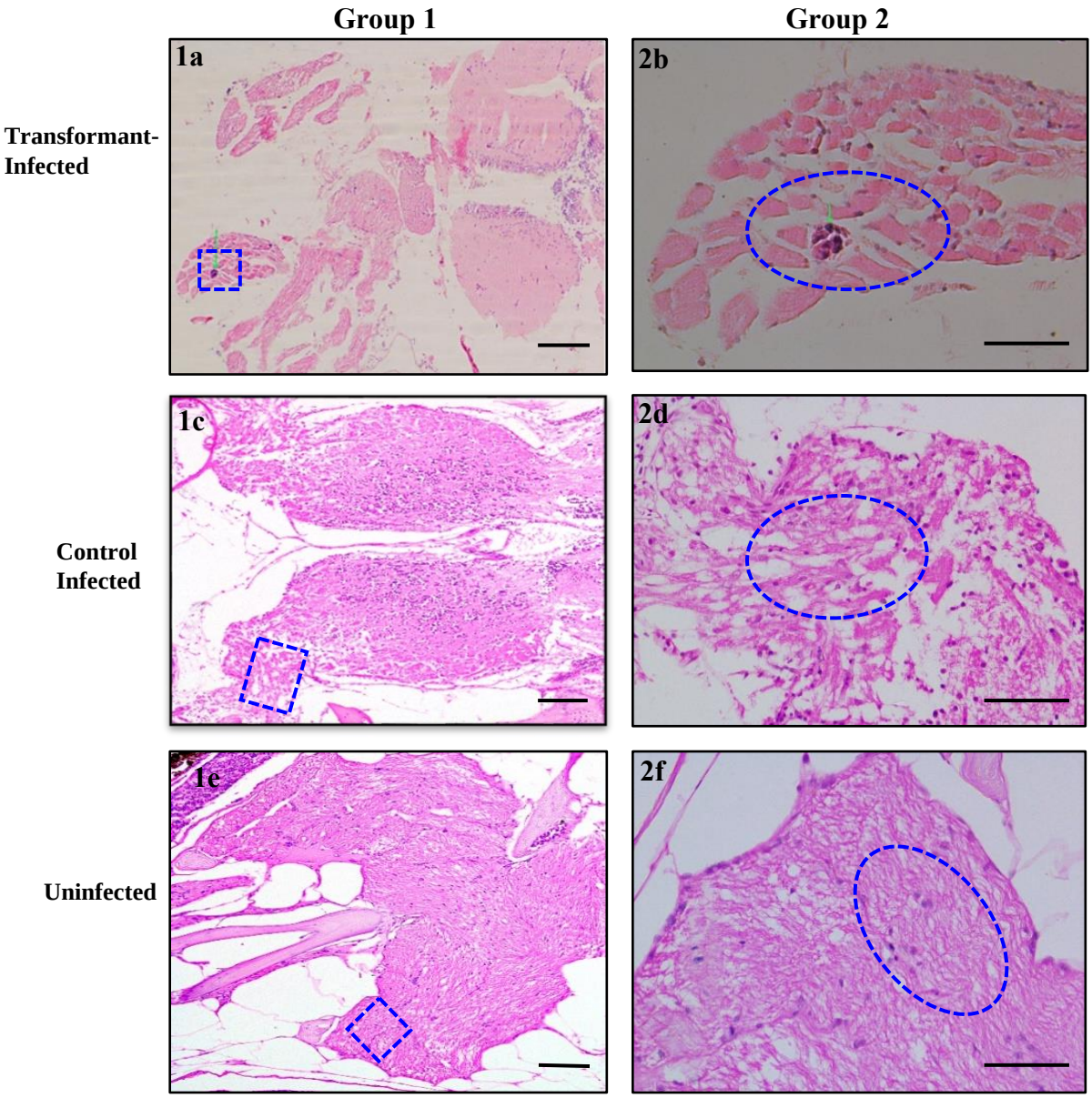

Figure 3. 16: Brain tissue sections of injected zebrafish stained with hematoxylin & eosin staining. Under **group 1**, picture **a** shows the granuloma-like lesion and the large overview of the surrounding area of the brain tissue of transformant *M. marinum* E11 infected zebrafish; **c** and **e** indicate the similar region without the granulomatous structure in the brain of control *M. marinum* E11 infected zebrafish and uninfected fish, respectively. Scale bars for **a, c,e** =200um. In **group 2**, **b** shows the enlarged granuloma-like lesion and, **d** and **f** show the enlarged similar region in control and uninfected zebrafish, respectively. Scale bars for **b, d, f** =50um.

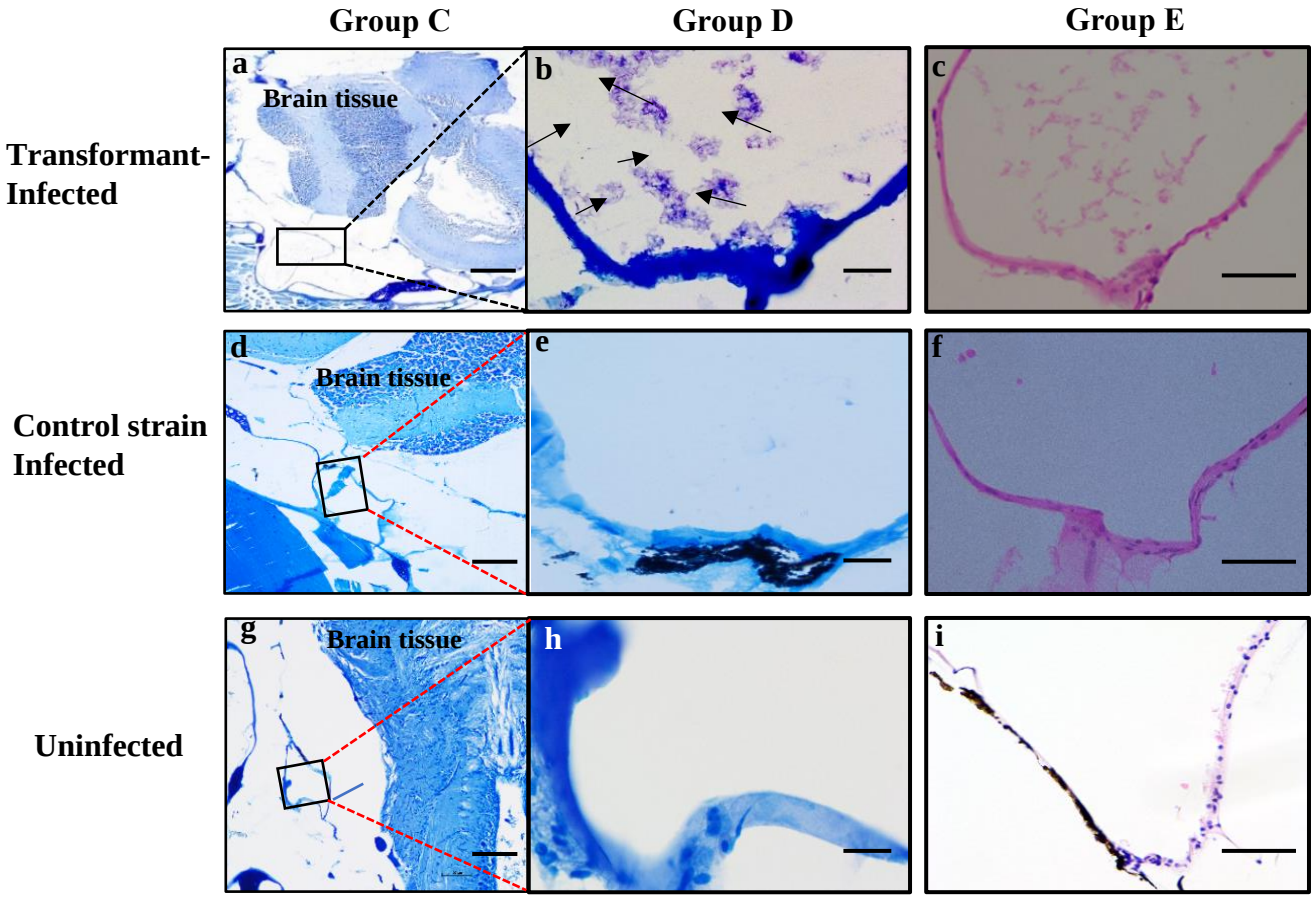

Figure 3. 17: Mycobacterial bacilli in the tissue adjacent to the brain of transformant *M. marinum* E11 infected zebrafish and pathologically affected tissue compared with that of the control and uninfected zebrafish. Boxed areas represent parts of the tissues adjacent to the brain. **Group C** shows the large overviews of the adjacent tissue to the brain from transformant-infected zebrafish **(a**), unaffected adjacent tissue taken from control (**d**), and uninfected zebrafish (**g**) (10X). Scale bar for **a, d, g**=200um. The black arrows in picture **b** indicate Ziehl-Neelsen stained bacilli in the infected tissue (100X); **e** and **h** present the tissue taken from the control infected fish and uninfected fish, respectively, with no bacilli inside (100X). Scale bar for **b, e, h**=10um. **Group E** describes the tissues prepared from their respective zebrafish and stained with hematoxylin and eosin staining: **c** shows structural changes in the infected adjacent tissue (40X); **f** and **i** indicate the absence of structural changes in the tissues of control infected fish and uninfected fish (40X), respectively. Scale bars for **c, f, i** =50um.

.

3.9 Immunohistochemistry analysis of the brain tissue

Immunohistochemistry staining was performed on the brain tissue sections of the zebrafish with positive AFB microscopy. The results demonstrated the existence of the BFP expression in the brain tissues (**Figure 3.18**), confirming the presence of the *M. marinum* strains transformed with the BFP gene (i.e. control *M. marinum* and transformant *M. marinum)*.

The immunohistochemical staining with anti-L-plastin antibody was also conducted and identified aggregated leukocytes in granuloma-like lesions in the brain tissue of the zebrafish infected with transformant strain (**Figure 3.19d)**.

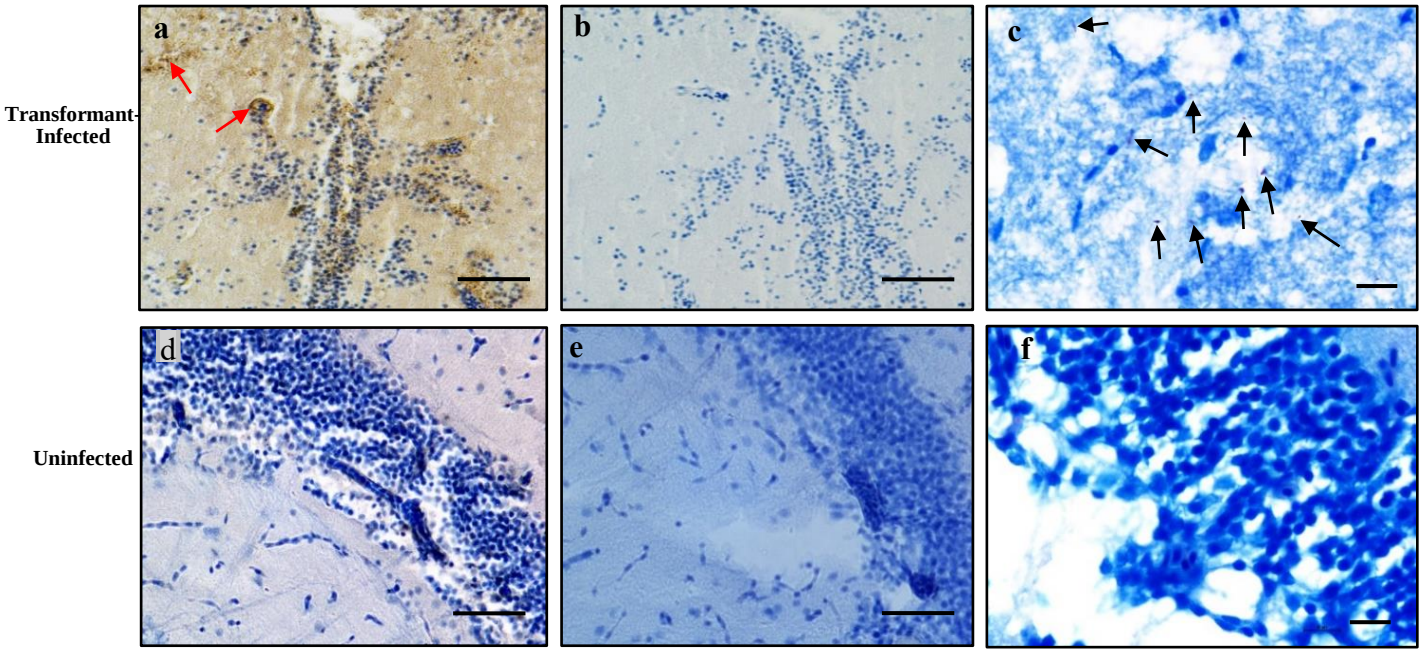

Figure 3. 18: The presence of blue fluorescence protein (red arrows) in the brain tissue section of transformant-infected zebrafish. Pictures **a, b**, and **c** were prepared from the same brain tissue of transformant-injected zebrafish. **a** is immunohistochemistry stained brain tissue based on peroxidase using an anti-blue fluorescent protein antibody. **c** indicates the presence of Ziehl-Neelsen (ZN) stained *M. marinum* bacilli (black arrows) in the same brain. Pictures **d, e**, and **f** are taken from the same brain of the control zebrafish. **d** is positive anti-blue fluorescent protein antibody control and showed the absence of the blue fluorescence protein in the control brain. **b** and **e** are negative anti-blue fluorescent protein antibody controls. **f** was the ZN-stained brain tissue section of the control fish and showed the absence of the bacilli in the tissue. Scale bar for **a,b,d,e**=50um, **c,f**=10um.

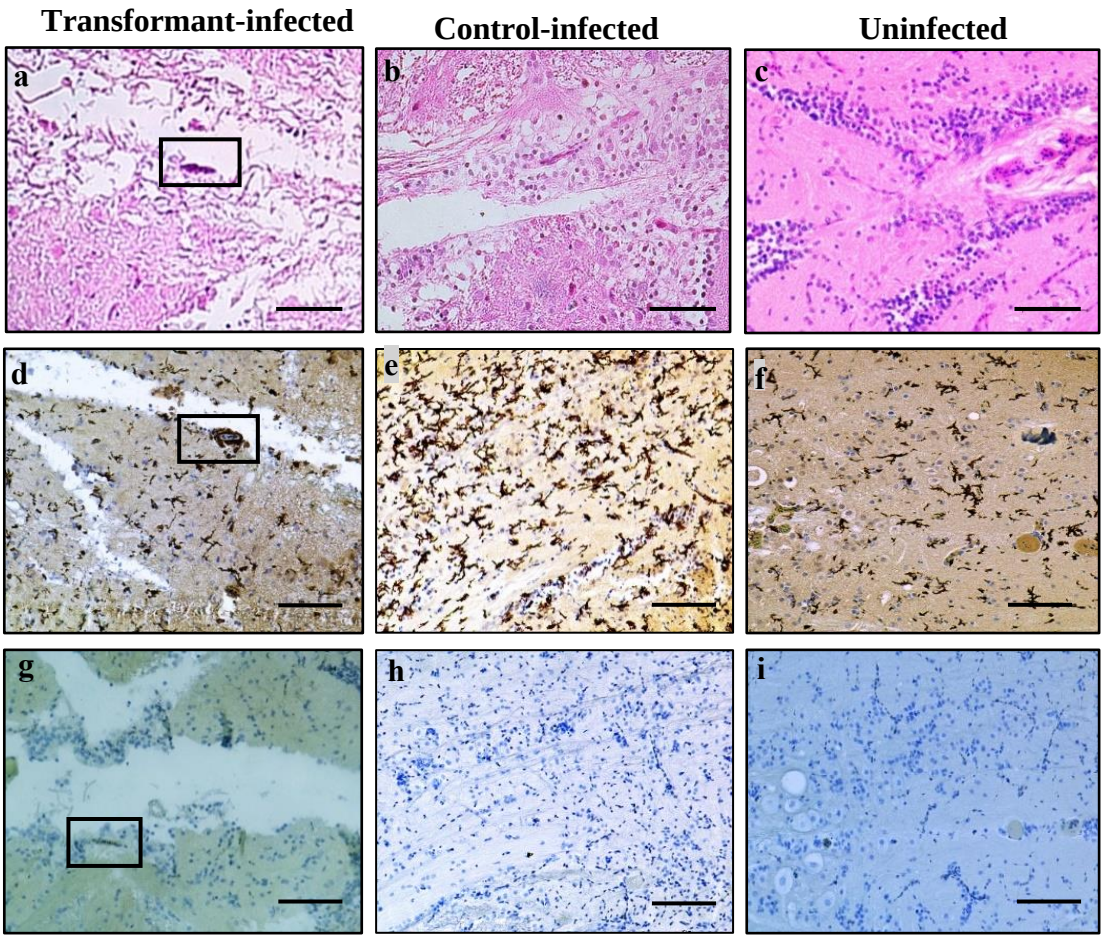

Figure 3. 19: Demonstrates the presence of L-plastin protein expressed from the components of the granuloma-like lesion in the brain of zebrafish. Picture **a, b** and **c** are tissue sections stained with the hematoxylin and eosin staining. a indicates a granuloma-like lesion in the hindbrain tissue of the transformant-infected zebrafish; **b** and **c** indicate the absence of the granulomatous structure in a similar region of the brain of the zebrafish infected with control strain and uninfected fish, respectively. Scale bars for **a-c**=50um. **d-i** represent the immunohistochemistry stained tissue section from their respective zebrafish. **d** shows the presence of the L-plastin protein which is brown in the granuloma-like lesion indicating the lesion is composed of leukocytes. **e** and **f** were taken from the control infected fish and uninfected fish, respectively, and indicate the absence of the lesion with L-plastin protein. **g-i** are negative anti-L-plastin antibody controls and show the absence of interaction with L-plastin protein. Scale bars for **d-i**=100um.

3.10 Association of death of zebrafish with brain infection in zebrafish after injection with the control and transformant *M. marinum* E11 strains.

The association of death with brain infection in the transformant-infected zebrafish was compared with that of the control-infected zebrafish. The result showed that among the zebrafish infected with the control strain and died, 6.25% (1/16) was positive for the bacilli in its brain and died on the 13th day of post-injection, whereas from those zebrafish infected with transformant and died, 47.37% (9/19) had the bacilli in their brain (**Table 3.2**). Among these zebrafish, 77.8% (7/9) died within 7 days of post-injection.

Table 3. 2: Death in the transformant *M. marinum* E11 infected zebrafish was significantly more associated with brain infection than that of the control group (P=0.0098).

Infection agent	Total No. of fish died	% of fish developed brain infection	Post-injection time at death for fish developed the brain infection
Control	16	6.25% (1/16)	13 days
M. marinum **Transformant** ***M. marinum***	19	47.37% (9/19)	7 within 7 days 1 at 10 days 1 at 16 days

3.11 Dissemination of blue fluorescent transformants and control strains in transparent zebrafish models along the infection course

Moreover, thirty transparent zebrafish were injected with blue fluorescent control *M. marinum* E11 (n=12), transformant *M. marinum* E11 (n=12), and Uninfected (n=6), following live-model examination with a fluorescence stereo microscope along the infection course. Among the zebrafish infected with the control strain, 50% (6/12) and 16.7% (2/12) developed blue fluorescent aggregates in their bodies and brains, respectively, on an average day 7 and 16. In the transformant group, 58.3% (7/12) showed the blue fluorescent signals in their body and 41.7% (5/12) of them also developed the signals in their brain on average day 6.6 and 12.4, respectively **(Table 3.3).** The total number of aggregated blue fluorescent signals observed in the whole body of transformant-infected zebrafish was 120, which was higher than that found in the control group (n=56). Two aggregated blue fluorescent signals were collectively detected in the brain region of the control strain-infected zebrafish, whereas eight blue fluorescent aggregates were observed in the brain region of transformant-infected zebrafish (**Table 3.3)**. The granuloma-like signals observed in the body and brain are shown in **Figures 3.20 and 3.21.**

The histological examination was subsequently performed for the zebrafish models which have detectable blue fluorescent signals in the brain region. Only one control strain infected zebrafish was positive for AFB microscopy in the brain tissue and

none of them showed granuloma-like lesion. In contrast, among transformant-infected zebrafish with blue fluorescent aggregates, acid-fast bacilli were observed in the brain of four zebrafish, and granuloma-like lesions were detected in the brain of two of them.

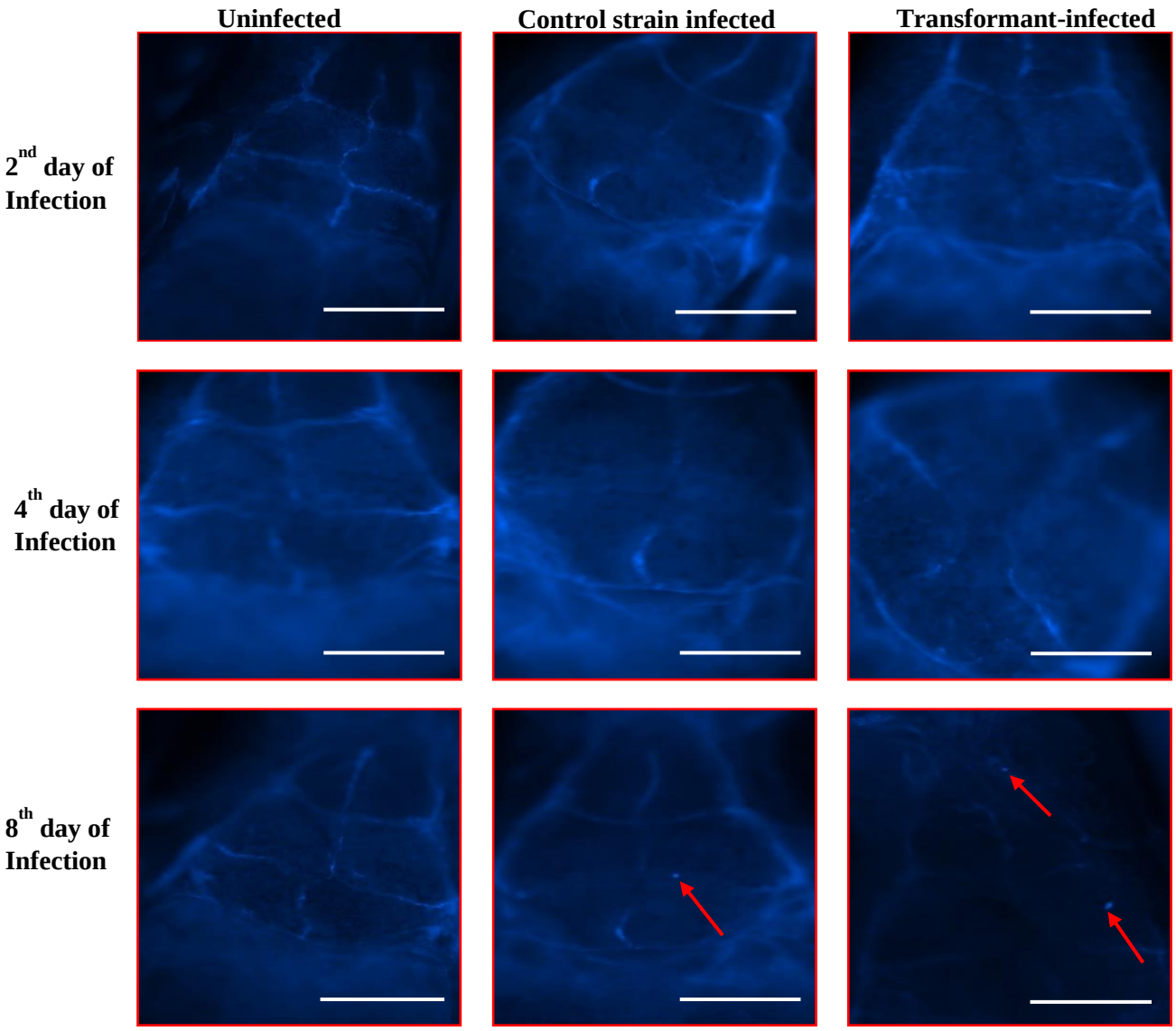

Figure 3. 20: Granuloma-like signals in the brain region of transparent zebrafish infected with control and transformant *M. marinum* E11. The signals appeared in the brain region on the 8th day of post-infection (red arrows) under the stereo fluorescence microscope. Scale bar =200µm. No signals appeared in the brain region until six days post-infection.

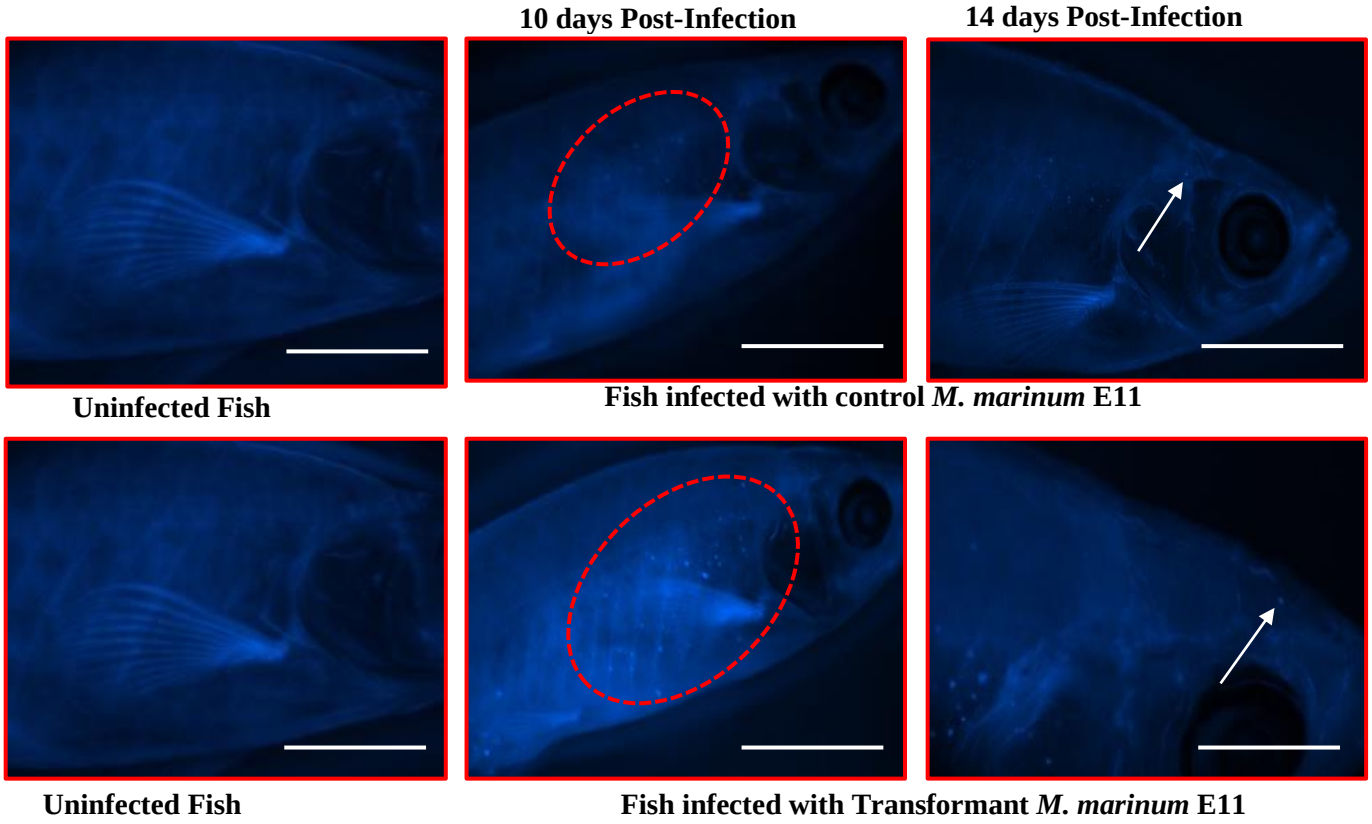

Figure 3. 21: The differences in the number and size of granuloma-like signals (blue dots) identified in the body and brain of zebrafish infected with control and transformant *M. marinum* strains. More granuloma-like signals were detected in the body of transformant-infected zebrafish than that in the control group. Among the signals, only one approached the brain in the control-infected zebrafish but entered the brain region in the situation of transformant-infected zebrafish on the 14th day of post-infection (white arrows). Scale bar=200µm.

Table 3. 3: Evaluation of granuloma-like signals in the brain and other body parts of infected transparent zebrafish.

Infection agent	Total No. of fish	No. of fish with granuloma signals		Total No. of granuloma signals	
		Body	Brain	Body	Brain
Control	12	6 (50%)	2(16.7%)	54	2
Transformant	12	7(58.3%)	5(41.7%)	112	8
Uninfected	6	-	-	-	-

3.12 Expression level of cytokines in zebrafish brain in response to transformants and control *M. marinum* infection

To measure the differences in the expression level of tumor necrosis factor-alpha (TNF-α) gene and interleukin-1 beta (IL-1ß) gene between zebrafish infected with transformant strain and the wild-type-infected group, RNA was extracted from the brain tissue of control, treatment and uninfected groups of zebrafish at 30 days of post-infection. The RNA of 8 and 7 zebrafish were analyzed for TNF-α and IL-1ß, respectively, using qPCR. The results showed that the level of TNF-α expression was reduced in the zebrafish infected with transformant strain relative to that of the control infected zebrafish even though their difference was not statistically significant (P=0.2186) (**Figure 3.22 A**).

However, the expression level of IL-1ß in the transformant-infected zebrafish was higher than that of the control strain infected zebrafish (P=0.5906) but lower than that of the uninfected zebrafish (P=0.4201). In the control infected zebrafish, the level of IL-1ß was significantly reduced relative to the uninfected zebrafish (P=0.0199) **(Figure 3.22 B).**

The relatively high statistical significance p-values indicates that the strain manipulates the immune system of the host not to induce the cytokines at the level it eliminates the bacilli from the body. This means the genes that are regulated by the PhoP, for example, ESX-1 facilitates the secretion of ESAT-6 and this modulates the Th1 cells and reduces the production of IFN-γ. This in turn inhibits further initiation of the macrophages that contain the bacilli to produce TNF-α. Reduction of the TNF-α level creates a suitable environment for the survival and intracellular growth of the bacilli.

A TNF-α

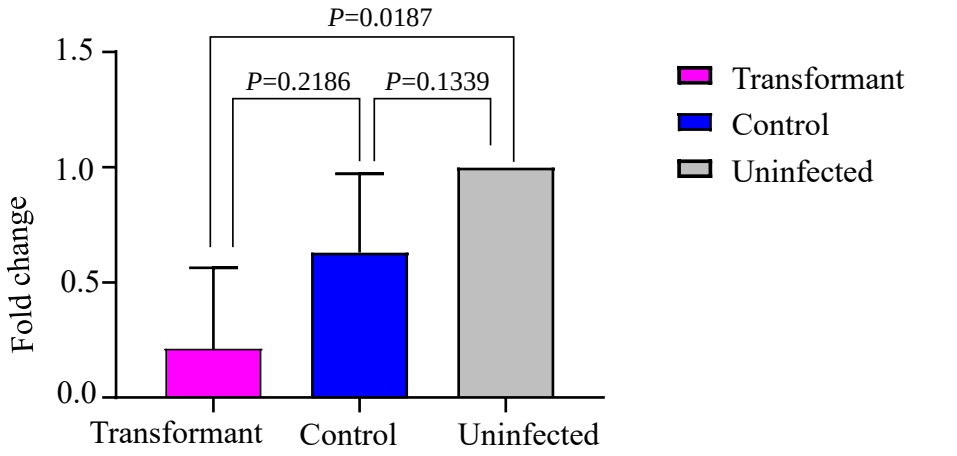

B IL-1ß

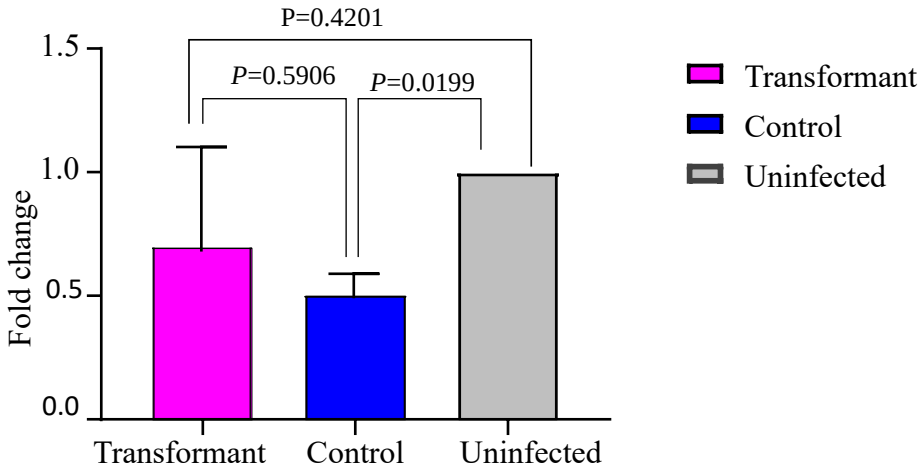

Figure 3. 22: Analysis of the expression level of TNF-α (A) and IL-1ß (B) in the brain tissue of zebrafish injected with transformants (n=6), control *M. marinum* (n=5), and Uninfected (n=2).

CHAPTER 4: DISCUSSION

In this study, we constructed transformant *M. marinum* with increased expression of *phoP* gene and examined its bacteriological and pathological features in the brain tissue of zebrafish, and compared it with that of the control *M. marinum* strains. These led us to validate the causative role of the differentially elevated expression of the *phoP* gene in the mycobacterial virulence in the pathogenesis of tuberculous meningitis inside the host.

In the constructed transformant *M. marinum,* we found the expression level of the *phoP* gene about 3-fold increase relative to that of the control *M. marinum.* This result is almost similar with that of the *phoP* expression level which was previously identified in the hypervirulent *M. tuberculosis* strain H112 (163), which was isolated from the cerebrospinal fluid of a patient suffering from TBM (162). Another study also found a highly up-regulated *phoP* gene expression in the transformant *Mycobacterium smegmatis* which was observed in one of the biggest multidrug-resistant tuberculosis outbreaks that occurred so far due to the B strain of *Mycobacterium bovis* (161). On the other hand, the mutation in the *phoP* gene resulted in the down-regulation of the gene expression and contributed to the avirulence of *M. tuberculosis*. For example, the attenuation of H37Ra has occurred as a result of the change in the amino acid from serine to leucine in the PhoP. This

happened due to the negative effects of the PhoP on the secretion of the major T-cell antigen ESAT-6 (159, 160). Thus, the change in the transcription level of the *phoP* gene highlights the significant genetic changes that occurred when mycobacteria increase their virulence level.

Histological and bacteriological experiments revealed consistently that transformant *M. marinum* infected zebrafish (wild-type) models have a higher bacterial load in the brain tissue and were more prone to have brain infection when compared with the control infected zebrafish. This result supported that overexpression of the *M. tuberculosis phoP* gene rendered the transformant *M. marimum* more neurotropic in zebrafish host. It is speculated that the elevated *phoP* expression may enhance the ability of *M. marinmum* to cross the blood-brain barrier (BBB) and establish infection in the brain parenchyma. As shown in our previous study, hypervirulent *M. tuberculosis* strains with enhanced *phoP* expression displayed a significantly higher intracellular growth in macrophages. Therefore, we believe that the bacterium infects macrophages and uses them as a carrier—like a Trojan Horse—to cross the BBB. However, the invasion is still challenging when the BBB is functionally intact (132) and the number of phagocytes entering the brain is limited. A previous study proposed that the ESX-1 secretion system of mycobacteria could be essential for the process of BBB-crossing (132). The ESX-

1 secretion contacts and interacts with the BBB and results in the damage of endothelial cells and basal lamina of the membrane and facilitates the entrance of the bacilli into the brain(132). Interestingly, the ESX-1 is one of the regulons that are positively regulated by the *phoP* gene (158). Therefore, the enhanced *phoP* gene expression, in turn, increases the function of ESX-1 and can be one of the reasons for the higher mycobacterial bacilli in the brain of the transformant-infected zebrafish in the current study. We hypothesize that differentially increased expression of *phoP* may favour the hypervirulent *M. tuberculosis* in dissemination, crossing the BBB and causing infection in the CNS through enhancing proper regulation of ESX-1 function (**Figure 4.1**).

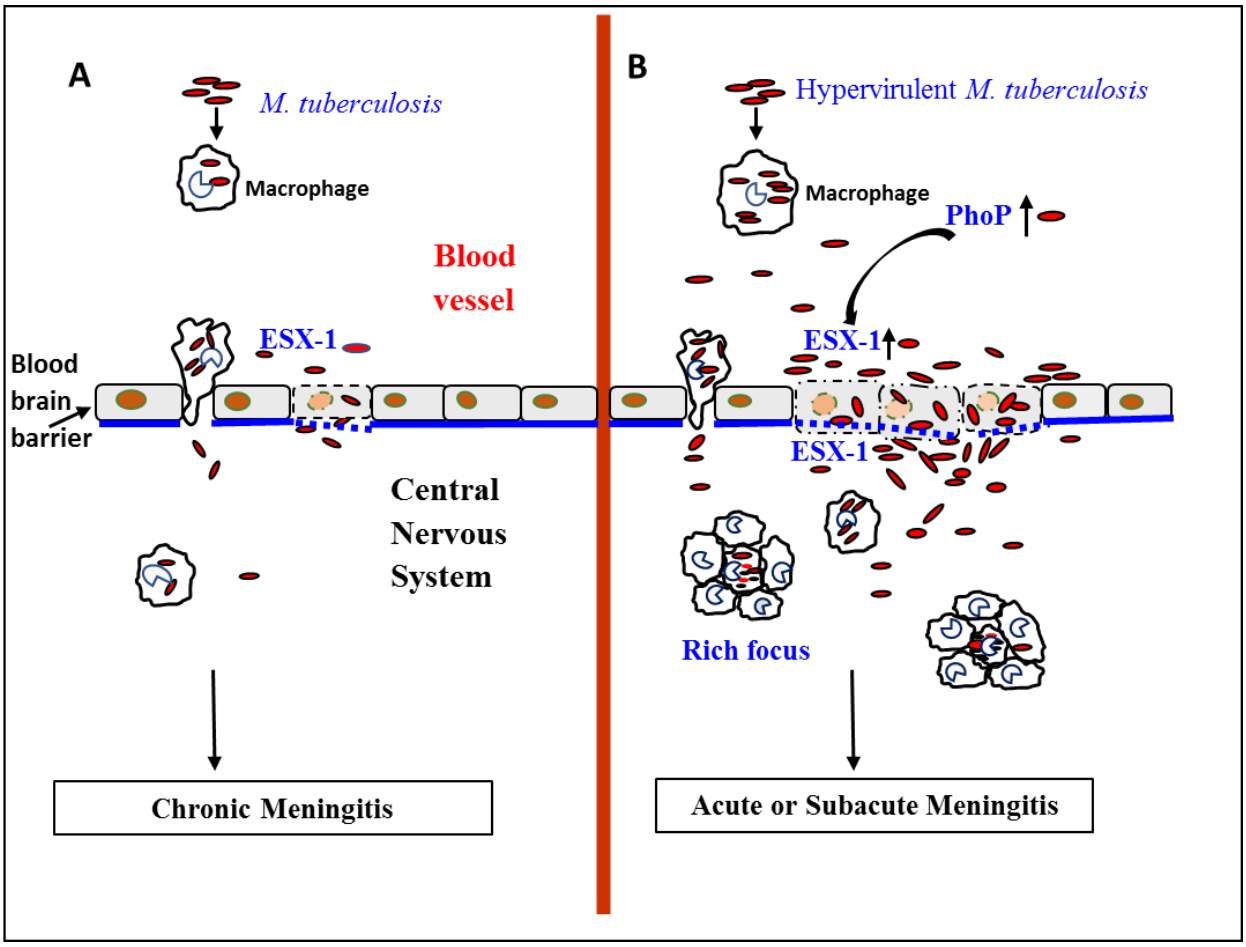

Figure 4. 1: Graphical presentation of our hypothesis on how the differentially elevated phoP gene expression contributes to the mycobacterial virulence in causing infection in the CNS. **A** indicates how the wild-type mycobacteria cross the BBB and enter the brain using macrophages and the ESX-1 secretion system with relatively limited access. **B** demonstrates how the differentially elevated *phoP* gene expression accelerates the entrance of the bacilli into the brain via the ESX-1 secretion system and helps in the development of tuberculous meningitis.

In the present study, we also observed granuloma-like lesions (Rich foci) in the brain tissue of transformant-infected zebrafish but not in the wild-type group. The formation of tuberculous granuloma by the host is initially to contain the dissemination of *M. tuberculosis* in the body. However, some *M. tuberculosis* bacilli take it as an advantage to survive and even multiply in the granuloma and disseminate in the body (43). It was reported that virulence determinants of mycobacteria enhance the formation of tuberculous granuloma. For instance, the molecular signal induced by the region of difference 1 (RD1) is able to attract macrophages and induce granuloma formation. This in turn facilitates the intracellular dissemination of the bacteria as well as increased bacterial numbers (209, 210). The function of RD1 is positively regulated by the *phoP* gene in mycobacteria (158). Increased expression of *phoP* may facilitate the RD1-related pathways to enhance the formation of granuloma-like lesions in the brain. This also favours the survival of hypervirulent strains in the central nervous system (CNS) of the host.

In the transformant-infected zebrafish, a large number of mycobacterial bacilli was not only found in the brain but also noted in the tissue adjacent to the brain and caused structural changes in the region. This may physically create pressure on the brain so that the brain cannot function properly. The infection may also gradually

spread and invade the brain and finally lead to the death of the zebrafish. This might also indicate that the transformant strain has more potential than the control strain in developing an infection in the CNS of the host.

Among the transformant-infected and died zebrafish, most of them (77.8%) died within a week after injection. In most cases of mycobacterial infection, meningitis occurred when the contents of pre-existing granuloma (Rich foci) in the meninges or brain tissue are discharged into the subarachnoid space (211, 212) and this leads to the late manifestation of the disease. However, some evidence showed that hematogenous dissemination in the form of miliary tuberculosis can lead to tuberculous meningitis in young children rapidly after infection (213), similar to the extracellular pathogens such as *Neisseria meningitidis*, *Hemophilus influenza*, and *Streptococcus pneumoniae* (211, 214). It was also shown that this type of brain tissue infection is facilitated by the gene under the regulation of PhoP (132). Thus, the earlier death and higher mortality of zebrafish associated with brain infection after being injected with transformant strain may indicate that the enhanced capacity of the transformant is at the level it can cause rapid onset of the disease before the formation of Rich foci in the CNS.

Monitoring the infection course of absolute (transparent) zebrafish models injected with the transformant strain showed that a higher number and bigger size of blue fluorescent aggregates were detected in both the body and brain regions of the transformant-infected zebrafish when compared to the control group. It suggested more rapid growth and intracellular survival of the transformant than that of the control strain after infection. A similar observation was obtained from previous study conducted on the hypervirulent *M. tuberculosis* strains that showed better intracellular growth and survival than other strains in the macrophages challenge experiments(162). This suggests that the enhanced intramacrophage survival and growth of the hypervirulent *M. tuberculosis* may facilitate the development of infection in the CNS.

Although the average day at which the blue fluorescent aggregates appeared in the body of both control strain infected transparent zebrafish and the transformant-infected group was nearly the same, the blue fluorescent signals appeared earlier in the brain region of the transformant-infected zebrafish than that of the control infected. The number of zebrafish that showed the blue fluorescent signals in their brain was also higher in the transformant-infected group. The small number of positive signals in both groups, on the other hand, restricts the interpretation of the result for differences in brain entry time between the two strains.

The present study also showed a lower level of TNF-α gene expression in the brain of transformant-infected wild-type zebrafish than that of the control strain infected zebrafish. However, the lower level of the expression didn't reach its significant level compared with that of the previous studies which showed significantly lower level in the hypervirulent *M. tuberculosis* strains than in the low virulent strains in infected macrophages. The hypervirulent strains also showed significantly better intracellular growth and survival than the low virulent and other strains in the macrophages (162, 163). Another study also indicated that the treatments of patients suffering from rheumatoid arthritis and Crohn's disease with monoclonal anti-TNF-α antibodies (infliximab) resulted in the reactivation of tuberculosis in the form of miliary and extrapulmonary tuberculosis including meningitis (215), reflecting the role of TNF-α in controlling the growth of mycobacteria in the host. Therefore, the lower level of TNF-α indicates the absence of an effective host immune response to remove the bacilli and facilitates the way for the mycobacterium to escape from the network of the host immune system. Hence, the lower level of TNF-α may also be one of the reasons for the increased mycobacterial load in the brain of those zebrafish infected with the transformant strain in this study.

In this study, the level of IL-1ß gene expression was higher in the brain of transformant-infected zebrafish when compared with that of the control infected zebrafish. This might be due to the increased secretion of ESAT-6 in the host. Because it has been recently identified that *M. tuberculosis* initiates the production of IL-1ß by macrophages through ESAT-6 dependent manner (216). Interestingly, the PhoP positively regulates the genes that are required for ESAT-6 secretion, and this might contribute to the situation. When the IL-1ß gene expression level in control infected zebrafish was compared with that of the uninfected zebrafish, it was significantly reduced. This result was highly deviated from what was obtained in the previous study which showed the highly up-regulated level of the gene expression as time post-infection increased (203). This difference might be attributed to the differences in the time of sample collection and the type of experiment used which is macrophage challenge in the previous study and the host in the current study.

CHAPTER 5:CONCLUSION REMARKS AND FUTURE DIRECTIONS

5.1 Conclusion

TB remains one of the most devastating health problems globally, with about 9.9 million cases and 1.5 deaths in 2020 (1). TBM is the most fatal and disabling clinical manifestation of TB, for which more than 100,000 new cases occurred per year (1, 217). Such a serious form of the disease is mainly associated with increased virulence level of the strains of the causative agent, *M. tuberculosis*. Lack of effective vaccines and drugs against the disease further exacerbated the problem. Previous studies identified a set of genetic mutations in the hypervirulent *M. tuberculosis* strains isolated from tuberculous meningitis patients (163). However, whether these genetic factors contribute to the enhanced mycobacterial virulence in causing this life-threatening form of tuberculosis in the CNS was not defined. The purpose of this study was to construct blue fluorescent, transformant *M. marinum* strain with enhanced *phoP* gene of *M. tuberculosis* and to examine the bacteriological and pathological features caused by the infection with the transformant *M. marinum* in the brain of zebrafish and compare it with that of the control strain.

We constructed the blue fluorescent, transformant *M. marinum* strain using transformation by electroporation and we found about 3-fold increased level of the *phoP* gene expression in the transformant strain relative to that of the control strain. The bacteriological and histopathological analyses showed that the transformant-infected zebrafish models had higher brain bacillary load and were more prone to have brain infection when compared with the control strain-infected group. Granuloma-like lesions were also observed in the brain tissue of transformant-infected zebrafish but not in that of the control infected. Notably, earlier mortality was observed in the transformant-infected zebrafish, and the death was more linked to brain infection than in the control-infected zebrafish. By monitoring the infection course of transparent zebrafish models, we also found more and larger blue fluorescent granuloma-like signals or aggregates in the body and brain region of transformant-infected zebrafish than in the situation of the control group. Furthermore, the qPCR analysis showed a lower expression level of the TNF-α gene in the brain of transformant-infected zebrafish than that of the control-infected zebrafish. Altogether, the results from the present study show that the transformant is more neurotropic and virulent than the control strains in zebrafish, suggesting differentially elevated expression of *phoP* gene may enhance the virulence of mycobacteria in causing infection in the CNS.

In a previous study, it was indicated that increased expression of the *phoP* gene enhanced intracellular survivability and growth of the hypervirulent *M. tuberculosis* in macrophages in in-vitro conditions which only explained the virulence mechanisms of the mycobacterium at the early stage of infection (163). In the current study, we identified a new causative role of the enhanced expression of the *phoP* gene in mycobacteria in the development of TBM in zebrafish. To the best of our knowledge, this work is the first to validate the functional impacts of the differentially elevated expression of the *phoP* gene specific to the hypervirulent *M. tuberculosis* particularly using animal model. Hence, our findings may provide a knowledge base for the development of novel and effective vaccines and drugs against tuberculosis, particularly TBM. For example, disruption of the related region of the *phoP* gene inside *M. tuberculosis* may result in a live attenuated strain of the mycobacterium which could be used as a potential candidate to produce new TB vaccines. By combining with the previous studies' findings, our findings may also pave the way for the development of new TB drugs if suppressing the corresponding pathways can attenuate the survival of the mycobacteria inside the macrophage and decrease the possibility of developing TBM and facilitate the condition for the host immune system to eliminate the mycobacteria.

There are some limitations to this study. First, the number of transparent zebrafish we used to study the course of events in the development of TBM in real life was small. However, we used more number of wild-type lines of zebrafish which is an alternative model to examine the presence of the bacilli in the brain tissue and evaluate the effect of the enhanced *phoP* gene on the virulence of *M. marinum* in causing brain infection. Second, the current study has focused only on the *phoP* gene among the genes affected by the genetic mutations specific to the hypervirulent *M. tuberculosis* strains. Even though the *phoP* gene was the one with RNA transcript and protein levels were consistently differentially elevated in the hypervirulent strains, investigation of the effects of other genes such as *higB*, *pip,* and *fadE5* is also needed. Third, we overexpressed the *phoP* gene of *M. tuberculosis* inside the *M. marinum*. Therefore, one can conduct gene knockout at the related region in the genome of *M. marinum* and confirm if the same situation occurred. One can also continue the research by taking the intergenic region at which the 2bp deletion occurred including the PhoPR operon from the H112 strain and inserting it into *M. marinum* using allelic exchange. Fourth, in the current study, we also used *M. marinum* transformed with the pVV16 plasmid-*BFP gene* as a control strain. It would also be better if further research is conducted using *M. marinum* transformed with pVV16 containing the *phoP* gene of H37Ra as a control strain. This helps to determine whether the observed virulence phenotype in zebrafish model is due to the additional copy effect or unique virulency of the

H37Rv *phoP*. It also helps to avoid the variation of outcomes that may arise from the size difference between the *phoP* of *M. tuberculosis* H37Rv and *M. marinum.* Moreover, we evaluated the levels of cytokines (TNF-α and IL-1ß) at a one-time point. The information would have been more comprehensive if the sample had been collected at different times and tested.

5.2 Recommendation and future directions

Future studies are recommended to determine whether the other virulence genes aforementioned contribute to the enhancement of mycobacterial virulence in the pathogenesis of TBM inside the host. The functional impacts of the genes (*higB, pip,* and *fadE5*) can be studied by transferring the mutated genes of hypervirulent *M. tuberculosis* strains into the relevant region of the genome of control *M. tuberculosis* using the allelic exchange method (218) or by taking the genes from the wild-type and transferring them into the genome of the hypervirulent strains (219). The impacts of the manipulated strains should be evaluated using cell culture and a proper animal model. The molecular mechanism or function pathways by which the differentially expressed *phoP* gene works on its regulon genes in causing the neurotropism of the hypervirulent *M. tuberculosis* strains in the CNS should also be determined through genetic manipulation.

Most importantly, rigorous functional validation of the differentially expressed *phoP* gene should also be conducted for *M. tuberculosis* using rabbits for evaluating the virulence of the mycobacterium. For example, the related gene can be disrupted in *M. tuberculosis* by using allelic exchange system (218) and the transformants are injected into the animal model. Then, the bacteriological, immunological, and pathological features of the infection will be examined and compared with that of the hypervirulent strains of *M. tuberculosis*. If the transformant *M. tuberculosis* is unable to cause the disease in the animal, it could be the potential candidate for a new vaccine against TB particularly TBM.

REFERENCES

1. World Health Organization. Global tuberculosis report 2021. Geneva: WHO; 2021.
2. Sia IG, Wieland ML. Current concepts in the management of tuberculosis. Mayo Clin Proc. 2011;86(4):348-61.
3. Nerlich AG, Haas CJ, Zink A, Szeimies U, Hagedorn HG. Molecular evidence for tuberculosis in an ancient Egyptian mummy. The Lancet. 1997;350(9088):1404.
4. Smith I. *Mycobacterium tuberculosis* pathogenesis and molecular determinants of virulence. Clinical Microbiology Reviews. 2003;16(3):463-96.
5. Gradmann C. Robert Koch and the pressures of scientific research: tuberculosis and tuberculin. Medical History. 2001;45(1):1-32.
6. Lipsitch M, Sousa AO. Historical intensity of natural selection for resistance to tuberculosis. Genetics. 2002;161(4):1599-607.
7. Frieden TR, Fujiwara PI, Washko RM, Hamburg MA. Tuberculosis in New York City-turning the tide. New England Journal of Medicine. 1995;333(4):229-33.

8. Coker R. Lessons from New York's tuberculosis epidemic: Tuberculosis is a political as much as a medical problem and so are the solutions. British Medical Journal. 1998;317(7159):616-20.

9. Young LS, Wormser GP. The resurgence of tuberculosis. Scandinavian Journal of Infectious Diseases. Supplementum. 1994;93:9-19.

10. Porter JD, McAdam KP. The re-emergence of tuberculosis. Annual Review of Public Health. 1994;15(1):303-23.

11. Pitchenik AE, Cole C, Russell BW, Fischl MA, Spira TJ, Snider Jr DE. Tuberculosis, atypical mycobacteriosis, and the acquired immunodeficiency syndrome among Haitian and non-Haitian patients in south Florida. Annals of Internal Medicine. 1984;101(5):641-5.

12. Theuer CP, Hopewell PC, Elias D, Schecter GF, Rutherford GW, Chaisson RE. Human immunodeficiency virus infection in tuberculosis patients. Journal of Infectious Diseases. 1990;162(1):8-12.

13. Elliott AM, Luo N, Tembo G, Halwiindi B, Steenbergen G, Machiels L, Pobee J, Nunn P, Hayes RJ, McAdam KP. Impact of HIV on tuberculosis in Zambia: a cross sectional study. British Medical Journal. 1990;301(6749):412-5.

14. Huebner RE, Villarino ME, Snider DE, Jr. Tuberculin skin testing and the HIV epidemic. Jama. 1992;267(3):409-10.

15. Nakajima H. Tuberculosis: a global emergency. World Health. 1993;46(4):3.

16. Raviglione MC. The new stop TB strategy and the global plan to stop TB, 2006-2015. Bulletin of the World Health Organization. 2007;85:327.

17. World Health Organization. The Paradigm Shift 2016-2020 Global plan to end TB. World Heal Organ Doc. 2015;124.

18. World Health Organization. Global tuberculosis report 2020. Geneva: WHO; 2020.

19. Chang KC, Tam CM. Tuberculosis Control in Hong Kong. In Handbook of Global Tuberculosis Control 2017 (pp. 35-46). Springer, Boston, MA.

20. Vynnycky E, Borgdorff M, Leung C, Tam C, Fine P. Limited impact of tuberculosis control in Hong Kong: attributable to high risks of reactivation disease. Epidemiology & Infection. 2008;136(7):943-52.

21. Tuberculosis and Chest Service DoH, The Government of Hong Kong Special, Region. A. Statistics on tuberculosis. Hong Kong, 2021[cited on 2021 Sept 8]. Available from: https://www.chp.gov.hk/en/statistics/data/10/26/43/88.html.

22. Ray CG, Ryan KJ. Sherris medical microbiology: an introduction to infectious diseases. NY: McGraw-Hill; 2004.

23. Shinnick T, Good R. Mycobacterial taxonomy. European Journal of Clinical Microbiology and Infectious Diseases. 1994;13(11):884-901.

24. Wayne L. Cultivation of Mycobacterium for research purposes. Tuberculosis: pathogenesis, protection and control. In: Dalam: Bloom BR p, editor.: Washington DC: ASM Press; 1994.

25. Forrellad MA, Klepp LI, Gioffré A, Sabio y Garcia J, Morbidoni HR, Santangelo MD, Cataldi AA, Bigi F. Virulence factors of the *Mycobacterium tuberculosis* complex. Virulence. 2013;4(1):3-66.

26. Behr MA. Comparative genomics of mycobacteria: some answers, yet more new questions. Cold Spring Harbor Perspectives in Medicine. 2015;5(2):a021204.

27. Forbes BA. Mycobacterial taxonomy. Journal of Clinical Microbiology. 2017;55(2):380-3.

28. Portaels F, Johnson P, Meyers WM, World Health Organization, Global Buruli Ulcer Initiative. Buruli ulcer: diagnosis of *Mycobacterium ulcerans* disease: a manual for health care providers. World Health Organization; 2001.

29. Brosch R, Gordon SV, Marmiesse M, Brodin P, Buchrieser C, Eiglmeier K, Garnier T, Gutierrez C, Hewinson G, Kremer K, Parsons LM. A new evolutionary scenario for the *Mycobacterium tuberculosis* complex. Proceedings of the National Academy of Sciences. 2002;99(6):3684-9.

30. Dye C, Watt CJ, Bleed DM, Hosseini SM, Raviglione MC. Evolution of tuberculosis control and prospects for reducing tuberculosis incidence, prevalence, and deaths globally. Jama. 2005;293(22):2767-75.

31. Balows A. Manual of clinical microbiology 8th edition: PR Murray, EJ Baron, JH Jorgenson, MA Pfaller, and RH Yolken, eds. Diagnostic Microbiology and Infectious Disease. ASM Press, 2003;47(4):625.

32. Fitzgerald DW, Sterling TR, Haas DW. *Mycobacterium tuberculosis* In: Mandell GL, Bennets JE, Dolin R. Principles and practice of infectious disease. Philadelphia, Elsevier Churchill Livingstone; 2010.

33. Murray P, Baron E, Pfaller M, Jorgensen J, Yolken R. Manual of Clinical Microbiology 8thEdition Washington DC: ASM Press; 2003.

34. Todar K. Todar's online textbook of bacteriology. Madison, USA: University of Wisconsin-Madison, Department of Bacteriology; 2006.

35. Wells W. Aerodynamics of droplet nuclei. Airborne contagion and air hygiene. 1955:13-9.

36. Sweany HC. The tubercle bacillus in the pulmonary lesion of man: histobacteriology and its bearing on the therapy of pulmonary tuberculosis. Diseases of the Chest. 1955;28(6):699-701.

37. Palomino JC, Leão SC, Ritacco V. Tuberculosis 2007: from basic science to patient care. Amedeo Challenge; 2007.

38. Mfinanga SG, Mørkve O, Kazwala RR, Cleaveland S, Sharp JM, Shirima G, Nilsen R. The role of livestock keeping in tuberculosis trends in Arusha, Tanzania. The International Journal of Tuberculosis and Lung Disease. 2003;7(7):695-704.

39. Skuce RA, Hughes MS, Taylor MJ, Neill SD. Detection of pathogenic mycobacteria of veterinary importance. In PCR Detection of Microbial Pathogens. Springer; 2003. p. 201-21.

40. Muñoz L, Stagg HR, Abubakar I. Diagnosis and management of latent tuberculosis infection. Cold Spring Harbor Perspectives in Medicine. 2015;5(11):a017830.

41. Khayat M, Fan H, Vali Y. COVID-19 promoting the development of active tuberculosis in a patient with latent tuberculosis infection: A case report. Respiratory Medicine Case Reports. 2021;32:101344.

42. Kirenga BJ, Ssengooba W, Muwonge C, Nakiyingi L, Kyaligonza S, Kasozi S, et al. Tuberculosis risk factors among tuberculosis patients in Kampala, Uganda: implications for tuberculosis control. BMC Public Health. 2015;15(1):1-7.

43. Silva Miranda M, Breiman A, Allain S, Deknuydt F, Altare F. The tuberculous granuloma: an unsuccessful host defence mechanism providing a safety shelter for the bacteria? Clinical and Developmental Immunology. 2012;2012:1-14.

44. Müller A. How TB infects the body: The tubercle.[Internet] 2011[updated 2016 March 31; cited 2022 April 02]; Available from: https://www.tbonline.info/posts/2016/3/31/how-tb-infects-body-tubercle-1/.

45. Chin JH. Tuberculous meningitis: diagnostic and therapeutic challenges. Neurology: Clinical Practice. 2014;4(3):199-205.

46. Getahun H, Matteelli A, Chaisson RE, Raviglione M. Latent *Mycobacterium tuberculosis* infection. New England Journal of Medicine. 2015;372(22):2127-35.

47. Cohen A, Mathiasen VD, Schön T, Wejse C. The global prevalence of latent tuberculosis: a systematic review and meta-analysis. European Respiratory Journal. 2019;54(3):1900655.

48. O'Garra A, Redford PS, McNab FW, Bloom CI, Wilkinson RJ, Berry MP. The immune response in tuberculosis. Annual Review of Immunology. 2013;31:475-527.

49. Nayak S, Acharjya B. Mantoux test and its interpretation. Indian Dermatology Online Journal. 2012;3(1):2.

50. Pahal P, Sharma S. PPD skin test. Treasure Island (FL): StatPearls Publiching; 2020.

51. Diel R, Loddenkemper R, Nienhaus A. Predictive value of interferon-γ release assays and tuberculin skin testing for progression from latent TB infection to disease state. Chest. 2012;142(1):63-75.

52. Wilkinson RJ, Rohlwink U, Misra UK, Van Crevel R, Mai NT, Dooley KE, Caws M, Figaji A, Savic R, Solomons R, Thwaites GE. Tuberculous meningitis. Nature Reviews Neurology. 2017;13(10):581-98.

53. Katti MK. Pathogenesis, diagnosis, treatment, and outcome aspects of cerebral tuberculosis. Medical Science Monitor. 2004;10(9):RA215-RA29.

54. Meyers BR. Tuberculous Meningitis. Medical Clinics of North America. 1982;66(3):755-62.

55. Marais S, Pepper DJ, Schutz C, Wilkinson RJ, Meintjes G. Presentation and outcome of tuberculous meningitis in a high HIV prevalence setting. PloS One. 2011;6(5):e20077.

56. Tho DQ, Török ME, Yen NT, Bang ND, Lan NT, Kiet VS, van Vinh Chau N, Dung NH, Day J, Farrar J, Wolbers M. Influence of antituberculosis drug resistance and *Mycobacterium tuberculosis* lineage on outcome in HIV-associated tuberculous meningitis. Antimicrobial Agents and Chemotherapy. 2012 Jun;56(6):3074-9.

57. Berenguer J, Moreno S, Laguna F, Vicente T, Adrados M, Ortega A, González-LaHoz J, Bouza E. Tuberculous meningitis in patients infected

with the human immunodeficiency virus. New England Journal of Medicine. 1992 Mar 5;326(10):668-72.

58. Malhotra KP, Kulshreshtha D. Pathology of Tuberculosis of the Nervous System (Tuberculous Meningitis, Tuberculoma, Tuberculous Abscess). In Tuberculosis of the Central Nervous System 2017 (pp. 33-53). Springer, Cham.

59. Rich AR. The pathogenesis of tuberculous meningitis. Bull John Hopkins Hosp. 1933;52:5-37.

60. Thwaites G, Fisher M, Hemingway C, Scott G, Solomon T, Innes J. British Infection Society guidelines for the diagnosis and treatment of tuberculosis of the central nervous system in adults and children. Journal of Infection. 2009;59(3):167-87.

61. Nelson CA, Zunt JR. Tuberculosis of the central nervous system in immunocompromised patients: HIV infection and solid organ transplant recipients. Clinical Infectious Diseases. 2011;53(9):915-26.

62. Rock RB, Olin M, Baker CA, Molitor TW, Peterson PK. Central nervous system tuberculosis: pathogenesis and clinical aspects. Clinical Microbiology Reviews. 2008;21(2):243-61.

63. Thwaites GE, van Toorn R, Schoeman J. Tuberculous meningitis: more questions, still too few answers. The Lancet Neurology. 2013;12(10):999-1010.

64. Christopher R, Gourie-Devi M. The syndrome of inappropriate antidiuretic hormone secretion in tuberculous meningitis. Journal of Association of Physicians of India. 1997;45(12):933-5.

65. Hajia M, Amirzargar AA, Nazari M, Davodi NR, Zarandi MK. A five years study of tuberculous meningitis in Iran. Iranian Journal of Pathology. 2015;10(4):290.

66. Jain SK, Paul-Satyaseela M, Lamichhane G, Kim KS, Bishai WR. *Mycobacterium tuberculosis* invasion and traversal across an in vitro human blood-brain barrier as a pathogenic mechanism for central nervous system tuberculosis. The Journal of Infectious Diseases. 2006;193(9):1287-95.

67. Peterson PK, Gekker G, Hu S, Sheng WS, Anderson WR, Ulevitch RJ, Tobias PS, Gustafson KV, Molitor TW, Chao CC. CD14 receptor-mediated uptake of nonopsonized *Mycobacterium tuberculosis* by human microglia. Infection and Immunity. 1995;63(4):1598-602.

68. Rock RB, Hu S, Gekker G, Sheng WS, May B, Kapur V, Peterson PK. *Mycobacterium tuberculosis*–induced cytokine and chemokine expression by human microglia and astrocytes: effects of dexamethasone. The Journal of Infectious Diseases. 2005;192(12):2054-8.

69. Wright SD, Ramos RA, Tobias PS, Ulevitch RJ, Mathison JC. CD14, a receptor for complexes of lipopolysaccharide (LPS) and LPS binding protein. Science. 1990;249(4975):1431-3.

70. Davis AG, Rohlwink UK, Proust A, Figaji AA, Wilkinson RJ. The pathogenesis of tuberculous meningitis. Journal of Leukocyte Biology. 2019;105(2):267-80.

71. Hsu NJ, Francisco NM, Keeton R, Allie N, Quesniaux VF, Ryffel B, Jacobs M. Myeloid and T cell-derived TNF protects against central nervous system tuberculosis. Frontiers in Immunology. 2017;8:180.

72. Spanos JP, Hsu N-J, Jacobs M. Microglia are crucial regulators of neuro-immunity during central nervous system tuberculosis. Frontiers in Cellular Neuroscience. 2015;9:182.

73. Pieters J. *Mycobacterium tuberculosis* and the macrophage: maintaining a balance. Cell Host & Microbe. 2008;3(6):399-407.

74. Gordon S. Elie Metchnikoff: father of natural immunity. European Journal of Immunology. 2008;38(12):3257-64.

75. Kierdorf K, Prinz M, Geissmann F, Perdiguero EG. Development and function of tissue resident macrophages in mice. Seminars in Immunology. 2015; 27(6): 369-378.

76. Tao X, Xu A. Basic knowledge of immunology. In Amphioxus immunity 2016(pp. 15-42). Academic Press.

77. Ferrari G, Langen H, Naito M, Pieters J. A coat protein on phagosomes involved in the intracellular survival of mycobacteria. Cell. 1999;97(4):435-47.

78. Kaufmann SH. How can immunology contribute to the control of tuberculosis? Nature Reviews Immunology. 2001;1(1):20-30.

79. Lerner TR, Borel S, Gutierrez MG. The innate immune response in human tuberculosis. Cell Microbiol. 2015;17(9):1277-85.

80. Via LE, Deretic D, Ulmer RJ, Hibler NS, Huber LA, Deretic V. Arrest of mycobacterial phagosome maturation is caused by a block in vesicle fusion between stages controlled by rab5 and rab7. Journal of Biological Chemistry. 1997;272(20):13326-31.

81. Clemens DL, Horwitz MA. Characterization of the *Mycobacterium tuberculosis* phagosome and evidence that phagosomal maturation is inhibited. The Journal of Experimental Medicine. 1995;181(1):257-70.

82. Rohde K, Yates RM, Purdy GE, Russell DG. *Mycobacterium tuberculosis* and the environment within the phagosome. Immunological Reviews. 2007;219(1):37-54.

83. Vergne I, Chua J, Deretic V. Tuberculosis toxin blocking phagosome maturation inhibits a novel Ca2+/calmodulin-PI3K hVPS34 cascade. The Journal of Experimental Medicine. 2003;198(4):653-9.

84. Kang PB, Azad AK, Torrelles JB, Kaufman TM, Beharka A, Tibesar E, et al. The human macrophage mannose receptor directs *Mycobacterium tuberculosis* lipoarabinomannan-mediated phagosome biogenesis. The Journal of Experimental Medicine. 2005;202(7):987-99.

85. Schüller S, Neefjes J, Ottenhoff T, Thole J, Young D. Coronin is involved in uptake of *Mycobacterium bovis* BCG in human macrophages but not in phagosome maintenance. Cell Microbiology. 2001;3(12):785-93.

86. Flynn JL, Chan J. Immune evasion by *Mycobacterium tuberculosis*: living with the enemy. Current Opinion in Immunology. 2003;15(4):450-5.

87. Ma J, Yang B, Yu S, Zhang Y, Zhang X, Lao S, et al. Tuberculosis antigen-induced expression of IFN-α in tuberculosis patients inhibits production of IL-1β. The FASEB Journal. 2014;28(7):3238-48.

88. Zhai W, Wu F, Zhang Y, Fu Y, Liu Z. The immune escape mechanisms of *Mycobacterium tuberculosis*. International Journal of Molecular Sciences. 2019;20(2):340.

89. Pandey AK, Sassetti CM. Mycobacterial persistence requires the utilization of host cholesterol. Proceedings of the National Academy of Sciences. 2008;105(11):4376-80.

90. Gutierrez MG, Mishra BB, Jordao L, Elliott E, Anes E, Griffiths G. NF-kappa B activation controls phagolysosome fusion-mediated killing of mycobacteria by macrophages. Journal of Immunology. 2008;181(4):2651-63.

91. Loui C, Chang AC, Lu S. Role of the ArcAB two-component system in the resistance of *Escherichia coli* to reactive oxygen stress. BMC Microbiology. 2009;9(1):1-14.

92. Imlay JA. Transcription factors that defend bacteria against reactive oxygen species. Annual Review of Microbiology. 2015;69:93-108.

93 Chan J, Fan X, Hunter S, Brennan P, Bloom B. Lipoarabinomannan, a possible virulence factor involved in persistence of *Mycobacterium tuberculosis* within macrophages. Infection and Immunity. 1991;59(5):1755-61.

94. Ehrt S, Schnappinger D. Mycobacterial survival strategies in the phagosome: defence against host stresses. Cellular Microbiology. 2009;11(8):1170-8.

95. Fang FC. Perspectives series: host/pathogen interactions. Mechanisms of nitric oxide-related antimicrobial activity. The Journal of Clinical Investigation. 1997;99(12):2818-25.

96. Mehta M, Singh A. *Mycobacterium tuberculosis* WhiB3 maintains redox homeostasis and survival in response to reactive oxygen and nitrogen species. Free Radic Biol Med. 2019;131:50-8.

97. Darwin KH, Nathan CF. Role for nucleotide excision repair in virulence of *Mycobacterium tuberculosis.* Infection and Immunity. 2005;73(8):4581-7.

98. Van Der Veen S, Tang CM. The BER necessities: the repair of DNA damage in human-adapted bacterial pathogens. Nature Reviews Microbiology. 2015;13(2):83-94.

99. Russell DG, VanderVen BC, Lee W, Abramovitch RB, Kim MJ, Homolka S, Niemann S, Rohde KH. *Mycobacterium tuberculosis* wears what it eats. Cell host & microbe. 2010;8(1):68-76.

100. Marcela Rodriguez G, Neyrolles O. Metallobiology of tuberculosis. Microbiology Spectrum. 2014;2(3):2-3.

101. Cole S, Brosch R, Parkhill J, Garnier T, Churcher C, Harris D, Gordon SV, Eiglmeier K, Gas S, Barry C3, Tekaia F. Deciphering the biology of *Mycobacterium tuberculosis* from the complete genome sequence. Nature. 1998;396(6707):190.

102. Ryndak MB, Wang S, Smith I, Rodriguez GM. The *Mycobacterium tuberculosis* high-affinity iron importer, IrtA, contains an FAD-binding domain. J Bacteriol. 2010;192(3):861-9.

103. Agoro R, Mura C. Iron supplementation therapy, a friend and foe of mycobacterial infections? Pharmaceuticals. 2019;12(2):75.

104. Agranoff D, Monahan IM, Mangan JA, Butcher PD, Krishna S. *Mycobacterium tuberculosis* expresses a novel pH-dependent divalent cation transporter belonging to the Nramp family. The Journal of Experimental Medicine. 1999;190(5):717-24.

105. Horwitz LD, Horwitz MA. The exochelins of pathogenic mycobacteria: unique, highly potent, lipid-and water-soluble hexadentate iron chelators with multiple potential therapeutic uses. Antioxidants & Redox Signaling. 2014;21(16):2246-61.

106. Sritharan M. Iron homeostasis in *Mycobacterium tuberculosis*: mechanistic insights into siderophore-mediated iron uptake. Journal of Bacteriology. 2016;198(18):2399-409.

107. Gobin J, Horwitz MA. Exochelins of *Mycobacterium tuberculosis* remove iron from human iron-binding proteins and donate iron to mycobactins in the *M. tuberculosis* cell wall. The Journal of Experimental Medicine. 1996;183(4):1527-32.

108. Inoue M, Niki M, Ozeki Y, Nagi S, Chadeka EA, Yamaguchi T, Osada-Oka M, Ono K, Oda T, Mwende F, Kaneko Y. High-density lipoprotein suppresses tumor necrosis factor alpha production by mycobacteria-infected human macrophages. Scientific Reports. 2018;8(1):1-1.

109. Flynn JL, Goldstein MM, Chan J, Triebold KJ, Pfeffer K, Lowenstein CJ, Schrelber R, Mak TW, Bloom BR. Tumor necrosis factor-α is required in the protective immune response against *Mycobacterium tuberculosis* in mice. Immunity. 1995;2(6):561-72.

110. Ghazaei C. *Mycobacterium tuberculosis* and lipids: Insights into molecular mechanisms from persistence to virulence. Journal of Research in Medical Sciences. 2018;23:63.

111. Reed MB, Domenech P, Manca C, Su H, Barczak AK, Kreiswirth BN, Kaplan G, Barry CE. A glycolipid of hypervirulent tuberculosis strains that inhibits the innate immune response. Nature. 2004;431(7004):84-7.

112. Redford P, Murray P, O'garra A. The role of IL-10 in immune regulation during *M. tuberculosis* infection. Mucosal Immunology. 2011;4(3):261-70.

113. Toossi Z, Ellner JJ. The role of TGFβ in the pathogenesis of human tuberculosis. Clinical Immunology and Immunopathology. 1998;87(2):107-14.

114. Giacomini E, Iona E, Ferroni L, Miettinen M, Fattorini L, Orefici G, Julkunen I, Coccia EM. Infection of human macrophages and dendritic cells with *Mycobacterium tuberculosis* induces a differential cytokine gene expression that modulates T cell response. The Journal of Immunology. 2001;166(12):7033-41.

115. Geijtenbeek TB, Van Vliet SJ, Koppel EA, Sanchez-Hernandez M, Vandenbroucke-Grauls CM, Appelmelk B, Van Kooyk Y. Mycobacteria target DC-SIGN to suppress dendritic cell function. The Journal of Experimental Medicine. 2003;197(1):7-17.

116. Guirado E, Schlesinger L. Modeling the *Mycobacterium tuberculosis* granuloma–the critical battlefield in host immunity and disease. Frontiers in Immunology. 2013;4:98.

117. Ramakrishnan L. Revisiting the role of the granuloma in tuberculosis. Nature Reviews Immunology. 2012;12(5):352-66.

118. Gil O, Díaz I, Vilaplana C, Tapia G, Díaz J, Fort M, Cáceres N, Pinto S, Caylà J, Corner L, Domingo M. Granuloma encapsulation is a key factor for containing tuberculosis infection in minipigs. PloS One. 2010;5(4):e10030.

119. Sharma AK, Dhasmana N, Dubey N, Kumar N, Gangwal A, Gupta M, Singh Y. Bacterial virulence factors: secreted for survival. Indian Journal of Microbiology. 2017;57(1):1-10.

120. Casadevall A, Pirofski La. Host-Pathogen Interactions: The Attributes of Virulence. The Journal of Infectious Diseases. 2001;184(3):337-44.

121. Jarlier V, Nikaido H. Mycobacterial cell wall: structure and role in natural resistance to antibiotics. FEMS Microbiology Letters. 1994;123(1-2):11-8.

122. Wu Y, Zhou A. In situ, real-time tracking of cell wall topography and nanomechanics of antimycobacterial drugs treated *Mycobacterium JLS* using atomic force microscopy. Chemical Communications. 2009(45):7021-3.

123. Marrakchi H, Lanéelle M-A, Daffé M. Mycolic acids: structures, biosynthesis, and beyond. Chemistry & Biology. 2014;21(1):67-85.

124. Hett EC, Rubin EJ. Bacterial growth and cell division: a mycobacterial perspective. Microbiology and Molecular Biology Reviews. 2008;72(1):126-56.

125. Jankute M, Cox JA, Harrison J, Besra GS. Assembly of the mycobacterial cell wall. Annual Review of Microbiology. 2015;69:405-23.

126. Bhat ZS, Rather MA, Maqbool M, Lah HU, Yousuf SK, Ahmad Z. Cell wall: a versatile fountain of drug targets in *Mycobacterium tuberculosis*. Biomedicine & Pharmacotherapy. 2017;95:1520-34.

127. Brennan PJ. Structure, function, and biogenesis of the cell wall of *Mycobacterium tuberculosis*. Tuberculosis. 2003;83(1-3):91-7.

128. Finlay BB, Falkow S. Common themes in microbial pathogenicity revisited. Microbiology and Molecular Biology Reviews. 1997;61(2):136-69.

129. Abdallah AM, Gey van Pittius NC, DiGiuseppe Champion PA, Cox J, Luirink J, Vandenbroucke-Grauls CM, Appelmelk BJ, Bitter W. Type VII

secretion—mycobacteria show the way. Nature Reviews Microbiology. 2007;5(11):883-91.

130. Mahairas GG, Sabo PJ, Hickey MJ, Singh DC, Stover CK. Molecular analysis of genetic differences between *Mycobacterium bovis* BCG and virulent *M. bovis*. Journal of Bacteriology. 1996 Mar;178(5):1274-82.

131. Conrad WH, Osman MM, Shanahan JK, Chu F, Takaki KK, Cameron J, Hopkinson-Woolley D, Brosch R, Ramakrishnan L. Mycobacterial ESX-1 secretion system mediates host cell lysis through bacterium contact-dependent gross membrane disruptions. Proceedings of the National Academy of Sciences. 2017;114(6):1371-6.

132. van Leeuwen LM, Boot M, Kuijl C, Picavet DI, van Stempvoort G, van der Pol SM, de Vries HE, van der Wel NN, van der Kuip M, van Furth AM, van der Sar AM. Mycobacteria employ two different mechanisms to cross the blood–brain barrier. Cellular Microbiology. 2018;20(9):e12858.

133. Augenstreich J, Arbues A, Simeone R, Haanappel E, Wegener A, Sayes F, Le Chevalier F, Chalut C, Malaga W, Guilhot C, Brosch R. ESX-1 and phthiocerol dimycocerosates of *Mycobacterium tuberculosis* act in concert to cause phagosomal rupture and host cell apoptosis. Cellular Microbiology. 2017;19(7):e12726.

134. Schuessler DL, Cortes T, Fivian-Hughes AS, Lougheed KE, Harvey E, Buxton RS, Davis EO, Young DB. Induced ectopic expression of HigB

toxin in *Mycobacterium tuberculosis* results in growth inhibition, reduced abundance of a subset of mRNAs and cleavage of tmRNA. Molecular Microbiology. 2013;90(1):195-207.

135. Bordes P, Cirinesi AM, Ummels R, Sala A, Sakr S, Bitter W, Genevaux P. SecB-like chaperone controls a toxin–antitoxin stress-responsive system in *Mycobacterium tuberculosis.* Proceedings of the National Academy of Sciences. 2011;108(20):8438-43.

136. Fivian-Hughes AS, Davis EO. Analyzing the regulatory role of the HigA antitoxin within *Mycobacterium tuberculosis.* Journal of Bacteriology. 2010;192(17):4348-56.

137. Ramage HR, Connolly LE, Cox JS. Comprehensive functional analysis of *Mycobacterium tuberculosis* toxin-antitoxin systems: implications for pathogenesis, stress responses, and evolution. PLoS Genet. 2009;5(12):e1000767.

138. Mostowy S, Tsolaki AG, Small PM, Behr MA. The in vitro evolution of BCG vaccines. Vaccine. 2003;21(27):4270-4.

139. Ren H, Dover LG, Islam ST, Alexander DC, Chen JM, Besra GS, Liu J. Identification of the lipooligosaccharide biosynthetic gene cluster from *Mycobacterium marinum.* Molecular Microbiology. 2007;63(5):1345-59.

140. Ru H, Liu X, Lin C, Yang J, Chen F, Sun R, Zhang L, Liu J. The impact of genome region of difference 4 (RD4) on mycobacterial virulence and BCG efficacy. Frontiers in Cellular and Infection Microbiology. 2017;7:239.

140. Kocíncová D, Sondén B, de Mendonça-Lima L, Gicquel B, Reyrat J-M. The Erp protein is anchored at the surface by a carboxy-terminal hydrophobic domain and is important for cell-wall structure in *Mycobacterium smegmatis*. FEMS Microbiology Letters. 2004;231(2):191-6.

142. Cosma CL, Klein K, Kim R, Beery D, Ramakrishnan L. *Mycobacterium marinum* Erp is a virulence determinant required for cell wall integrity and intracellular survival. Infection and Immunity. 2006;74(6):3125-33.

143. Ganaie AA, Trivedi G, Kaur A, Jha SS, Anand S, Rana V, Singh A, Kumar S, Sharma C. Interaction of Erp protein of *Mycobacterium tuberculosis* with Rv2212 enhances intracellular survival of *Mycobacterium smegmatis*. Journal of Bacteriology. 2016;198(20):2841-52.

144. Echeverria-Valencia G, Flores-Villalva S, Espitia CI. Virulence factors and pathogenicity of Mycobacterium. Intech Open Mycobacterium Research and Development. 2018:231-55.

145. Tundup S, Akhter Y, Thiagarajan D, Hasnain SE. Clusters of PE and PPE genes of *Mycobacterium tuberculosis* are organized in operons: Evidence that PE Rv2431c is co-transcribed with PPE Rv2430c and their gene products interact with each other. FEBS Letters. 2006;580(5):1285-93.

146. Fishbein S, Van Wyk N, Warren RM, Sampson SL. Phylogeny to function: PE/PPE protein evolution and impact on *Mycobacterium tuberculosis* pathogenicity. Molecular Microbiology. 2015;96(5):901-16.

147. Tufariello JM, Chapman JR, Kerantzas CA, Wong K-W, Vilchèze C, Jones CM, et al. Separable roles for *Mycobacterium tuberculosis* ESX-3 effectors in iron acquisition and virulence. Proceedings of the National Academy of Sciences. 2016;113(3):E348-E57.

148 Rodrigue S, Provvedi R, Jacques P-E, Gaudreau L, Manganelli R. The σ factors of *Mycobacterium tuberculosis*. FEMS Microbiology Reviews. 2006;30(6):926-41.

149. Wu S, Barnes PF, Samten B, Pang X, Rodrigue S, Ghanny S, Soteropoulos P, Gaudreau L, Howard ST. Activation of the eis gene in a W-Beijing strain of *Mycobacterium tuberculosis* correlates with increased SigA levels and enhanced intracellular growth. Microbiology. 2009;155(Pt 4):1272.

150. Wu S, Howard ST, Lakey DL, Kipnis A, Samten B, Safi H, Gruppo V, Wizel B, Shams H, Basaraba RJ, Orme IM. The principal sigma factor sigA mediates enhanced growth of *Mycobacterium tuberculosis* in vivo. Molecular Microbiology. 2004;51(6):1551-62.

151. Manganelli R, Dubnau E, Tyagi S, Kramer FR, Smith I. Differential expression of 10 sigma factor genes in *Mycobacterium tuberculosis*. Molecular Microbiology. 1999;31(2):715-24.

152. Abdul-Majid K-B, Ly LH, Converse PJ, Geiman DE, McMurray DN, Bishai WR. Altered cellular infiltration and cytokine levels during early *Mycobacterium tuberculosis* sigC mutant infection are associated with late-stage disease attenuation and milder immunopathology in mice. BMC Microbiology. 2008;8(1):1-14.

153. Broset E, Martín C, Gonzalo-Asensio J. Evolutionary landscape of the *Mycobacterium tuberculosis* complex from the viewpoint of PhoPR: implications for virulence regulation and application to vaccine development. MBio. 2015;6(5):e01289-15.

154. Bretl DJ, Demetriadou C, Zahrt TC. Adaptation to environmental stimuli within the host: two-component signal transduction systems of *Mycobacterium tuberculosis.* Microbiology and Molecular Biology Reviews. 2011;75(4):566-82.

155. Solans L, Gonzalo-Asensio J, Sala C, Benjak A, Uplekar S, Rougemont J, Guilhot C, Malaga W, Martin C, Cole ST. The PhoP-dependent ncRNA Mcr7 modulates the TAT secretion system in *Mycobacterium tuberculosis*. PLoS Pathogens. 2014;10(5):e1004183.

156. Fontán PA, Aris V, Alvarez ME, Ghany S, Cheng J, Soteropoulus P, Trevani A, Pine R, Smith I. Virulence and pathogenicity. Revista de Salud Pública. 2010;12(2):5-9.

157. Ryndak M, Wang S, Smith I. PhoP, a key player in *Mycobacterium tuberculosis* virulence. Trends in Microbiology. 2008;16(11):528-34.

158. Gonzalo-Asensio J, Mostowy S, Harders-Westerveen J, Huygen K, Hernández-Pando R, Thole J, Behr M, Gicquel B, Martín C. PhoP: a missing piece in the intricate puzzle of *Mycobacterium tuberculosis* virulence. PloS One. 2008;3(10):e3496.

159. Frigui W, Bottai D, Majlessi L, Monot M, Josselin E, Brodin P, Garnier T, Gicquel B, Martin C, Leclerc C, Cole ST. Control of *M. tuberculosis* ESAT-6 secretion and specific T cell recognition by PhoP. PLoS Pathogens. 2008;4(2):e33.

160. Lee JS, Krause R, Schreiber J, Mollenkopf HJ, Kowall J, Stein R, Jeon BY, Kwak JY, Song MK, Patron JP, Jorg S. Mutation in the transcriptional regulator PhoP contributes to avirulence of *Mycobacterium tuberculosis* H37Ra strain. Cell Host & Microbe. 2008;3(2):97-103.

161. Soto CY, Menéndez MC, Pérez E, Samper S, Gómez AB, García MJ, Martín C. IS 6110 mediates increased transcription of the phoP virulence gene in a multidrug-resistant clinical isolate responsible for tuberculosis outbreaks. Journal of Clinical Microbiology. 2004;42(1):212-9.

162. Wong KC, Leong WM, Law HK, Ip KF, Lam JT, Yuen KY, Ho PL, Tse WS, Weng XH, Zhang WH, Chen S. Molecular characterization of clinical

isolates of *Mycobacterium tuberculosis* and their association with phenotypic virulence in human macrophages. Clinical and Vaccine Immunology. 2007;14(10):1279-84.

163. Rajwani R, Yam WC, Zhang Y, Kang Y, Wong BK, Leung KS, Tam KK, Tulu KT, Zhu L, Siu GK. Comparative whole-genomic analysis of an ancient L2 lineage *Mycobacterium tuberculosis* reveals a novel phylogenetic clade and common genetic determinants of hypervirulent strains. Frontiers in Cellular and Infection Microbiology. 2018;7:539.

164. Rajwani R. Genetic mechanism of enhanced virulence in *Mycobacterium tuberculosis* strain isolated from patient with tuberculosis meningitis [Ph.D thesis]. Hong Kong: THe Hong Kong Polytechnic University; 2019.

165. Mangtani P, Abubakar I, Ariti C, Beynon R, Pimpin L, Fine PE, Rodrigues LC, Smith PG, Lipman M, Whiting PF, Sterne JA. Protection by BCG vaccine against tuberculosis: a systematic review of randomized controlled trials. Clinical Infectious Diseases. 2014;58(4):470-80.

166. Roy A, Eisenhut M, Harris RJ, Rodrigues LC, Sridhar S, Habermann S, Snell L, Mangtani P, Adetifa I, Lalvani A, Abubakar I. Effect of BCG vaccination against *Mycobacterium tuberculosis* infection in children: systematic review and meta-analysis. Bmj.2014;349.

167. Andersen P, Doherty TM. The success and failure of BCG — implications for a novel tuberculosis vaccine. Nature Reviews Microbiology. 2005;3(8):656-62.

168. Andersen P. Tuberculosis vaccines—an update. Nature Reviews Microbiology. 2007;5(7):484-7.

169. Wixon J. Featured organism: Danio rerio, the zebrafish. Yeast. 2000;17(3):225-31.

170. Grunwald DJ, Eisen JS. Headwaters of the zebrafish—emergence of a new model vertebrate. Nature Reviews Genetics. 2002;3(9):717-24.

171. Streisinger G, Walker C, Dower N, Knauber D, Singer F. Production of clones of homozygous diploid zebra fish (Brachydanio rerio). Nature. 1981;291(5813):293-6.

172. Bradford YM, Toro S, Ramachandran S, Ruzicka L, Howe DG, Eagle A, Kalita P, Martin R, Taylor Moxon SA, Schaper K, Westerfield M. Zebrafish models of human disease: gaining insight into human disease at ZFIN. ILAR Journal. 2017;58(1):4-16.

173. Doke SK, Dhawale SC. Alternatives to animal testing: a review. Saudi Pharmaceutical Journal. 2015;23(3):223-9.

174. Blackburn JS, Liu S, Raimondi AR, Ignatius MS, Salthouse CD, Langenau DM. High-throughput imaging of adult fluorescent zebrafish with an LED fluorescence macroscope. Nature Protocols. 2011;6(2):229-41.

175. Fleming A, Diekmann H, Goldsmith P. Functional characterisation of the maturation of the blood-brain barrier in larval zebrafish. PloS One. 2013;8(10):e77548.

176. Kuipers J, Kalicharan RD, Wolters AH, van Ham TJ, Giepmans BN. Large-scale scanning transmission electron microscopy (nanotomy) of healthy and injured zebrafish brain. Journal of visualized experiments: JoVE. 2016(111):e53635.

177. Rallis E, Koumantaki-Mathioudaki E. Treatment of *Mycobacterium marinum* cutaneous infections. Expert Opinion on Pharmacotherapy. 2007;8(17):2965-78.

178. Von Betegh L. More reviews on experimental tuberclosis of marine fish. Zentrablatt für Bakteriologie, Parasitenkunde, Infektionskrankheiten und Hygiene. Abteilung. 1910;153:54.

179. Aronson JD. Spontaneous tuberculosis in salt water fish. The Journal of Infectious Diseases. 1926:315-20.

180. Akram SM, Rathish B, Saleh D. *Mycobacterium chelonae*. Treasure Island (FL): StatPearls Publishing; 2017.

181. Clark HF, Shepard CC. Effect of environmental temperatures on infection with *Mycobacterium marinum* (Balnei) of mice and a number of poikilothermic species. Journal of Bacteriology. 1963;86(5):1057-69.

182. El Amrani M, Adoui M, Patey O, Asselineau A. Upper extremity *Mycobacterium marinum* infection. Orthopaedics & Traumatology: Surgery & Research. 2010;96(6):706-11.

183. Humphrey JD. Systemic pathology of fish: a text and atlas of normal tissues in teleosts and their responses in disease. Scotian Press; 2006. 199-214.

184. van Leeuwen LM, Van Der Kuip M, Youssef SA, De Bruin A, Bitter W, van Furth AM, Van Der Sar AM. Modeling tuberculous meningitis in zebrafish using *Mycobacterium marinum*. Disease Models & Mechanisms. 2014;7(9):1111-22.

185. Chen Z, Shao X-y, Wang C, Hua M-h, Wang C-n, Wang X, et al. *Mycobacterium marinum* infection in zebrafish and microglia imitates the early stage of tuberculous meningitis. Journal of Molecular Neuroscience. 2018;64(2):321-30.

186. Prouty MG, Correa NE, Barker LP, Jagadeeswaran P, Klose KE. Zebrafish-*Mycobacterium marinum* model for mycobacterial pathogenesis. FEMS Microbiology Letters. 2003;225(2):177-82.

187. Myllymäki H, Bäuerlein CA, Rämet M. The zebrafish breathes new life into the study of tuberculosis. Frontiers in Immunology. 2016;7:196.

188. Tobin DM, Ramakrishnan L. Comparative pathogenesis of *Mycobacterium marinum* and *Mycobacterium tuberculosis*. Cellular Microbiology. 2008;10(5):1027-39.

189. Stinear TP, Jenkin GA, Johnson PD, Davies JK. Comparative genetic analysis of *Mycobacterium ulcerans* and *Mycobacterium marinum* reveals evidence of recent divergence. Journal of Bacteriology. 2000 Nov 15;182(22):6322-30.

190. Tønjum T, Welty D, Jantzen E, Small P. Differentiation of *Mycobacterium ulcerans*, *M. marinum*, and *M. haemophilum*: mapping of their relationships to *M. tuberculosis* by fatty acid profile analysis, DNA-DNA hybridization, and 16S rRNA gene sequence analysis. Journal of Clinical Microbiology. 1998;36(4):918-25.

191. Ramakrishnan L, Falkow S. *Mycobacterium marinum* persists in cultured mammalian cells in a temperature-restricted fashion. Infection and Immunity. 1994;62(8):3222-9.

192. Van Der Sar AM, Abdallah AM, Sparrius M, Reinders E, Vandenbroucke-Grauls CM, Bitter W. *Mycobacterium marinum* strains can be divided into two distinct types based on genetic diversity and virulence. Infection and Immunity. 2004;72(11):6306-12.

193. Don EK, Formella I, Badrock AP, Hall TE, Morsch M, Hortle E, Hogan A, Chow S, Gwee SS, Stoddart JJ, Nicholson G. A Tol2 gateway-compatible toolbox for the study of the nervous system and neurodegenerative disease. Zebrafish. 2017;14(1):69-72.

194. Parikh A, Kumar D, Chawla Y, Kurthkoti K, Khan S, Varshney U, Nandicoori VK. Development of a new generation of vectors for gene expression, gene replacement, and protein-protein interaction studies in mycobacteria. Applied and Environmental Microbiology. 2013;79(5):1718-29.

195. Goude R, Parish T. Electroporation of mycobacteria. JoVE (Journal of Visualized Experiments). 2008(15):e761.

196. Young JL, Dean DA. Electroporation-mediated gene delivery. Advances in Genetics. 2015;89:49-88.

197. Baumeister R. Cross-species studies for target validation. Briefings in Functional Genomic Proteomic. 2002;1(1):53-65.

198. Lekanne Deprez RH, Fijnvandraat AC, Ruijter JM, Moorman AFM. Sensitivity and accuracy of quantitative real-time polymerase chain reaction using SYBR green I depends on cDNA synthesis conditions. Analytical Biochemistry. 2002;307(1):63-9.

199. Rutledge RG, Stewart D. Critical evaluation of methods used to determine amplification efficiency refutes the exponential character of real-time PCR. BMC Molecular Biology. 2008;9(1):1-2.

200. Rao X, Huang X, Zhou Z, Lin X. An improvement of the 2ˆ (–delta delta CT) method for quantitative real-time polymerase chain reaction data analysis. Biostatistics, Bioinformatics and Biomathematics. 2013;3(3):71.

201. Takaki K, Davis JM, Winglee K, Ramakrishnan L. Evaluation of the pathogenesis and treatment of *Mycobacterium marinum* infection in zebrafish. Nature Protocols. 2013;8(6):1114-24.

202. Benard EL, van der Sar AM, Ellett F, Lieschke GJ, Spaink HP, Meijer AH. Infection of zebrafish embryos with intracellular bacterial pathogens. JoVE (Journal of Visualized Experiments). 2012(61):e3781.

203. Watkins BY, Joshi SA, Ball DA, Leggett H, Park S, Kim J, Austin CD, Paler-Martinez A, Xu M, Downing KH, Brown EJ. *Mycobacterium marinum* SecA2 promotes stable granulomas and induces tumor necrosis factor alpha in vivo. Infection and Immunity. 2012;80(10):3512-20.

204. Moore JL, Aros M, Steudel KG, Cheng KC. Fixation and decalcification of adult zebrafish for histological, immunocytochemical, and genotypic analysis. Biotechniques. 2002;32(2):296-8.

205. Lamar Jones M. Histotechnology: a self instructional text. Journal of Histotechnology. 2015; 38(3): 97-97.

206. Sheehan DC, Hrapchak BB. Theory and practice of histotechnology. Mosby; 1980.

207. Schmittgen TD, Livak KJ. Analyzing real-time PCR data by the comparative CT method. Nature Protocols. 2008;3(6):1101-8.

208. Kent PT. Public health mycobacteriology: a guide for the level III laboratory. US Department of Health and Human Services, Public Health Service, Centers for Disease Control; 1985.

209. Volkman HE, Clay H, Beery D, Chang JC, Sherman DR, Ramakrishnan L, Akira S. Tuberculous granuloma formation is enhanced by a mycobacterium virulence determinant. PLoS Biology. 2004;2(11):e367.

210. Davis JM, Ramakrishnan L. The role of the granuloma in expansion and dissemination of early tuberculous infection. Cell. 2009;136(1):37-49.

211. Panackal AA, Williamson KC, van de Beek D, Boulware DR, Williamson PR. Fighting the Monster: Applying the host damage framework to human central nervous system infections. MBio. 2016;7(1):e01906-e1915.

212. Donald PR, Van Toorn R. Use of corticosteroids in tuberculous meningitis. The Lancet. 2016;387(10038):2585-7.

213. Donald P, Schaaf H, Schoeman J. Tuberculous meningitis and miliary tuberculosis: the Rich focus revisited. Journal of Infection. 2005;50(3):193-5.

214. Van Sorge NM, Doran KS. Defense at the border: the blood–brain barrier versus bacterial foreigners. Future Microbiology. 2012;7(3):383-94.

215. Keane J, Gershon S, Wise RP, Mirabile-Levens E, Kasznica J, Schwieterman WD, Siegel JN, Braun MM. Tuberculosis associated with

infliximab, a tumor necrosis factor α–neutralizing agent. New England Journal of Medicine. 2001;345(15):1098-104.

216. Jung B-G, Vankayalapati R, Samten B. *Mycobacterium tuberculosis* stimulates IL-1β production by macrophages in an ESAT-6 dependent manner with the involvement of serum amyloid A3. Molecular Immunology. 2021;135:285-93.

217. Wilkinson RJ, Rohlwink U, Misra UK, Van Crevel R, Mai NT, Dooley KE, Caws M, Figaji A, Savic R, Solomons R, Thwaites GE. Tuberculous meningitis. Nature Reviews Neurology. 2017;13(10):581-98.

218. Gopinath K, Warner DF, Mizrahi V. Targeted gene knockout and essentiality testing by homologous recombination. In Mycobacteria protocols 2015 (pp. 131-149). Humana Press, New York, NY.

219. Siu GKH, Yam WC, Zhang Y, Kao RYT. An upstream truncation of the furA-katG operon confers high-level isoniazid resistance in a *Mycobacterium tuberculosis* clinical isolate with no known resistance-associated mutations. Antimicrobial Agents and Chemotherapy. 2014;58(10):6093-100.